PAPERS AND PROCEEDINGS OF

THE ROYAL SOCIETY OF TASMANIA

Edited by M. Davies

and Published by the Society

Hobart

Tasmania

MUSEUM VICTORIA
20 MAR 2005

29 OCTOBER 2004

VOLUME 138

PAPERS AND PROCEEDINGS OF

THE ROYAL SOCIETY OF TASMANIA

Edited by M. Davies

and Published by the Society

Hobart

Tasmania

Printing Authority of Tasmania

ISSN 0080-4703

OCTOBER 2004

VOLUME 138

ROYAL SOCIETY OF TASMANIA

Council and Office Bearers from March 2004 to March 2005

Patron
His Excellency Mr Richard Butler, AC
Governor of Tasmania
(until 9 August 2004)

President
Dr Michael Readett

Vice-President
Dr David Leaman

Immediate Past President
Dr Andrew Rozefelds

Council
Mr Warren Boyles
Professor John Hunn
Dr Harvey Marchant
Dr Penny McCartney
Professor Patrick Quilty
Professor Jim Thompson
Mr Elvin Fist*
Mr Brian East*
(*Northern Branch Nominees)

Honorary Secretary
Ms Carol Bacon

Honorary Treasurer
Dr Albert Goede

Honorary Editor
Dr Margaret Davies

Honorary Librarian
Mr Graeme Rayner

Statements of opinions expressed in papers in this volume reflect the views of the author(s) and are not necessarily those of the Royal Society of Tasmania.

PAPERS AND PROCEEDINGS OF THE ROYAL SOCIETY OF TASMANIA
VOLUME 138

Contents

page

HARLOW, L. D., WATKINS, W. B. & KOUTOULIS, A. — An ultrastructural and functional assessment of nasal cilia and spermatozoa in an infertile human male and healthy controls 1

EVERARD, J. L., SUTHERLAND, F. L. & ZWINGMANN, H. — A Cretaceous phonolite dyke from the Tomahawk River, northeast Tasmania 11

MORRIS, D. I. — *Laxmannia morrisii* Keighery (Anthericaceae) a synonym of *L. squarrosa* Lindl., not a native of Tasmania 35

KIRKPATRICK, J. B., LEAMAN, T., PENNINGTON, A. & POLLARD, T. — Characteristics and dynamics of the sand dune vegetation at North Bay, Tasmania 37

LEESON, K. E. & KIRKPATRICK, J. B. — Vegetation patterns associated with a large rock plate in the Meehan Range, Tasmania 47

GATES, G. M. & RATKOWSKY, D. A. — A preliminary census of the macrofungi of Mt Wellington, Tasmania – the non-gilled Basidiomycota 53

NELSON, M. — Distribution of the Western paragalaxias (*Paragalaxias julianus*) (Pisces: Galaxiidae) on the Western Central Plateau, Tasmania 61

WALSH, R. G. J., SHIEL, R. J. & TYLER, P. A. — Reconnaissance limnology of Tasmania VIII. Tasmanian coastal lagoons – epicentres of endemism in the Australian aquatic microbiota 67

BANKS, M. R. — Mr Gordon Hale 1921–2004, Honorary Life Member, Royal Society of Tasmania: Obituary 77

Instructions to Authors 79

TASMANIA

UNIVERSITY OF TASMANIA

Publication of this volume was generously supported by the Government of Tasmania and the University of Tasmania.

AN ULTRASTRUCTURAL AND FUNCTIONAL ASSESSMENT OF NASAL CILIA AND SPERMATOZOA IN AN INFERTILE HUMAN MALE AND HEALTHY CONTROLS

by Lucy D. Harlow, William B. Watkins and Anthony Koutoulis

(with six plates and four tables)

HARLOW, L. D., WATKINS, W. B. & KOUTOULIS, A., 2004 (29.x): An ultrastructural and functional assessment of nasal cilia and spermatozoa in an infertile human male and healthy controls. *Papers and Proceedings of the Royal Society of Tasmania* 138: 1–10. ISSN 0080–4703. Cell Biology Group, School of Plant Science, University of Tasmania, Private Bag 55, Hobart, Tasmania 7001, Australia (LDH, AK*); 141 Hampden Rd, Hobart, Tasmania 7000, Australia (WBW). * Author for correspondence.

Ciliary disorders are complex and enigmatic, and can lead to infertility and respiratory complications. Human males who produce spermatozoa with defective flagella may also possess defective cilia. In this study, the motility and ultrastructure of nasal cilia/cells and spermatozoa of an infertile Tasmanian male patient were examined in order to elucidate the cause of his infertility. A detailed examination of the variation in cilia and spermatozoa of control subjects was also conducted. The axonemal structure of all nasal samples from control subjects showed a low frequency of abnormalities; however, when present, abnormalities varied between samples. The nasal cells and spermatozoa of the infertile patient were distinct from control samples, both in terms of motility and ultrastructure. The spermatozoa axonemes of the patient displayed the normal 9+2 microtubule ultrastructure; however, the proportion of immotile spermatozoa and ultrastructural abnormalities was higher than in control samples. All of the patient's nasal cilia were functionally immotile and approximately 70% of ciliated cells displayed extensive ciliary fusion; a feature not found in controls and not previously described. Despite having immotile nasal cilia, this patient was healthy with no obvious respiratory ailments. Additionally, the nasal cells of the patient possessed mitochondria with distended membranes, internalised membranous material, cilia with vesicles and internalised axonemes. These features suggest that ciliary deployment and membrane deposition was compromised in the patient.

Key Words: nasal cilia, spermatozoa, flagella, infertility.

INTRODUCTION

In humans, coordinated ciliary beating is important for clearing the airways of mucus and trapped foreign particles (Houtmeyers *et al.* 1999, Ma *et al.* 1999), while the flagella of spermatozoa propel them to ova to facilitate fertilisation. Consequently, defects in cilia/flagella may be associated with respiratory ailments and lowered fertility, as well as impaired sensory organ and/or brain function (Afzelius *et al.* 1975, Afzelius & Elaisson 1983, Mygind & Pedersen 1983, Afzelius 1998). The ultrastructure of cilia and flagella are essentially identical and the terms are sometimes used interchangeably (Dentler & Witman 1995), as is the case in this study.

Accurate diagnosis of ciliary disorders requires functional and ultrastructural analysis of cilia (Santamaria *et al.* 1999, Holzmann *et al.* 2000) from different systems (e.g., reproductive and respiratory) (Afzelius 1976, El-Sayed *et al.* 1997) and different areas within the one system as well as an understanding of the inherent variation that occurs within healthy populations (Nelson *et al.* 1995, Bush *et al.* 1998). Shared ultrastructural defects in cilia of different tissues would imply a genetic rather than an acquired disorder (Sturgess & Turner 1990, de Longh & Rutland 1995, Afzelius 1999).

This study examined the motility and ultrastructure of two different ciliated samples, nasal cells and spermatozoa. An infertile Tasmanian male patient who consistently produced an abnormally low proportion of motile spermatozoa was studied in order to elucidate the cause of his infertility, and examine whether his nasal cilia were affected. Samples from healthy subjects provided a standard from which to draw comparisons. The study aimed to quantify and describe variation in the axoneme and enhance our understanding of the role of cilia.

MATERIALS AND METHODS

Nasal Cilia

Ethics approval for this research was obtained from the Royal Hobart Hospital Ethics Committee, Hobart, Tasmania. Consent for biopsy of nasal cells was obtained from all participants. Nasal cells were collected from 13 control subjects (eight females and five males, aged 21–42) and a 37-year-old male infertile patient using the nasal brushing technique (Rutland *et al.* 1982). Neither the controls nor the patient had suffered recently from a respiratory illness, nor did they have a history of exposure to agents (particulate matter/chemicals and/or smoke) that may affect nasal cilia. Furthermore, the controls were non-smokers of whom none consumed more than an average of one to two glasses of alcohol per week. The patient consumed alcohol approximately once a fortnight and did not suffer from headaches, frequent colds or a persistent cough.

Individuals were requested to not consume: (i) caffeine for at least 4 h prior to sampling; or (ii) alcohol for at least 24 h prior to sampling (see Rossman *et al.* 1981). To increase tissue yield, patients blew their nose to clear excess secretions. A qualified physician performed the nasal brushings, using a 2 mm diameter nylon brush. The brush was first moistened in 5% Delbecco's Minimum Essential Medium (DMEM) (GibcoBRL, USA) and the nasal passage brushed for a few seconds. Adherent epithelia were immediately dislodged from the brush by brisk agitation directly into a pre-warmed plastic vial containing 2 ml of 5% DMEM. The brush was rinsed in 2 ml of 2.5% glutaraldehyde in 0.1 M Pipes buffer to fix the remaining cells for transmission electron microscopy (TEM). Post collection, cells in 5% DMEM were kept in a 37°C water bath to permit inspection of live material by light microscopy. Cells in fixative were stored at 4°C until processed for TEM.

Small strips of epithelia (up to 1 mm) and/or individual nasal cells were observed under the light microscope immediately after collection. Ciliary beat frequency (CBF) (scored as [i] none, [ii] some or [iii] rapid), the proportion of ciliated cells to non-ciliated cells, cell morphology, ciliary morphology and beat pattern, and any abnormalities, were observed. The number of cilia per cell was recorded as normal or abnormal. Three slides of the same sample were examined such that an overall impression of the sample and the variability within the sample were obtained. Samples were recorded by video using a Nikon Labophot microscope. In all cases, pre-warmed (37°C) slides and coverslips were used.

Spermatozoa

Semen samples were collected from two controls and the infertile patient. The control samples were from donors of an IVF programme and these have been used successfully in the programme. All specimens were collected after a minimum of 48 h but no longer than seven days of sexual abstinence, as recommended by the IVF laboratory. Samples collected away from the laboratory were delivered within 1 h of collection and specimens kept as close to body temperature as possible. Samples were collected into a sterile plastic container pre-warmed to body temperature. An aliquot of the semen was centrifuged at low speed for 5–10 min until a pellet had formed. The supernatant was removed and the pellet resuspended in 2.5% glutaraldehyde in 0.1 M Pipes buffer and stored at 4°C until processed for TEM.

Macroscopic analysis of semen included appearance, volume and viscosity. The sample was allowed to liquefy at 37°C for a minimum of 15 min and mixed thoroughly with a swirling motion for 20–30 sec. The sample was examined immediately after liquefaction. A normal sample has a homogenous, gray opalescent appearance. The volume was measured with a sterile graduated pipette. Viscosity was estimated by allowing the semen to drop from the pipette and observing the drops or length of the thread. A sample with normal viscosity leaves the pipette with discrete drops. Increased viscosity can range from slightly increased to moderately increased, to grossly increased depending on the length of the thread (this can be up to 2 cm long). Viscosity may also be decreased if the semen is watery.

Light microscopy was used for detailed analysis. A 5 µl drop of the sample was placed on a Makler chamber and the number of motile/non-motile spermatozoa was counted. A minimum of 200 spermatozoa were counted and the count repeated with a second aliquot of the sample (the count and motility were averaged). Progression or degree of forward movement was assessed according to the following scale: (i) poor – no forward motion (wavering) or slight forward motion; (ii) average – slow meandering forward motion; (iii) fair – more direct but slow forward motion; (iv) good – faster straight line motion; and (v) excellent – very rapid direct motion.

For detailed morphological observations, a slide was prepared from the raw semen sample. A drop of semen was placed between two slides. The slides were pulled apart gently and one smear was stained with hematoxylin and eosin, and fixed with DePeX mounting medium (Gurr, USA). Slides were left for a minimum of 24 h to set. Spermatozoa were documented as having a normal or abnormal morphology. Abnormalities were grouped into four categories: (i) cytoplasmic droplets; (ii) head defects; (iii) mid-piece defects; and (iv) tail defects. After initial observations spermatozoa were recorded by video using a Nikon Labophot microscope. In all cases, pre-warmed (37°C) slides and coverslips were used. Slides of fixed spermatozoa were re-examined and more detailed observations of morphology conducted.

Transmission Electron Microscopy (TEM)

After initial fixation in 2.5% glutaraldehyde in 0.1 M Pipes buffer, samples were washed three times for 3 min in 0.1 M Pipes buffer, fixed in 1% OsO_4 in water for 2 h, washed three times for 3 min in sterile water and stained in 4% aqueous uranyl acetate for 2 h. Following staining, samples were washed three times for 3 min in sterile water and dehydrated in a graded series of ethanol (25%, 50%, 75%, 100%) for 20 min per concentration. Two further 20 min-exposures to 100% ethanol were performed to ensure all water was removed. Cells were embedded in Spurr's resin (Spurr 1969) at 25% increments (25%, 50%, 75%, 100%) over a period of 2 h. The 100% resin was changed twice, 20 min per change, followed by an overnight change and polymerised at 65°C for 25 h. Ultrathin sections were stained for 30 min in 4% aqueous uranyl acetate, washed four times for 3 min in distilled water, stained in lead citrate for 3 min, washed four times for 3 min in distilled water and examined in a Philips CM100 transmission electron microscope operated at 80 kV.

Initial observations consisted of documenting the variation in control ultrastructure, both of nasal cells and their associated cilia, and of spermatozoa and their associated cilium. For each sample, similarities and differences between control and the patient were documented. This included recording the percentage of apparently "normal" and "abnormal" cells and axonemes. All samples were examined by TEM. Extensive documentation was performed on seven randomly chosen control nasal samples and the two spermatozoa controls.

RESULTS

Control Nasal Cilia

The proportion of ciliated cells varied widely (15–80%) between controls. All control samples possessed a very similar beat pattern, number of cilia per cell and CBF (scored as rapid). Control nasal cells viewed by electron microscopy possessed numerous regularly-spaced cilia, interspersed by branched microvilli (pl. 1A–D). Microvilli were present on regions of the cell surface both with and without cilia, and dominated at junctions between cells (pl. 1A). Cilia were 6 µm in length and 200 nm wide, while microvilli were considerably shorter, up to 2 µm long, with a variable width. Microvilli sectioned towards their tip were 50–100 nm wide (pl. 1C), while microvilli sectioned at a branching point were up to 600 nm wide. The degree of branching varied from unbranched to six branches, with secondary branching common (pl. 1D).

The orientation of central pair (CP) microtubules of adjacent cilia was generally similar for controls; however, occasionally the CP microtubules were oriented in a different direction (pl. 1C). The ciliary membranes of control cilia were typically uniform in appearance (i.e., not "loose"or

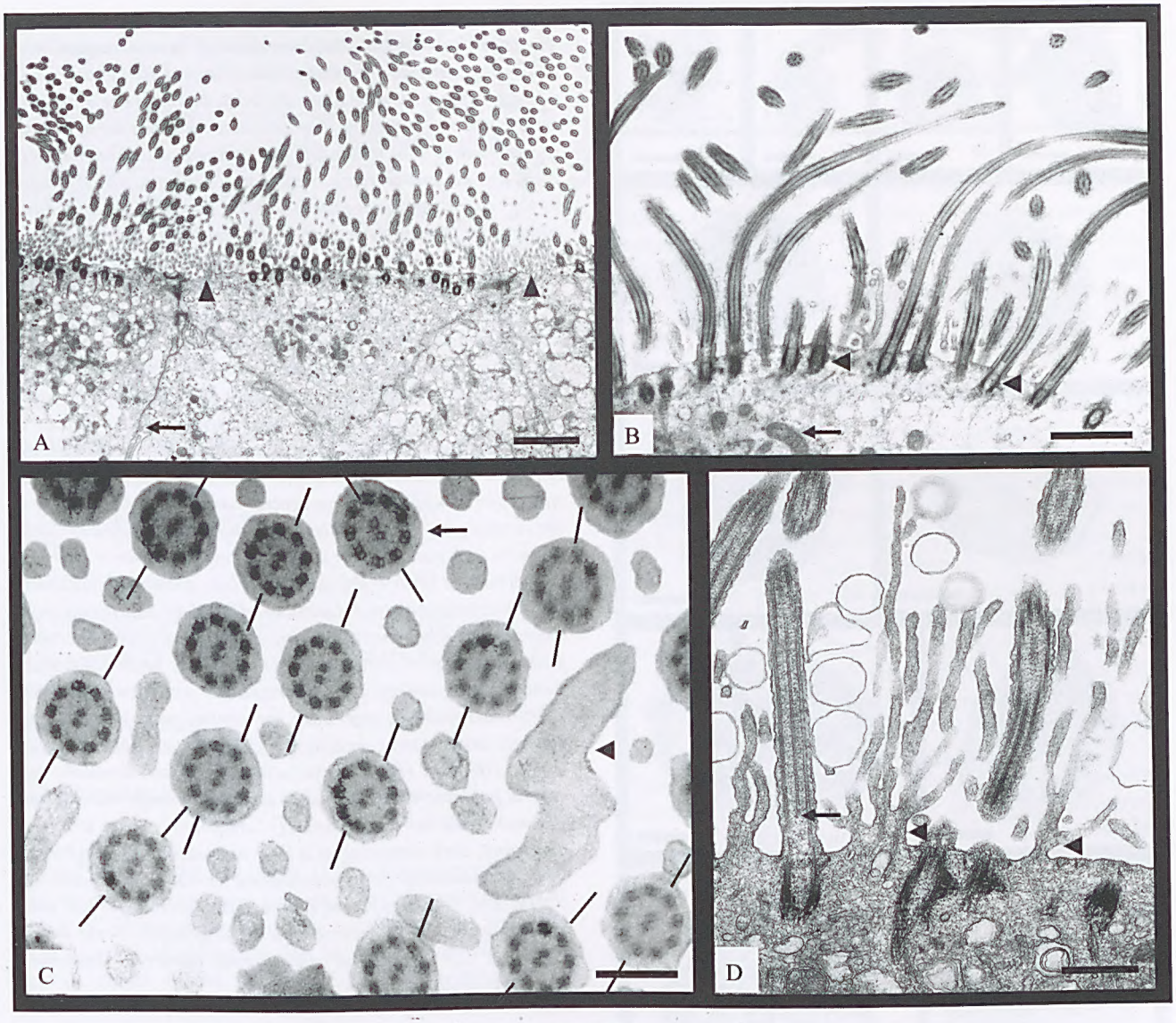

PLATE 1

Transmission electron micrographs of control nasal cells with cilia. (A) Oblique section showing numerous cilia and junctions between cells. Note cell membrane (arrow). Microvilli are interspersed between cilia at the cell surface and span the junction between cells (arrowheads). Scale bar = 2 μm. (B) Longitudinal section showing basal bodies (arrowheads). Note mitochondrion with uniform appearance of external and internal membranes (arrow). Scale bar = 1 μm. (C) Transverse section through a branched microvillus (arrowhead) and numerous cilia. The cilia possess the characteristic 9+2 microtubule arrangement. Ciliary orientation is defined by a line through the central pair microtubules. Note the cilium with misoriented central pair microtubules (arrow). Scale bar = 200 nm. (D) Longitudinal section through branched microvilli (arrowheads) and cilia. The central pair microtubules of the ciliary axoneme begin some distance above the cell proper (arrow). Scale bar = 500 nm.

wavy) (pl. 1C). Internal and external mitochondrial membranes in nasal cells also appeared uniform in controls (pl. 1B).

The axonemal structure showed distinct changes along the length of the cilium. The CP microtubules of the axoneme were present ~350 nm from the cell proper (pl. 1D), forming the characteristic 9+2 microtubular arrangement, consisting of nine outer doublet microtubules and two single CP microtubules. This arrangement continued up the length of the cilium until the tip, where the cilium tapered. In this region, microtubules were reduced in number and became disorganised resulting in a range of axonemal tip sections, all of which appeared abnormal (pl. 2A–D). Microtubule associated structures, such as dynein arms, occasionally persisted in tip regions (pl. 2C–D).

In all controls, microtubule associated structures (inner/outer dynein arms, radial spokes, CP projections) were evident. Sections in which this detail could be seen were rare and could be documented only as present or absent. In the majority of sections, outer dynein arms were clearly visible. The proportion of normal axonemes (9d+2cp = 9 doublet microtubules with outer dynein arms + 2 single CP microtubules), including tip sections, ranged from 81.8–94.9% in controls (table 1). A variety of different tip axonemal structures was observed in which single (s) microtubules were commonly present in place of doublet (d) microtubules and one or both CP microtubules were absent (pl. 2A). The following tip sections were observed in controls: 9d+1cp, 9d+0cp, 8d+1s+2cp, 8d+2cp, 8d+1s+0cp, 8d+0cp, 7d+2s+0cp, 6d+2cp, 5d+4s+2cp, 5d+4s+0cp, 4d+3s+0cp, 4d+0cp, 3d+3s+2cp, 3d+0cp, 2d+7s+0cp,

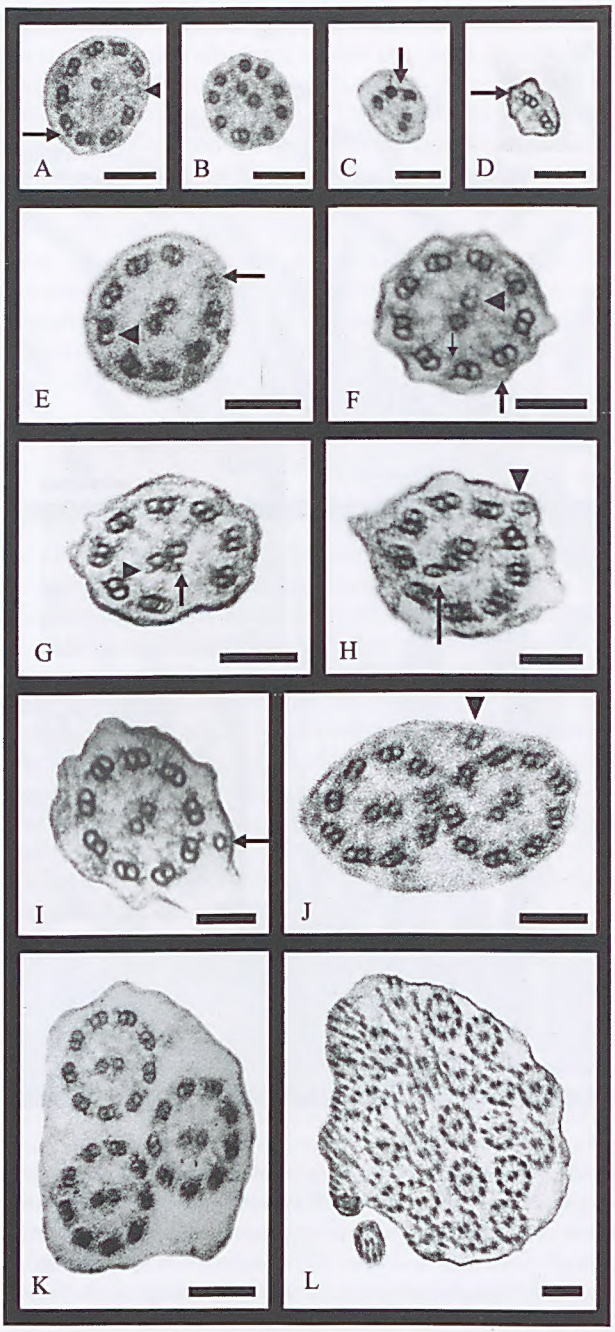

PLATE 2

Transmission electron micrographs of control nasal cilia exhibiting variation from the 9+2 microtubule arrangement. (A) Axoneme with nine outer doublets, but only one of the two central pair microtubules. The nine outer doublets are not evenly spaced leading to a noticeable gap (arrowhead). Outer dynein arms can be seen (arrow). Scale bar = 100 nm. (B) Axomene at the ciliary tip region with one outer doublet and eight outer singlets, all lacking dynein arms. The central pair microtubules are present, but off-centre. Scale bar = 100 nm. (C) Axoneme at the ciliary tip region with two singlet microtubules, possibly the central pair, and three outer doublet microtubules with outer dynein arms (arrow). Scale bar = 100 nm. (D) Axoneme at the ciliary tip region with two outer doublets with outer dynein arms (arrow). Scale bar = 100 nm. (E) Axoneme with eight outer doublets and one outer singlet (arrow). The B-tubule of one of the outer doublets is not completely associated with the A-tubule (arrowhead). Scale bar = 100 nm. (F) Axoneme with nine outer doublets and two central pair microtubules. One of the central pair microtubules is incomplete (arrowhead). Some doublets lack outer dynein arms (arrows). Scale bar = 100 nm. (G) Axoneme with eight outer doublets, abnormal placement of central pair projection (arrowhead) and an additional small microtubule-like structure (arrow) associated with the central pair. Scale bar = 100 nm. (H) Axoneme with nine outer doublets, two central pair microtubules and two additional single microtubules; one near the central pair microtubules (arrow) and one near the ciliary membrane (arrowhead). Scale bar = 100 nm. (I) Axoneme with nine outer doublets, two central pair microtubules and an additional single microtubule (arrow). Scale bar = 100 nm. (J) Compound cilium with two axonemes, each consisting of a 9+2 microtubule arrangement, and an additional single microtubule (arrowhead). Scale bar = 100 nm. (K) Compound cilium with three axonemes, each consisting of a 9+2 microtubule arrangement. Scale bar = 100 nm. (L) Compound cilium with numerous axonemes. Scale bar = 200 nm.

2d+3s+2cp, 2d+1s+0cp, 2d+0cp, 1d+0cp, 9s+2cp, 9s+1cp, 9s+0cp, 8s+2cp, 8s+0cp and 2–5 random microtubules.

Ciliary abnormalities in controls occurred at a low frequency (10.4%) (table 1). Microtubule abnormalities fell into three categories: (i) missing microtubules (1.8%) (pl. 2E, G); (ii) misplaced microtubules (0.2%); and (iii) extra microtubules, either inside (pl. 2H) or outside (pl. 2I) the axoneme (0.8%). Incomplete or broken microtubules were observed; either the B-tubule of an outer doublet was not fully connected to the A-tubule (pl. 2E), or there was a break in a CP microtubule (pl. 2F). The most common abnormality observed in controls was compound cilia (>1 axoneme within the ciliary membrane). The extent of compound cilia ranged greatly in controls, from one and a half axonemes to over six (pl. 2J–L), with an average occurrence of 5.4% (table 1).

Patient Nasal Cilia

The nasal cells and nasal cilia of the patient showed an unusual morphology by light microscopy. Approximately 30% of ciliated cells displayed varying degrees of fusion of cilia, ranging from what appeared to be separate cilia with normal morphology as seen in controls to partially fused cilia (pl. 3A, B), while the majority of ciliated cells (~70%) possessed cilia that appeared completely fused (pl. 3C). Fused cilia did not beat, while the tips of some non-fused cilia showed tiny abnormal movements (CBF scored as none), only detectable upon detailed examination of video recordings. Therefore, all nasal cilia in the patient were deemed functionally immotile. Fused cilia were not found in any controls.

The patient possessed cilia with the 9+2 axonemal structure and the appropriate microtubule associated structures. However, the patient possessed an unusually low number of normal axonemes, only 39% compared to the

TABLE 1
Comparison of control and patient nasal ciliary ultrastructure

	Control (range)	Patient
% Normal TS* (no tips)	69.7 (46.2-89.3)	19.5
% Normal TS	89.6 (81.8-94.9)	39
% Abnormal TS	10.4 (5.1-18.2)	61
% Half axoneme	0	4.8
% Internalised microtubules	0	9.7
% Missing microtubules	1.8 (0-10.8)	8.1
% Misplaced microtubules	0.2 (0-1.1)	3.7
% Extra-numerary microtubules	0.8 (0-2.5)	1.6
% Ciliary vesicles	1.8 (0-6.1)	45.2
% Compound (>1 axoneme)	5.4 (2.3-11.5)	7.8
% Abnormal TS excluding compound	5 (0-15.9)	53.2
Total # TS examined	405 (58)	77

* TS = transverse sections

control mean of 89.6% (table 1). Furthermore, abnormal cilia were six times more frequent than the control mean (table 1). Although unfused cilia were found (pl. 4A), the high number of abnormal cilia in the patient was largely due to ciliary fusion (pl. 4B, C) and the presence of vesicles between the axoneme and ciliary membrane (pl. 4D). The patient displayed microtubule abnormalities not found in controls such as half axonemes and off-centre CP microtubules. Additionally, the patient possessed cells with a high proportion of internal microtubules and/or internal axonemes (pl. 4E, table 1).

Ciliary abnormalities found in the patient, at a frequency greater than the control range, included misplaced microtubules and ciliary vesicles. Cilia of the patient also possessed "loose" ciliary membranes giving a wavy appearance (pl. 4F), while cells possessed distended mitochondria (pl. 4A) and significant amounts of internalised membraneous or fibrous material (pl. 4G). The frequency of compound cilia in the patient (7.8%) was within the control range (2.3–11.5%) (table 1). Mis-orientation of adjacent cilia (pl. 4F) occurred at a slightly higher frequency in the patient than controls.

Control and Patient Spermatozoa

The patient possessed an unusually low proportion (33%) of motile spermatozoa compared to the control mean (69%) and possessed spermatozoa with a low rate of forward movement or "progression" (table 2). Furthermore, his spermatozoa count was unusually low (~half the control mean) and his semen volume was unusually low (0.5 ml compared to a control average of 5.4 ml) (table 2).

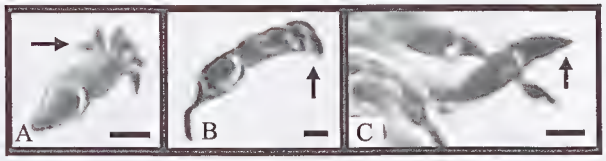

PLATE 3
Light microscope images of ciliated nasal cells of the patient showing different degrees of ciliary fusion. All scale bars = 4 μm. (A) Cilia (arrow) with apparent normal morphology (i.e., separate cilia), as seen in control samples. (B-C) Nasal cells with different degrees of ciliary fusion (arrows).

At the light microscope level, some spermatozoa in the patient's samples displayed the same appearance as normal spermatozoa in control samples (pl. 5A). Spermatozoa often displayed multiple defects. The proportion of patient spermatozoa with an abnormal morphology (78%) was within the control range (78–83%) (table 3). A range of different head abnormalities was observed (pl. 5B, C). Unlike controls, some patient spermatozoa possessed cytoplasmic droplets, which accounted for 1% of abnormal spermatozoa (table 3). Cytoplasmic droplets were either distending from the acrosome or the mid-piece region. Spermatozoa with pin heads (pl. 5B), double heads, double tails, short tails (pl. 5D, G) and mid-piece abnormalities (pl. 5B, D–G) were found in control and patient samples.

Spermatozoa examined by TEM (pl. 6) were analysed according to whether they were sectioned transversely (pl. 6A) or longitudinally (pl. 6B) (table 4). Spermatozoa with internal axonemes formed a large proportion of the abnormalities in the patient and the controls; these internal axonemes were often accompanied by the outer thick fibre, and mid-piece mitochondria or tail region fibrous sheaths typical of human sperm. For instance, 73.1% of the patient's spermatozoa possessed internal axonemes (pl. 6F, G), while 57.9% of control spermatozoa possessed internal axonemes (pl. 6C) (table 4). The percentage of the patient's spermatozoa with a normal ultrastructure in longitudinal view (17.9%) was considerably lower than the control range (56.7–60.5%) (table 4). This was also the case in transverse view; 29% in the patient and 34–50% in controls (table 4).

Microtubule abnormalities could be evaluated more easily in transverse section than longitudinal section and were grouped into a range of sub-categories (table 4), which could be scored more than once if an axoneme possessed multiple defects or an axoneme was sectioned more than once (e.g., internalised axonemes). Generally, the patient possessed a higher percentage of defects compared to the controls. Compound cilia were rare in controls (0.75%), but more common in the patient (6.8%) (table 4). Unlike nasal cilia, the only form of compound cilia found in spermatozoa was those with two axonemes within the ciliary membrane. Other infrequent abnormalities found in controls included twisting of the outer doublet microtubules and unusually wide cilia (pl. 6D).

The patient also possessed unusually wide cilia; however, unlike controls, microtubules were sometimes absent from these cilia (pl. 6G). The fibre bundles of the cilium displayed a similar set of abnormalities as the axoneme. Fibres were documented as missing, misplaced, extra-numerary (pl. 6E) or internalised.

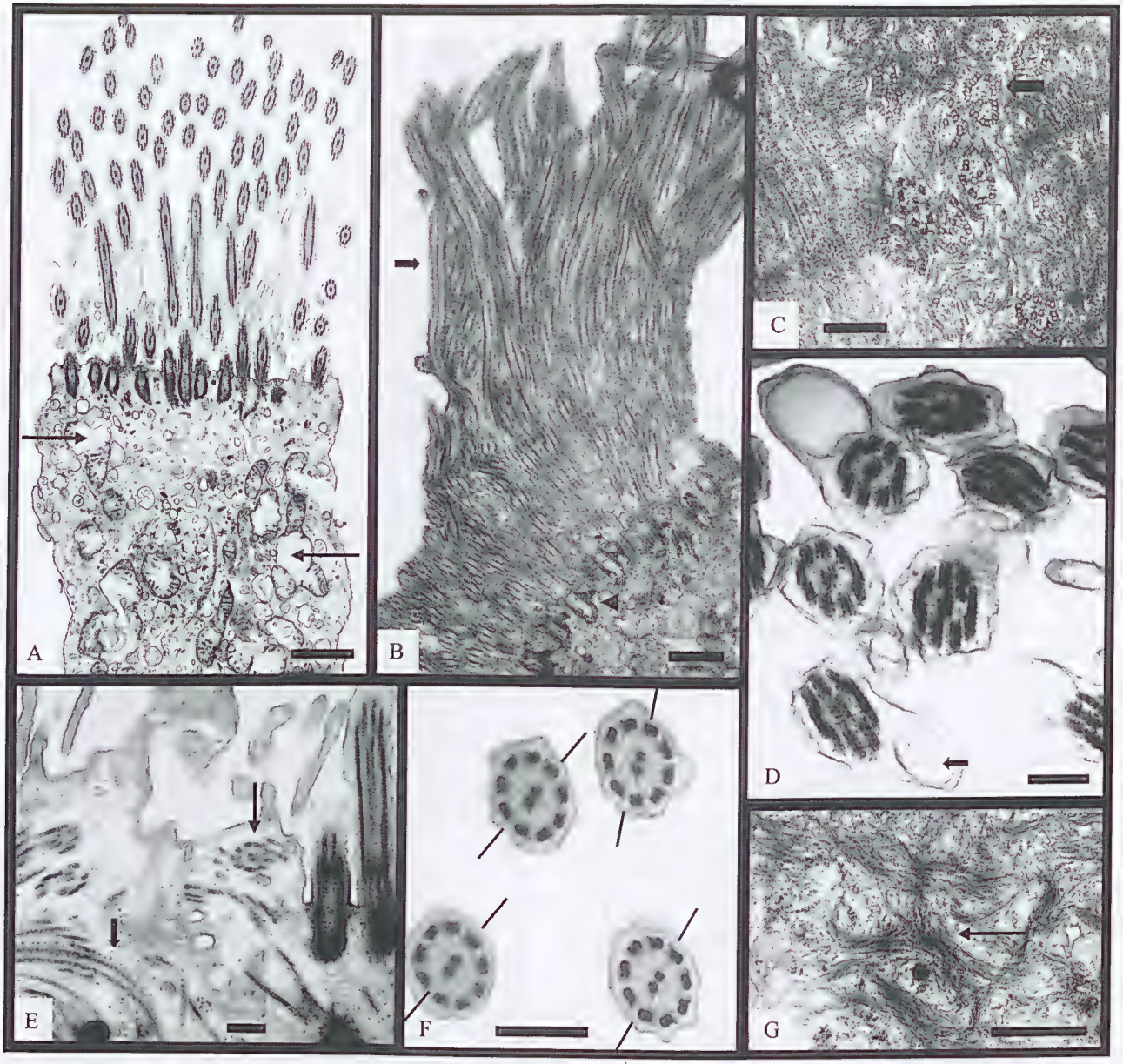

PLATE 4

Transmission electron micrographs of patient nasal cells and cilia. (A) Longitudinal section of nasal cell with apparently normal ciliary arrangement. Cilia are not fused and there are no vesicles within the ciliary membrane; however, mitochondria possess distended membranes (arrows). Scale bar = 1 μm. (B) Nasal cell with fused cilia (arrow). Note basal bodies (arrowhead). Scale bar = 500 nm. (C) Glancing section of fused cilia. Some axonemes are sectioned transversely and exhibit the 9+2 microtubule arrangement (arrow). Axonemes are intertwined with additional membranous material. Scale bar = 200 nm. (D) Cilia with vesicles within ciliary membrane (arrow). Scale bar = 200 nm. (E) Nasal cell with numerous internalised microtubules (short arrow) and internalised axonemes with 9+2 microtubule arrangement (long arrow). Scale bar = 200 nm. (F) Transverse section through cilia with normal microtubular arrangment, normal ciliary orientation (as determined by the lines) and the presence of dynein arms, radial spokes and central pair projections. Scale bar = 200 nm. (G) Copious membranous or fibrous material (arrow) within a nasal cell. Scale bar = 500 nm.

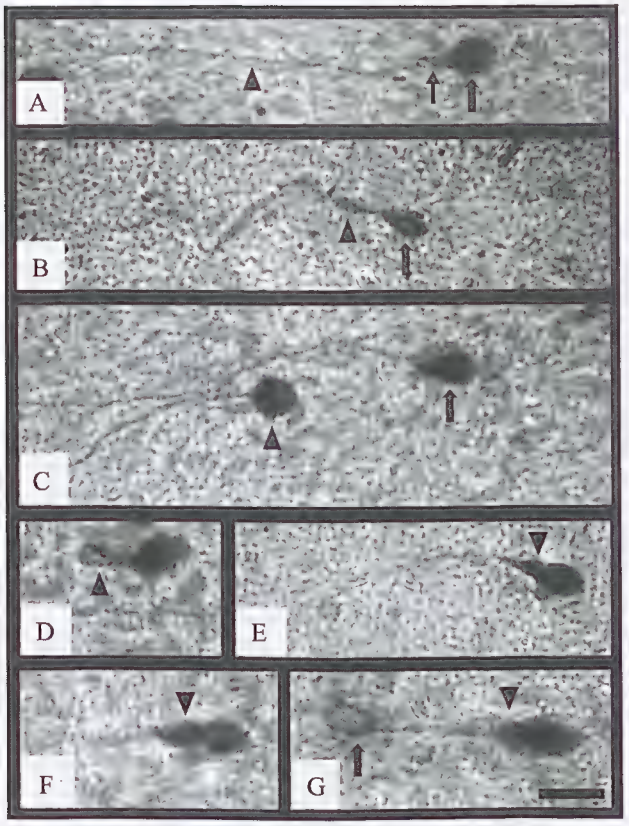

PLATE 5

Light microscope images of fixed and stained spermatozoa from the patient. Scale bar for all images = 5 μm. (A) Normal spermatozoon as seen in control samples. Note the three distinct regions of the cell: acrosome (thick arrow), mid-piece (thin arrow) and tail (arrowhead). (B)-(G) Defective spermatozoa which can also be found in control samples. (B) Spermatozoon with pin-head (arrow) and thick mid-piece (arrowhead). (C) Spermatozoa with abnormally shaped heads: one head is unusually tapered (arrow), while the other is more spherical (arrowhead). (D) Spermatozoon with a stumpy tail (arrowhead) that may be internalised. (E) Spermatozoon with enlarged mid-piece (arrowhead). (F) Spermatozoon with enlarged mid-piece (arrowhead). Note the enlargement is far more pronounced than the spermatozoon shown in (E). (G) Spermatozoon with enlarged mid-piece (arrowhead) and coiled tail (arrow).

TABLE 2
Macroscopic examination and light microscopy of semen

	Control (range)	Patient (range)
# Samples averaged	2	7
% Motility	69 (64–74)	33 (14–49)
Progression (1–5)	Good (4–4)	Fair (3–3)
Count (x10^6 ml^{-1})	93 (52–168)	48 (31–93)
Volume (ml)	5.4 (3.6–7)	0.5
Viscosity	Normal-moderately increased	Slightly increased*

*Within control range

TABLE 3
Light microscope evaluation of the morphology of control and patient spermatozoa

	Controls (range)	Patient (range)
# Samples averaged	2	3
% Normal forms	19.5 (17–22)	22 (21–24)
% Abnormal forms	80.5 (78–83)	78
% Cytoplasmic droplet	0	1 (0–3)
% Abnormal head	80 (78–82)	64.7 (59–70)
% Abnormal mid-piece	0.5 (0–1)	12.3 (9–14)
% Abnormal tail*	0	0

*Some spermatozoa with abnormal tails also fell into the abnormal head and/or abnormal mid-piece categories, and these were not scored twice.

TABLE 4
Comparison of control and patient spermatozoa ultrastructure

	Control (range)	Patient
# Cells/axonemal longitudinal sections	34 (30–38)	67
% Cells with internalised axonemes	57.9 (50–65.8)	73.1
% Normal axonemes	58.6 (56.7–60.5)	17.9
% Abnormal axonemes	41.4 (39.5–43.3)	82.1
% Cells with internalised microtubules	10.4 (5.3–13.3)	17.9
# Axonemal transverse sections excluding tips	59.5 (53–66)	74
% Normal axomenes	42 (34–50)	29
% Compound (>1 axoneme)	0.75 (0–1.5)	6.8
% Half axoneme	11.7 (4.5–18.9)	25.7
% Missing microtubules	26.5 (22.7–30.2)	29.7
% Extra-numerary microtubules	0.95 (0–1.9)	4.1
% Disorganised microtubules*	13.8 (10.6–17)	35.2
% Abnormal fibres**	2.25 (0–4.5)	8.1
% Other***	0.95 (0–1.9)	3.3

Note: percentage of axonemal abnormalities in transverse section exceeds 100 because some axonemes possessed more than one defect.

* Includes axonemes with misplaced microtubules, off-centre CP and CP too close.

** Includes missing, misplaced, extra-numerary and internalised fibres.

*** Includes abnormally wide cilia, ciliary vesicles, twisted outer doublets (LS) and B-tubule broken off A-tubule.

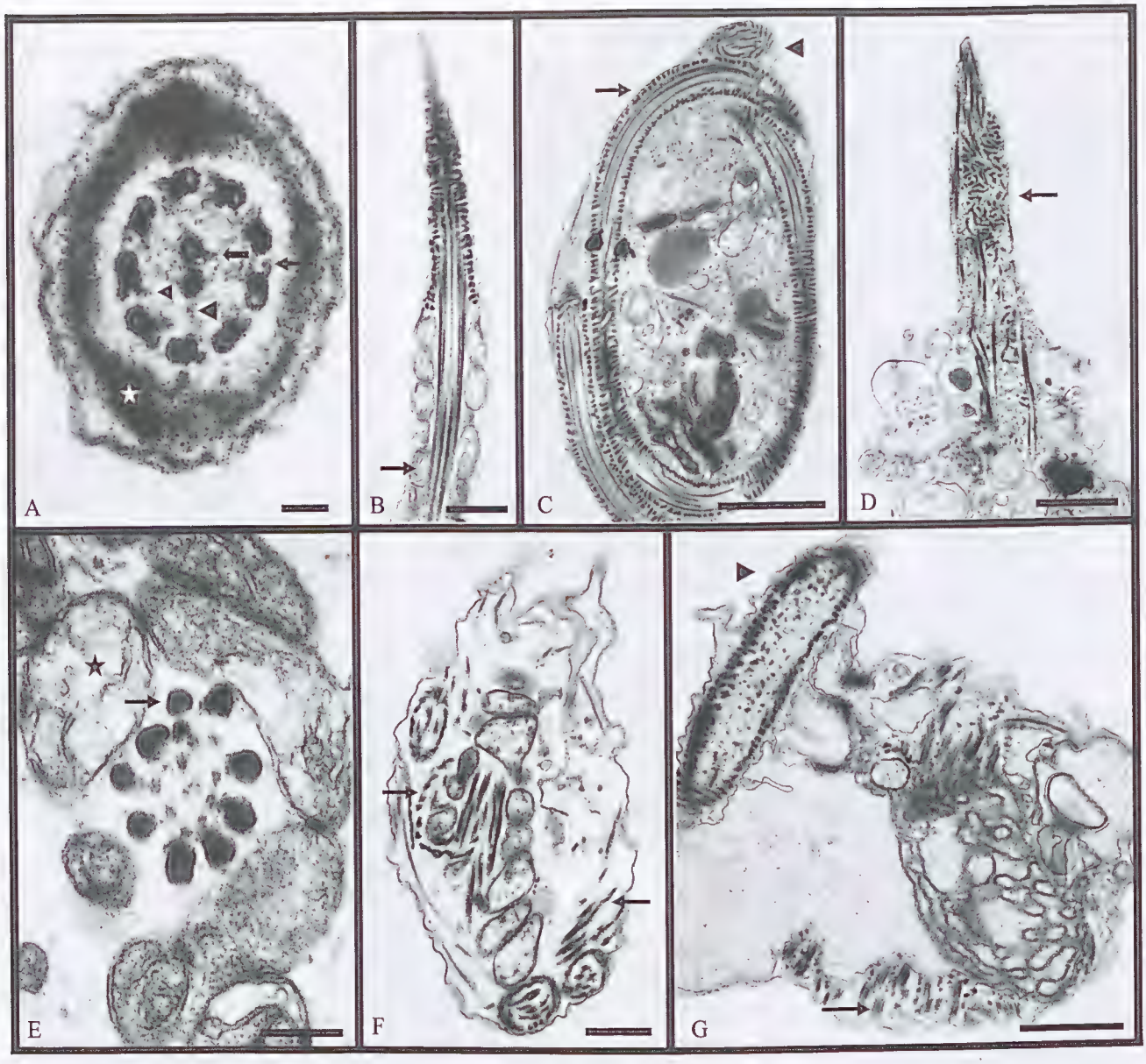

PLATE 6

Transmission electron micrographs of spermatozoa. (A) Transverse section through a control cilium with a 9+2 microtubule arrangement surrounded by a fibrous sheath (star). Note microtubule projections, including outer dynein arms (thin arrow), inner dynein arms (small arrowhead) radial spokes (large arrowhead) and central pair projections (thick arrow). Scale bar = 50 nm. (B) Longitudinal section through a control cilium at the junction between the mid-piece (with mitochondrial profiles [arrow]) and the tail region (with fibrous sheath [top of section]). Scale bar = 500 nm. (C) Control spermatozoon showing variation. Note coiled internalised axoneme sectioned longitudinally (arrow) and almost transversely (arrowhead). Scale bar = 1 µm. (D) Control spermatozoon showing variation. Note short broad cilium containing extra-numerary, apparently disorganised microtubules or fibrous sheath components (arrow). Scale bar = 1 µm. (E) Transverse section through basal region of a cilium from a patient spermatozoon showing an additional or split fibre bundle (arrow). Mitochondria surround the axoneme (star). Scale bar = 250 nm. (F) Section through a patient spermatozoon showing internalised microtubules (arrows), some of which may represent axonemal profiles. Scale bar = 500 nm. (G) Section through a patient spermatozoon showing internalised axoneme that is twice the width of a normal cilium and lacks microtubules (arrowhead). Scale bar = 500 nm.

DISCUSSION

Patient Summary

The nasal cells/cilia and spermatozoa of the patient were functionally immotile but this was not attributable to a lack of co-ordination (misorientation of ciliary axonemes) or an axonemal defect(s). The patient's cilia were clearly distinct from controls and displayed a higher frequency of abnormalities at the ultrastructural level. Strikingly, the patient's nasal cells displayed extensive ciliary fusion, vesicles within the ciliary membrane, distended mitochondria and internal microtubules/axonemes (also in spermatozoa). These observations suggest that membrane deposition or deployment is compromised in the patient resulting in abnormal ciliogenesis. Internalised axonemes may result from a lack of ciliary deployment; vesicles may be a product of excess ciliary membrane; mitochondrial membranes may be

produced copiously or malformed, resulting in the observed distention; and excess membranes within the cell proper may cause ciliary axonemes to become matted or "fused". Unlike other membrane defects such as cilia with finlike extensions (Herzon 1983), individual membranes were absent from fused axonemes such that these cilia were unable to beat. Therefore, although the patient does not have an axonemal problem *per se*, his ciliated cells were affected.

The cause of the patient's infertility was less obvious than the immotility of his nasal cilia. Male infertility is complex and men can often have spermatozoa with an impaired motility but an apparently "normal" ultrastructure (Greenstone *et al.* 1983, Santamaria *et al.* 1999), or vice versa (de Longh & Rutland 1995). It is known that the spermatozoa of the patient are incapable of fertilising an ovum under normal conditions, while those of the two donor controls are capable of fertilisation. Distinct features of the patient's semen were the: (i) extremely low volume collected; (ii) high proportion of immotile spermatozoa and spermatozoa with reduced progression; (iii) unusually low number of spermatozoa; and (iv) unusually high proportion of spermatozoa with an abnormal ultrastructure. It appears that the high proportion of immotile spermatozoa in the patient's samples reflects the high proportion of spermatozoa with internalised axonemes and the degree of internalisation. It is presumed that spermatozoa with internal axonemes would be functionally immotile and hence incapable of fertilisation. More specific axonemal abnormalities did not appear to be connected to patient infertility.

Control Ciliary Variation

It is expected that ciliary abnormalities found in control subjects are an attribute of environmental factors, and are therefore acquired. The main causes of acquired ciliary defects are infectious or toxic exposures (Sleigh 1983, Toremalm 1983). Damage commonly arises as a result of cigarette smoke (Fox *et al.* 1983, Knoll & Talbot 1998), alcohol and/or caffeine (Johnsen *et al.* 1974). In addition, some local anaesthetics (Afzelius & Elaisson 1983) as well as bacterial (de Longh & Rutland 1995, Nelson *et al.* 1995) and fungal (Pieckova & Jesenska 1998) products temporarily inhibit ciliary motility. Infections may cause ciliary damage but do not appear to affect spermatozoa motility (Afzelius 1998). Such factors may account for the baseline level of ciliary disorientation, compound cilia (Nielsen *et al.* 1983), and the wide variability in the types of ciliary abnormalities found in control subjects and the patient.

Caution is required when determining diagnostic features. Previous studies have not looked extensively at control variation in nasal samples. Certain microtubule arrangements documented in controls in this study (e.g., axonemal sections with only two doublet microtubules) have been reported as abnormal by previous studies (Arden & Fox 1979) when these arrangements are the natural tapering of the cilium at its tip. Interestingly, branching microvilli, a "normal" feature of nasal cells, do not appear to have been previously documented.

The average frequency of abnormal nasal cilia for controls was 10.4% compared to 1% (Levison *et al.* 1983) and < 5% (Rossman *et al.* 1983) for previous studies. This may reflect the range of variation in controls that has in the past been attributed to ciliary disorders. Similarly, control spermatozoa exhibited a range of abnormalities both externally (i.e., at the light microscope level) and internally (i.e., at the TEM level). This seemingly high proportion of abnormal spermatozoa reflects the high IVF laboratory standards for spermatozoa with a normal morphology. The main abnormality of control spermatozoa, observed at the TEM level, was internalised axonemes (i.e., a tail defect). When these spermatozoa are observed under the light microscope they appear to have an abnormally large head and acrosome region (i.e., a head defect). Current clinical diagnosis of infertility may therefore be biased towards head defects.

Defining Fused Cilia

Large cilia have been described previously in the form of compound cilia (a term used interchangeably with fused cilia and megacilia) of various forms (Takasaka *et al.* 1980, Corbeel *et al.* 1981, Wright 1982, Bryan 1983 [not illustrated], Zahm *et al.* 1990 [no TEM images]), cilia with cyst-like structures (Tsang *et al.* 2000) and so-called fusion cilia (Herzon 1983). These fusion cilia are not the same as those described in our study. Fusion cilia, whether complete or partial, are usually not much larger than a single 9 + 2 size (Herzon 1983). Although membrane defects such as finlike extensions from the ciliary membrane or defects of the shaft membrane have been described (Herzon 1983), the fused cilia in our study do not resemble these, nor are they compound cilia. Use of the term "fused" in literature is inconsistent and needs clarification. The fused cilia in our study do not appear to have been previously documented and may represent a novel disorder. Extensive research would be necessary to determine how common this disorder may be.

Conclusions

Interpretation of these results is complex and warrants further study, given the inability to analyse data statistically because of a single experimental subject. In particular, study of control variation and the effect of fused cilia on mucociliary clearance would be rewarding. Continuation of this work could involve examining a broader range of samples, with a particular focus on membranes. It is important to note that spermatozoa possess only one cilium (flagellum) such that ciliary fusion cannot occur.

It would have been interesting to include relatives of the patient in further genetic studies. However, during the course of this research, the male patient's partner was successful in becoming pregnant using IVF technology. Once this occurred, the male patient did not want to participate in any further research. Potentially, the infertility of this patient represents a novel disorder. Interestingly, the patient leads a healthy life and does not suffer from symptoms of impaired ciliary function (such as respiratory infections, coughs, frequent colds or headaches). He describes himself as being quite fit, and it could be that his fitness compensates for the defects found in this study. Similarly, organs that possess axonemal structures such as sensory organs (e.g., auditory hair cells and photoreceptors of the eye) do not appear affected (i.e., vision, balance and hearing were not impaired). The patient's anatomy displayed the normal left-right asymmetry.

Clearly there is much to learn about: (i) the functioning of respiratory cilia and their significance for healthy airways; and (ii) the complex factors that affect fertility. Interestingly,

examination of nasal cilia may facilitate clinical diagnosis of infertility, specifically in males whose spermatozoa have lowered motility and abnormal function.

ACKNOWLEDGEMENTS

We thank the patient and volunteers who acted as controls in this study. We also thank Dr Tara Andersen at the Royal Hobart Hospital, Tasmania, for performing the nasal brushings and IVF laboratory staff at the St Helen's Private Hospital, Tasmania, for their assistance.

REFERENCES

AFZELIUS, B.A., 1976: A human syndrome caused by immotile cilia. *Science* 193: 317–319.

AFZELIUS, B.A., 1998: Immotile cilia syndrome: past, present, and prospects for the future. *Thorax* 53: 894–897.

AFZELIUS, B.A., 1999: Asymmetry of cilia and of mice and men. *International Journal of Developmental Biology* 43: 283–286.

AFZELIUS, B.A. & ELAISSON, R., 1983: Male and female infertility problems in the immotile-cilia syndrome. *European Journal of Respiratory Disease* 64: 144–147.

AFZELIUS, B.A., ELIASSON, R., JOHNSEN, O. & LINDHOLMER, C., 1975: Lack of dynein arms in immotile human spermatozoa. *Journal of Cell Biology* 66: 225–232.

ARDEN, G.B. & FOX, B., 1979: Increased incidence of abnormal nasal cilia in patients with retinitis pigmentosa. *Nature* 279: 534–536.

BRYAN, J.H.D., 1983: Abnormal cilia in a male-sterile mutant mouse. *Virchows Archiv* 400: 77–86.

BUSH, A., COLE, P., HARIRI, M., MACKAY, I., PHILLIPS, G., O'CALLAGHAN, C., WILSON, R. & WARNER, J.O., 1998: Primary ciliary dyskinesia: diagnosis and standards of care. *European Respiratory Journal* 12: 982–988.

CORBEEL, L., CORNILLIE, F., LAUWERYNS, J., BOEL, M. & VAN DEN BERGHE, G., 1981: Ultrastructural abnormalities of bronchial cilia in children with recurrent airway infections and bronchiectasis. *Archives of Disease in Childhood* 56: 929–933.

DE LONGH, R. & RUTLAND, J., 1995: Ciliary defects in healthy subjects, bronchiectasis, and primary ciliary dyskinesia. *American Journal of Respiratory and Critical Care Medicine* 151: 1559–1567.

DENTLER, W. & WITMAN, G., 1995: Cilia and flagella. *Methods in Cell Biology* 47. Academic Press, San Diego.

EL-SAYED, Y., AL-SARHANI, A. & AL-ESSA, A.R., 1997: Otological manifestations of primary ciliary dyskinesia. *Clinical Otolaryngology and Allied Sciences* 22: 266–270.

FOX, B., BULL, T.B. & OLIVER, T.N., 1983: The distribution and assessment of electron-microscopic abnormalities of human cilia. *European Journal of Respiratory Disease* 64: 11–18.

GREENSTONE, M.A., DEWAR, A. & COLE, P.J., 1983: Ciliary dyskinesia with normal ultrastructure. *Thorax* 38: 875–876.

HERZON, F.S., 1983: Nasal ciliary structural pathology. *Laryngoscope* 93: 63–67.

HOLZMANN, D., OTT, P.M. & FELIX, H., 2000: Diagnostic approach to primary ciliary dyskinesia: a review. *European Journal of Pediatrics* 159: 95–98.

HOUTMEYERS, E., GOSSELINK, R., GAYAN-RAMIREZ, G. & DECRAMER, M., 1999: Effects of drugs on mucous clearance. *European Respiratory Journal* 14: 452–467.

JOHNSEN, O., ELIASSON, R. & ABDEL KADER, M.M., 1974: Effects of caffeine on the motility and metabolism of human spermatozoa. *Andrologia* 6: 53.

KNOLL, M. & TALBOT, P., 1998: Cigarette smoke inhibits oocyte cumulus complex pick-up by the oviduct *in vitro* independent of ciliary beat frequency. *Reproductive Toxicology* 12: 57–68.

LEVISON, H., MINDORFF, C.M., CHAO, J., TURNER, J.A.P., STURGESS, J.M. & STRINGER, D.A., 1983: Pathophysiology of the ciliary motility syndromes. *European Journal of Respiratory Disease* 64: 78–90.

MA, W., KORNGREEN, A., UZLANER, N., PRIEL, Z. & SILBERBERG, S.D., 1999: Extracellular sodium regulates airway ciliary motility by inhibiting a P2X receptor. *Nature* 400: 894–897.

MYGIND, N. & PEDERSEN, M., 1983: Nose-, sinus- and ear-symptoms in 27 patients with primary ciliary dyskinesia. *European Journal of Respiratory Disease* 64: 96–101.

NELSON, S., MASON, C.M., KOLLS, J. & SUMMER, W.R., 1995: Pathophysiology of pneumonia. *Clinics in Chest Medicine* 16: 1–12.

NIELSEN, M.H., PEDERSEN, M., CHRISTENSEN, B. & MYGIND, N., 1983: Blind quantitative electron microscopy of cilia from patients with primary ciliary dyskinesia and from normal subjects. *European Journal of Respiratory Disease* 64: 19–30.

PIECKOVA, E. & JESENSKA, Z., 1998: Molds on house walls and the effect of their chloroform-extractable metabolites on the respiratory cilia movement of one-day-old chicks *in vitro*. *Folia Microbiologica* 43: 672–678.

ROSSMAN, C.M., FORREST, J.B., LEE, R.M.K.W., NEWHOUSE, A.F. & NEWHOUSE, M.T., 1981: The dyskinetic cilia syndrome: abnormal ciliary motility in association with abnormal ciliary ultrastructure. *Chest* 80: 860–863.

ROSSMAN, C.M., LEE, R.M.K.W., FORREST, J.B. & NEWHOUSE, M.T., 1983: Nasal cilia in normal man, primary ciliary dyskinesia: analysis of motility and ultrastructure. *European Journal of Respiratory Disease* 64: 64–70.

RUTLAND, J., DEWAR, A., COX, T. & COLE J., 1982: Nasal brushing for the study of ciliary ultrastructure. *Journal of Clinical Pathology* 35: 357–359.

SANTAMARIA, F., DE SANTI, M.M., GRILLO, G., SARNELLI, P., CATERINO, M. & GRECO, L., 1999: Ciliary motility at light microscopy: a screening technique for ciliary defects? *Acta Paediatrica* 88: 853–857.

SLEIGH, M.A., 1983: Kartagener's syndrome, ciliary defects and ciliary function. *European Journal of Respiratory Disease* 64: 157–161.

SPURR, A.R., 1969: A low-viscosity epoxy resin embedding medium for electron microscopy. *Journal of Ultrastructure Research* 26: 31–43.

STURGESS, J.M. & TURNER, J.A.P., 1990: The Immotile Cilia Syndrome. In V. Chernick (Ed.): *Kendig's Disorders of the Respiratory Tract in Children.* 5th edn. W.B. Saunders Company, Philadelphia: 675–768.

TAKASAKA, T., SATO, M. & ONODERA, A., 1980: Atypical cilia of the nasal mucos. *Annals of Otolaryngology* 89: 37–45.

TOREMALM, N.G., 1983: What can we learn about ENT diseases from Kartagener's syndrome? *European Journal of Respiratory Disease* 64: 148–150.

TSANG, K.W.T., TIPOE, G., SUN, J., HO, J.C.M., LAM, B., ZHENG, L., OOI, G.C., IP, M. & LAM, W., 2000: Severe bronchiectasis in patients with 'cystlike' structures within the ciliary shafts. *American Journal of Respiratory and Critical Care Medicine* 161: 1300–1305.

WRIGHT, A., 1982: Giant cilia in the human organ of corti. *Clinical Otolaryngology and Allied Sciences* 7: 193–199.

ZAHM, J.M., PIERROT, D., HINNRASKYK, J., FUCHEY, C., CHEVILLARD, M., GAILLARD, D. & PUCHELLE, E., 1990: Functional activity of ciliated outgrowths from cultured human nasal and tracheal epithelia. *Biorheology* 27: 559–565.

(accepted 2 February 2004)

A CRETACEOUS PHONOLITE DYKE FROM THE TOMAHAWK RIVER, NORTHEAST TASMANIA

by J. L. Everard, F. L. Sutherland and H. Zwingmann

(with 11 tables, 13 text-figures and six plates)

EVERARD, J. L., SUTHERLAND, F. L. & ZWINGMANN, H., 2004 (29.x): A Cretaceous phonolite dyke from the Tomahawk River, northeast Tasmania. *Papers and Proceedings of the Royal Society of Tasmania* 138: 11–33. ISSN 0080–4703. Tasmanian Geological Survey, Mineral Resources Tasmania, PO Box 56, Rosny Park, Tasmania 7018, Australia (JLE*); Geodiversity Research Centre, Australian Museum, 6 College Street, Sydney, New South Wales 2010, Australia (FLS); CSIRO Division of Petroleum Resources and Centre of Excellence in Mass Spectrometry, School of Applied Geology, Curtin University, Western Australia 6102, Australia (HZ). *Author for correspondence.

Field mapping and ground magnetics indicate that a phonolite dyke, which intrudes Devonian granite in the upper Tomahawk River area, Tasmania, is 3.2 km long and shallowly west-dipping with a true thickness of 10–15 m. The rock contains microphenocrysts of anorthoclase, sparse fayalitic olivine and low-Ti magnetite, and rare biotite in a groundmass of aligned alkali feldspar laths, with interstitial clinopyroxene (hedenbergite to aegirine), amphibole (either hastingsite or arfvedsonite), sodalite, nepheline, analcime and accessory apatite. It is peralkaline and exceptionally strongly evolved, even for phonolites, with very low TiO_2, MgO and CaO, and high Na_2O and incompatible elements. However, relatively high Sr and Ba and the absence of a negative Eu anomaly suggest little feldspar fractionation in its petrogenesis. Its Late Cretaceous age (K/Ar 80.4 ± 1.6 Ma, $^{40}Ar/^{39}Ar$ plateau 75.8 ± 0.3 Ma, $^{40}Ar/^{39}Ar$ total fusion 76 ± 3.1 Ma) and geochemistry are unique for Tasmania and it represents a newly recognised, although very minor, igneous episode. It may be related to a change in dynamic regime following continental rifting, the opening of the Tasman Sea and the subsidence of Bass Basin.
Key Words: phonolite, peralkaline rocks, pyroxenes, amphiboles, arfvedsonite, K/Ar dating, $^{40}Ar/^{39}Ar$ dating, Cretaceous, Tasmania.

INTRODUCTION

Phonolites are felsic, volcanic or hypabyssal igneous rocks which, despite their relatively high SiO_2 content, are undersaturated in silica because of their very high alkali content ($Na_2O + K_2O$). Their most voluminous development is in and around the East African Rift Valley (e.g., Lippard 1973, Price *et al.* 1985). Elsewhere they are relatively uncommon and usually subordinate to associated mafic rocks. There are well-documented Cainozoic examples in other continental settings, usually also related to rifting, such as the Rhine Graben (e.g., Wörner & Schmincke 1984a, b), the Massif Central of France (Wilson *et al.* 1995) and the McMurdo Volcanic Province, which includes Mt Erebus, Antarctica (Kyle 1981, Kyle *et al.* 1992). Recently studied intra-plate oceanic examples occur on Tristan da Cunha (Le Roex *et al.* 1990), Tenerife (Ablay *et al.* 1998), Fernando de Noronha and Trinidade (Weaver 1990), Rarotonga (Thompson *et al.* 2001), Kaula, Hawaii (Garcia *et al.* 1986) and McDonald Island, Southern Ocean (Quilty & Wheller 2000). These are associated with ocean island basalts (OIB) and, together with the McMurdo Volcanic Province, appear to be related to upwelling mantle plumes ("hotspots"). Phonolites are rare in subduction-related or orogenic environments (e.g., Keller 1983, Sorensen 1974).

There are limited occurrences of phonolite, of Jurassic to Late Cainozoic age, in eastern Australia (Ewart *et al.* 1985, Knutson 1989, Sutherland *et al.* 1996). They have not been recorded previously in Tasmania, although feldspathoidal syenite, their approximate plutonic equivalent, is a subordinate component of the Cretaceous Cygnet alkaline complex (Edwards 1947, Ford 1983, Taheri & Bottrill 1999). A plug of Cainozoic basalt at Droughty Point near Hobart contains small (≤ 40 mm) coarse-grained late-stage segregations, some of which approach mafic phonolite in composition (Sutherland 1976).

PREVIOUS WORK

Baillie (1972) reported outcrops of dark green "lamprophyre" at three localities (EQ641638, EQ638646, EQ636652 (grid references refer to 1:25,000 Monarch (5646) and 1:100,000 Cape Portland (8416) topographic sheets; datum is AGD66) in the valley of the Tomahawk River, about 9–12 km south of Tomahawk township. They were thought to indicate a NNW-trending post-granitic dyke of unknown length but not more than 6 m wide. The rock was described as consisting of phenocrysts (25%) of oriented albite (80%), olivine (15%), lamprobolite amphibole (4%) and pyrite (1%) in an extremely fine-grained panidiomorphic granular groundmass containing a faintly green mineral, possibly actinolite.

On the Boobyalla 1:50,000 geological map (Baillie *et al.* 1978), the dyke is labelled "Ca?", a unit also used for Cretaceous appinitic rocks near Cape Portland (Jennings & Sutherland 1969). The dyke is shown as extending for about 1.5 km, partly concealed by Quaternary alluvium, with another small exposure 1.5 km further north, slightly offset to the east (EQ635664).

The local country rock is granite, comprising the Poimena and Little Mt Horror plutons of the Blue Tier Batholith (figs 1, 2; Groves 1977). Probably the most reliable published radiometric date from the Poimena pluton is a Rb-Sr mineral isochron of 379 ± 3 Ma (Middle Devonian) (McKenzie *et al.* 1988), although an unpublished SHRIMP U-Pb zircon age is about 5 Myr older (L. P. Black pers. comm.). On the

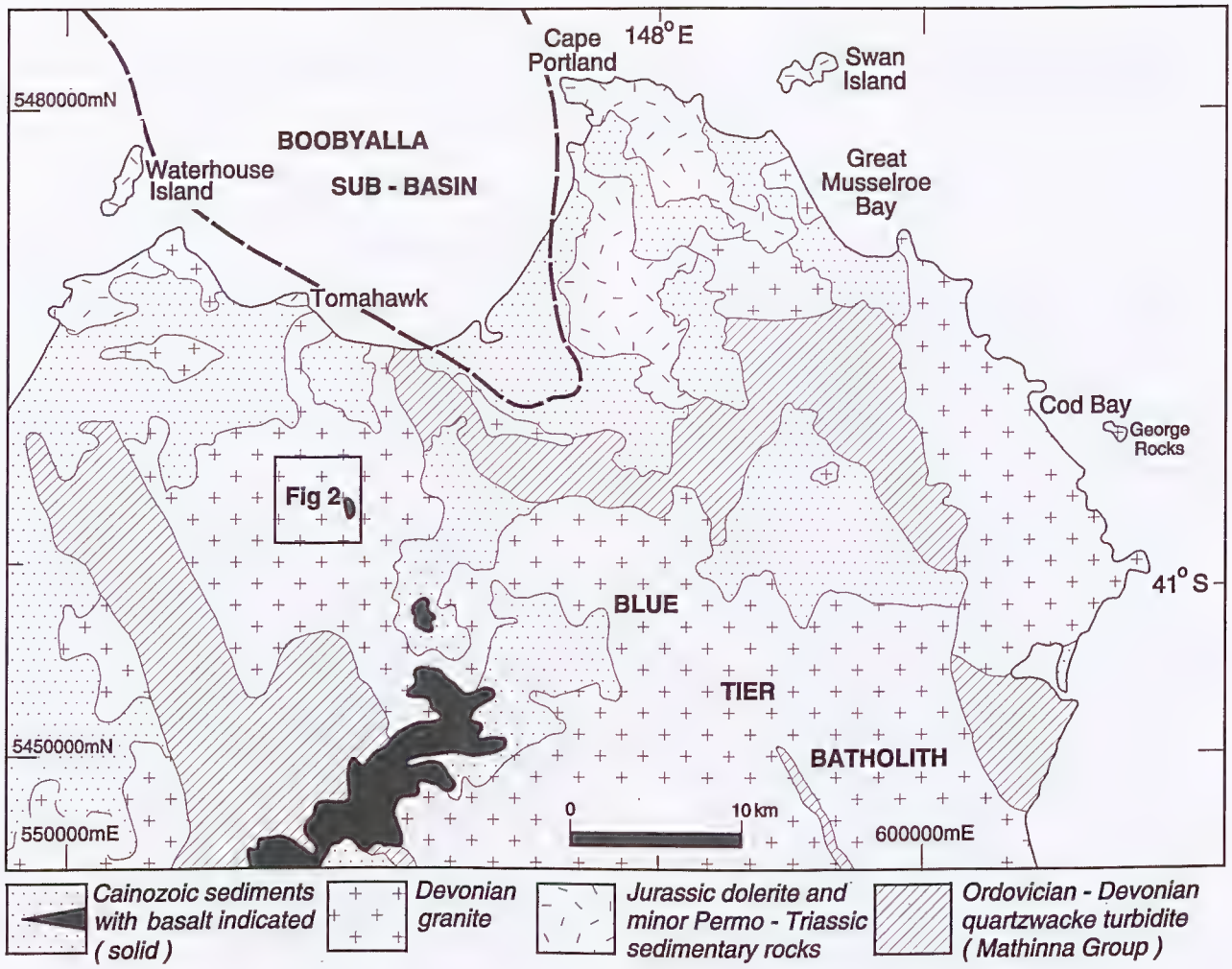

FIG. 1 — Simplified geology of part of northeast Tasmania showing location of Tomahawk River dyke and localities mentioned in text.

basis of intrusive relationships, the Little Mt Horror pluton is thought to be slightly younger than the Poimena pluton (Baillie 1972, McClenaghan *et al.* 1982).

FIELD RELATIONS AND GEOPHYSICS

The phonolite is a tough, dark bluish- to greenish-grey, fine-grained, massive aphanitic rock with locally well-developed platy jointing. Eight samples collected for petrological examination (table 1) are registered and stored at Mineral Resources Tasmania, Mornington.

The dyke can be traced along strike for about 3.2 km and has a slightly arcuate NNW to northerly trend (fig. 2). Its most southerly exposure is on the west bank of the Tomahawk River (EQ64106364), beyond which only granite was encountered. To the north, the dyke largely forms float on a series of low rocky knolls in rough pasture and light forest. In small cliffs just west of the river (EQ63376572), a steep western contact with fine-grained granite is exposed; here the dyke is about 20 m wide. About 400 m further north (near 63406620) a fault may offset the dyke dextrally by about 100 m, but outcrop is poor and a change in strike is possible. The dyke re-appears immediately west of a small gorge in the river (EQ63516633), and scattered float and rubbly outcrop continue for a further 400 m to EQ63476672.

The phonolite has a moderately high mean magnetic susceptibility of about 5.35 x 10^{-3} SI units (table 1) but it is not apparent on images of the area derived from regional aeromagnetic data (BMR, 1985). However, this survey had a 1.5 km line spacing and a 150–1000 m terrain clearance, probably inadequate to resolve any associated anomaly.

In order to constrain the dimensions and orientation of the body, six ground magnetometer traverses were measured across its southern segment, roughly perpendicular to strike (fig. 2). Survey details, data and interpretation are described in detail by Everard (2004).

The two northern profiles (A–A' and B–B') each contain an asymmetric anomaly peaking at about 60 nT above the local regional field, accompanied by a smaller negative anomaly to the east. They are easily modelled by a dipping dyke with a true thickness of 10–15 m, dipping west at 18–31° and extending very close to the surface. Profile D–D' is similar but was not modelled due to distortion of the field by several wire fences.

Profile C-C' defines a much broader and more subdued (15 nT) anomaly, consistent with a dyke dipping west at about 30°. It may have a maximum true thickness of about 13 m at a depth of 40 m, tapering out both downward and within about 2 m of the surface.

Profile E–E' is complex with several distinct peaks of up to about 50 nT spread out over an east-west distance of about 120 m, accompanied by a distinct negative anomaly to the

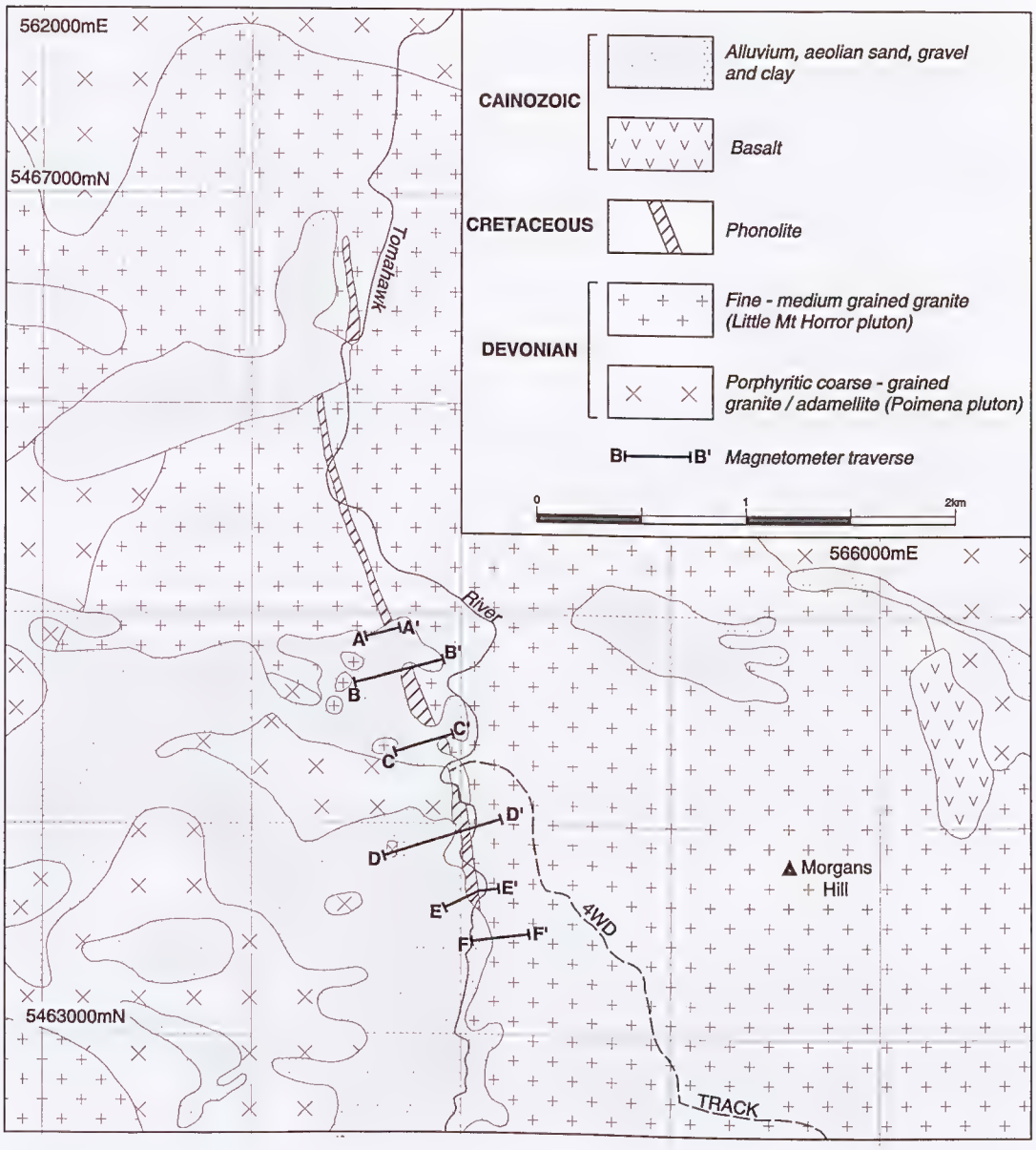

FIG. 2 — Detailed geology of upper Tomahawk River area (modified after Baillie et al. *1978) showing phonolite dyke and location of magnetometer traverses.*

TABLE 1
Sample locations and physical properties

Field no.	Reg. no.	metres E	metres N	Magnetic susceptibility ($x10^{-3}$ SI)				Density
		datum:AGD66		N	mean	min.	max	t/m^3
PHN[a]	C108641	563640	5465010					
PHS[a,b]	C108642	563770	5464660					
CPJ32[a,b]	R006569	564100	5463640	10	5.64	4.85	6.53	2.642
CPJ33[a]	R006570	564110	5463690					
CPJ38	R004373	563770	5464630					
CPJ39	R004374	563510	5465380					
CPJ40	R004375	563510	5466440	10	6.19	5.22	7.44	2.628
CPJ41[a]	R004376	563350	5465990	20	4.78	2.45	6.31	2.605

[a] mineral (electron microprobe) analyses (tables 4–10)

[b] whole rock analyses (table 11)

west. Modelling suggests that here the main dyke may be split into five sub-parallel splays, none more than about 10 m thick, each dipping west at about 30°. These may taper and pinch out southward, as profile F–F', about 200 m south of the southernmost phonolite outcrop, contains two small overlapping positive anomalies of about 12 nT and 8 nT, consistent with two thin (3–4 m) west-dipping dykes concealed by about 10 m of overburden.

GEOCHRONOLOGY

K-Ar Analysis

The selected sample CPJ32, with least alteration of K-bearing phases, was ground to 750 µm. K contents were determined by atomic absorption (Varian AA20), following procedures after Heinrichs & Herrmann (1990). The pooled error of duplicate K determinations and standards is better than 2%. K-Ar isotope determinations followed Bonhomme *et al.* (1975) and spiked isotopes were measured in a high sensitivity VG 3600 noble-gas mass spectrometer. The ^{38}Ar spike was calibrated against biotite GA1550 (95.5 Ma, McDougall & Roksandic 1974) together with measurements of standards (LP-6, HD-B1, GLO and GA 1550) and mass discrimination factors (airshots). Errors for Ar analysis were <1% and ^{40}Ar/^{36}Ar values for airshots were 293.39 ± 0.29 (2σ). The result with 2σ error (table 2) used ^{40}K abundances and decay constants recommended by Steiger & Jäger (1977).

^{40}Ar–^{39}Ar analysis

A detailed account of the ^{40}Ar-^{39}Ar dating technique (McDougall & Harrison 1999) underpins the dating presented here. A concentrate of separated feldspar from the rock was cleaned before wrapping in aluminium foil for loading into an aluminium package, along with biotite standard HD-B1 (24.21 ± 0.32 Ma, Hess & Lippolt 1994) to monitor the neutron flux gradient. The package was Cd-shielded and fast neutron irradiated in the McMaster University Nuclear Reactor, Hamilton, Canada, for 28.4 hours.

For infra-red laser step-heating, the mineral separate was loaded onto an aluminium palette and baked within an ultra-high vacuum laser sample chamber to 120°C overnight to remove absorbed atmospheric argon. A 110 W Spectron Laser systems continuous wave Nd-Y-Al-garnet (= λ1064 nm) laser was used to laser step treat the sample.

Gas cleanup and mass spectrometry removed active gases using Zr-Al getter pumps and the remaining noble gases were equilibrated into a Mass Analyser Product 215-50 static mass spectrometer with a Balzers multiplier detector. The Ar sensitivity of the ms multiplier detector was 2.71 x 10^{-10} cm^3/Volt. A Lab View program was used to measure isotope peak masses from 35–41 (10 times) in sequence lasting ~15 minutes, via a peak hopping routine. Blank analyses were run before and after.

Age calculation involved extrapolating peak intensities back to the inlet time and correcting for extraction line blanks, ms backgrounds, ms discrimination (^{40}Ar/^{36}Ar ratio of 281.0) and reactor interferences. The Ca and K correction factors in the data reduction were ^{39}Ar/^{37}Ar$_{Ca}$ = 0.00065, ^{36}Ar/^{37}Ar$_{Ca}$ = 0.000255 and ^{40}Ar/^{36}Ar$_K$ = 0.0015). Errors quoted are 1σ and Ar-Ar ages were calculated using decay constants of Steiger & Jäger (1977). Weighted mean ages were calculated (2σ errors) using the Ludwig (2001) Isoplot program (fig. 3).

TABLE 2
K-Ar analysis

Sample	%K (duplicate)	^{40}Ar[a] (x10^{-3} mol/g)	^{40}Ar/^{40}Ar$_{total}$	Age (Ma)	Error (±2δ)
CPJ32	3.31	4.720	0.927	80.40	1.60

[a] Denotes radiogenic argon.
Constants: ^{40}K = 0.01167 atom 96; λβ = 4.962, λε = 0.581 x 10^{-10}y^{-1}

Results

The K-Ar results (table 2) give an age of 80.40 ± 1.60 Ma. The Ar-Ar analysis (table 3, fig. 3) gives a weighted mean age of 75.77 ± 0.32 Ma from steps 4–5 (lowest-Ca steps and highest ^{40}Ar *yields) and a total fusion age of 76 ± 3.1 Ma. There was evidence of mixing with a Ca-rich phase in the feldspar separate. The total fusion Ar-Ar and K-Ar age are within error and with the weighted mean Ar-Ar age confirm a Late Cretaceous age for the phonolite crystallisation, with age limits between 75 and 81 Ma. On recent time-scales (e.g., Young & Laurie 1996) this is within the Campanian (73–83 Ma).

PETROGRAPHY

In thin section (pls 1–6), the samples are similar. Most are slightly porphyritic (pl. 1) to seriate (pl. 2), with microphenocrysts of anorthoclase (≤ 1.5 mm but commonly 500 µm–1 mm long) grading down in grain size to a usually pilotaxitic groundmass. Sparse to rare, usually corroded microphenocrysts include fayalite (≤ 0.1–1.0% by volume), magnetite (c. 0.3–1%) and rare biotite. These minerals are rare in the groundmass, probably due to a reaction relationship with it (pls 3, 4, 5).

The groundmass (pls 5, 6) consists of flow-aligned laths (commonly 50–100 µm long) of alkali feldspar (mainly anorthoclase), small platelets and prisms of clinopyroxene (hedenbergite to aegirine) and amphibole (hastingsite and/or arfvedsonite), together with interstitial sanidine, feldpathoids, zeolites, minor pale brown, slightly turbid glass, accessory apatite, and sometimes traces of biotite.

Electron microprobe analyses (see below) and X-ray diffraction of powdered samples indicate that the feldspathoids are nepheline and sodalite. The main zeolite is analcime, with substantial natrolite in CPJ39. Their identification is supported by the disappearance of their diffraction peaks after treatment of the powders with dilute HCl, which dissolves these minerals (R. N. Woolley, pers. comm.). Reconnaissance scanning electron microscope work (R. S. Bottrill) suggests the presence of small amounts of a Na-Ca silicate, possibly pectolite, as minute grains in one sample (PHS). The presence of pyrite, reported in the dyke by Baillie (1972), has not been substantiated.

There are small variations between samples in the abundance of feldspar microphenocrysts, groundmass

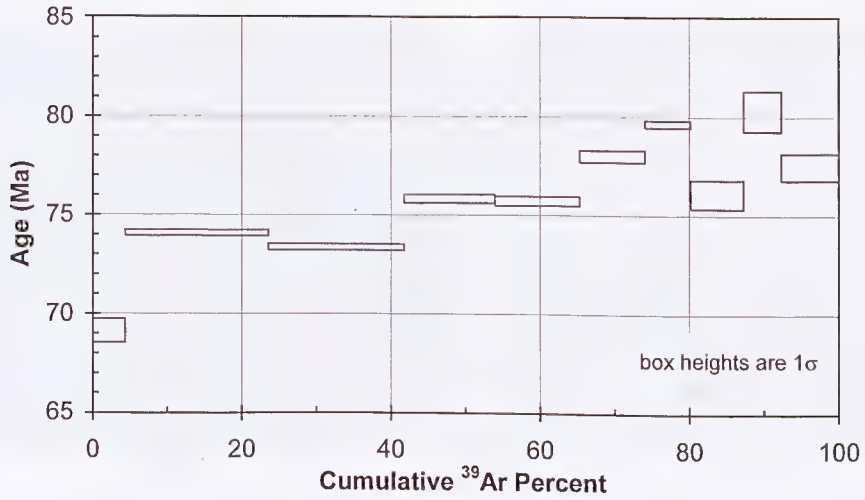

FIG. 3 — Step heating age spectrum (apparent age versus cumulative ^{39}Ar released) for ^{40}Ar/^{39}Ar analysis, Tomahawk phonolite sample CPJ32.

TABLE 3
^{40}Ar-^{39}Ar analysis, Tomahawk River phonolite; sample 412 (K-feldspar from sample CPJ32)

Step	Age (Ma)	^{40}Ar*/^{39}Ar	^{40}Ar/^{39}Ar	^{38}Ar/^{39}Ar	^{37}Ar/^{39}Ar	^{36}Ar/^{39}Ar	^{39}Ar (10^{-12}cm^3)	40Ar* (%)
1	69.13±0.69	5.90±0.05	7.49±0.01	0.01287±0.00035	0.06238±0.00417	0.00539±0.00017	77.74±0.06	78.7
2	74.08±0.39	6.33±0.01	7.08±0.01	0.01299±0.00011	0.04164±0.00095	0.00539±0.00004	342.45±0.22	89.3
3	73.36±0.39	6.26±0.01	6.79±0.01	0.01532±0.00008	0.03488±0.00100	0.00178±0.00004	324.82±0.24	92.2
4	75.83±0.43	6.48±0.02	6.97±0.01	0.01363±0.00012	0.02630±0.00067	0.00167±0.00006	218.22±0.16	92.9
5	75.72±0.44	6.47±0.02	6.88±0.01	0.01335±0.00013	0.02598±0.00143	0.00139±0.00007	204.05±0.16	94.0
6	78.00±0.48	6.67±0.03	7.26±0.01	0.01390±0.00017	0.02833±0.00186	0.00199±0.00009	156.00±0.09	91.9
7	79.64±0.43	6.81±0.02	7.33±0.02	0.01392±0.00013	0.02709±0.00006	0.00174±0.00000	108.85±0.24	93.0
8	76.08±0.82	6.50±0.06	7.38±0.01	0.01415±0.00024	0.05120±0.00230	0.00298±0.00021	126.75±0.08	88.1
9	80.31±1.09	6.87±0.09	7.49±0.01	0.01360±0.00030	0.04923±0.00972	0.00210±0.00030	89.96±0.08	91.7
10	77.47±0.78	6.62±0.06	7.44±0.02	0.01256±0.00020	0.03444±0.00672	0.00276±0.00020	137.22±0.27	89.0

Total fusion age = 75.96 ± 3.10 Ma
Irradiation standard used = HD-B1 biotite (24.21 ± 0.32 Ma)
J value = 0.006510 ± 0.000032
1σ errors
Weighted mean age (steps 4–5) = 75.77 ± 0.60 Ma (2σ)

grain-size, development of flow lamination and degree of alteration (especially of feldspar). In particular, CPJ38 and CPJ39 (pl. 3) are aphyric and relatively coarse-grained with randomly oriented feldspars (typically 400–600 µm x 50–100 µm), and may be slower-cooled rocks from near the centre of the dyke.

MINERALOGY AND MINERAL CHEMISTRY

Minerals from five polished thin sections were analysed using the Cameca SX-50 electron microprobe at the University of Tasmania. Representative analyses and calculated cation formulae are given in tables 4–10 and full data by Everard (2004).

The amphibole arfvedsonite is a new mineral species for Tasmania, although there is a very old and spurious record from Swan Island (Anon 1970).

Olivine (fayalite)

Pale yellow fayalite occurs sometimes as equant to oblong euhedral microphenocrysts (≤1 mm) (pls 1, 2) with slightly corroded, ragged margins, but commonly as deeply-embayed subhedra (typically 400–500 µm) (pls 2, 4) or anhedral granules (c. 100 µm) (pl. 3). Some of the larger microphenocrysts contain inclusions of apatite, as rod-like laths (up to 100 x 15 µm) and hexagonal sections (up to 120 µm across). In some samples, fayalite is altered to orange to amber-coloured fibrous alteration products (CPJ33) or dark red-brown "iddingsite" (PHS).

Analyses (table 4, fig. 4) are near-stoichiometric with significant MnO (≤4.25%) and MgO (≤3.83%) but a narrow compositional range ($Fa_{86.3\text{-}89.0}$ $Fo_{4.4\text{-}9.2}$ $Jo_{3.6\text{-}6.0}$). The CaO contents (0.28–0.59%) are those of low pressure, volcanic olivine (≥0.10%) rather than plutonic olivine (≤0.10%)(Simkin & Smith 1970).

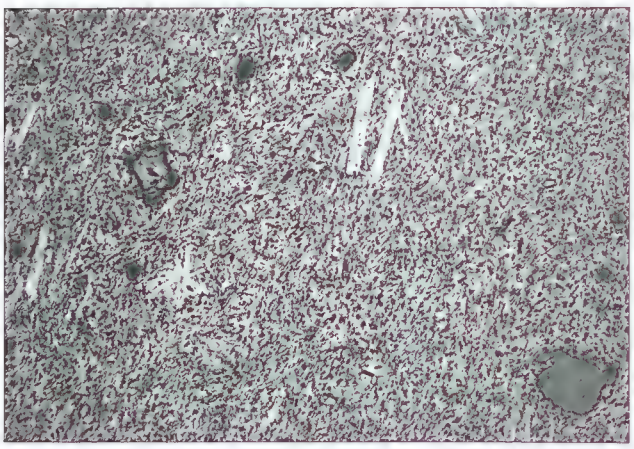

PLATE 1

Photomicrograph of phonolite (PHS), showing porphyritic texture with microphenocrysts of fayalite (left), anorthoclase (e.g., upper centre) and corroded biotite (lower right) in a fine-grained pilotaxitic groundmass (plane polarised light, field of view 4.5 x 3.4 mm).

PLATE 2

Photomicrograph of phonolite (CPJ32), showing porphyritic to seriate texture with microphenocrysts of fayalite (upper left, centre bottom, lower right), magnetite (lower right) and anorthoclase grading to the groundmass (plane polarised light, field of view 4.5 x 3.4 mm).

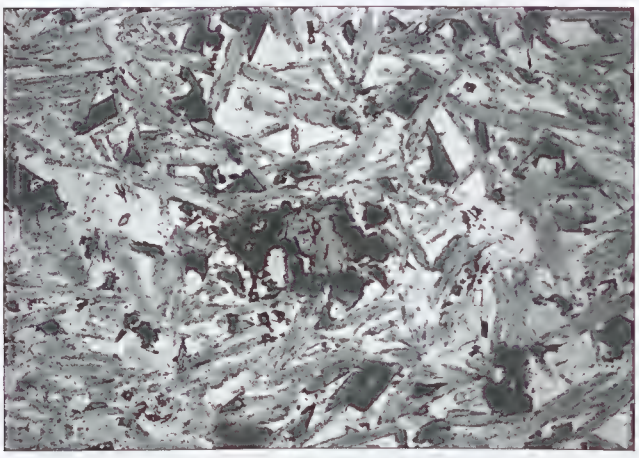

PLATE 3

Photomicrograph of phonolite (CPJ39), showing aphyric, relatively coarse-grained texture of mainly pyroxene and amphibole (dark), turbid alkali feldspar (grey) and interstitial feldspathoids and zeolites (clear). A central corroded fayalite grain has a narrow reaction rim of biotite and magnetite (plane polarised light, field of view 4.5 x 3.4 mm).

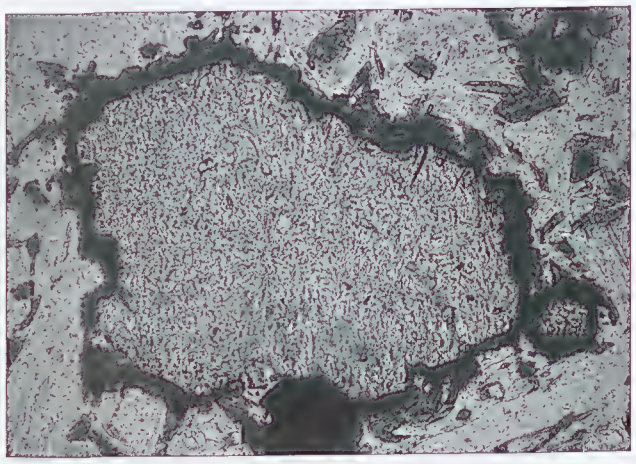

PLATE 4

Photomicrograph of phonolite (CPJ32) showing a corroded fayalite microphenocryst and abutting small magnetite microphenocryst (bottom), with narrow reaction rims of biotite (plane polarised light, field of view 730 x 550 µm).

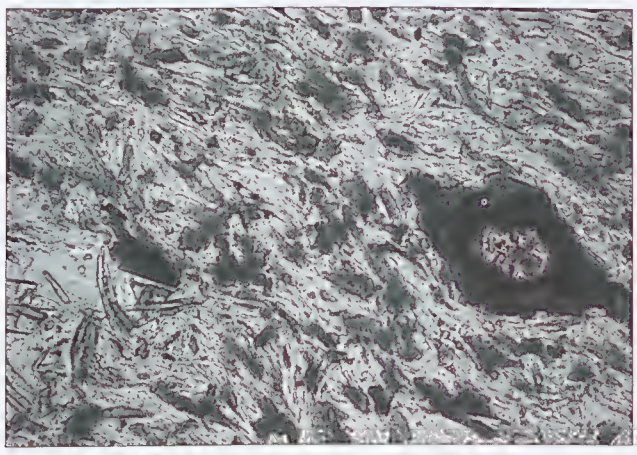

PLATE 5

Photomicrograph of phonolite (PHS) groundmass, showing aligned alkali feldspar laths with prisms of aegirine (grey) and arfvedsonite (dark grey, e.g., centre left). A fayalite granule (centre right) has a reaction rim of arfvedsonite (plane polarised light, field of view 730 x 550 µm).

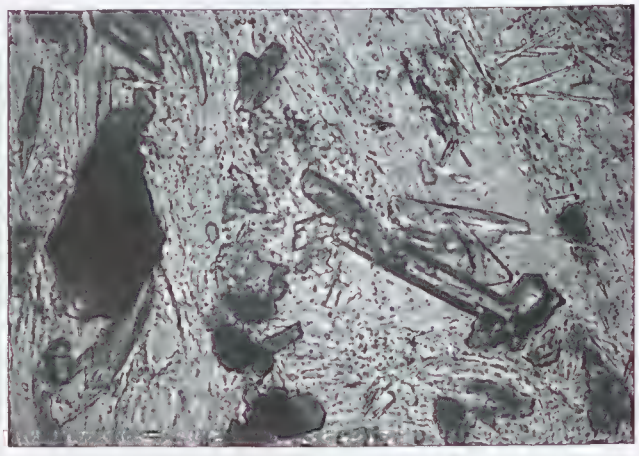

PLATE 6

Photomicrograph of phonolite (PHS) groundmass, showing prisms and sections of arfvedsonite (dark, e.g., left) and aegirine (e.g., centre right) with feldspars, feldspathoids, zeolite and acicular apatite (e.g., upper left)(plane polarised light, field of view 280 x 210 µm).

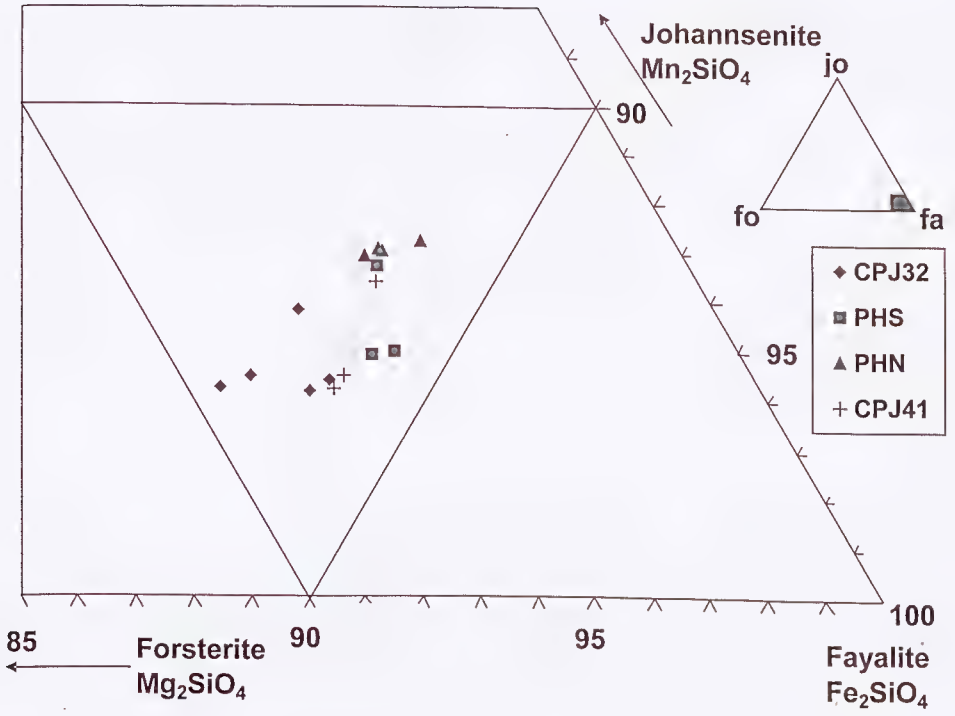

FIG. 4—Electron microprobe analyses of olivine (fayalite) phenocrysts, plotted in the plane Mg_2SiO_4 (forsterite)–Fe_2SiO_4 (fayalite)–Mn_2SiO_4 (johannsenite); small amounts of Ca_2SiO_4 component are included with Mn_2SiO_4.

TABLE 4
Representative mineral analyses: olivine (fayalite) phenocrysts

Sample	CPJ32	PHS	PHN
Analysis	R1/1	R7/4	R5/1
SiO_2	30.40	29.87	29.52
TiO_2	–	0.03	0.01
Cr_2O_3	0.02	0.01	–
FeO	63.34	64.16	63.20
MnO	2.75	3.21	4.18
NiO	0.07	–	–
MgO	3.83	2.42	1.78
CaO	0.30	0.31	0.76
Total	100.72	100.02	99.45
Cations calculated on the basis of (O) = 4			
Si	0.995	0.995	0.993
Ti	–	0.001	–
Cr	0.001	–	–
Fe^{II}	1.734	1.787	1.778
Mn	0.076	0.091	0.119
Ni	0.002	–	–
Mg	0.187	0.120	0.089
Ca	0.011	0.011	0.028
Total	3.005	3.004	3.007
Mg#	9.73	6.31	4.77

Magnetite

Opaque microphenocrysts (pls 2, 4) are equant, angular, polygonal (squarish to pseudohexagonal) to irregular or skeletal grains, exceptionally up to 1.5 x 1 mm, but commonly 150–400 μm across. They are identified in reflected light as magnetite, and can be drawn off the powdered samples by a magnet. Some of the larger microphenocrysts contain small (≤50 μm) inclusions of biotite and euhedral apatite. Usually, opaque phases are absent in the groundmass, except for rare small (c. 50 μm) partly oxidised magnetite grains in PHN.

Analyses (table 5) match low-Ti magnetite (TiO_2 ≤6.24%) in which Al_2O_3 (≤3.29%) and MnO (≤0.60%) are minor components. These values correspond to ≤18.0 mole % ulvospinel and ≤4.6 mole % hercynite in solid solution.

Biotite

Biotite is an uncommon mineral in the phonolite, but has three distinct parageneses. All are iron-rich biotites (table 6) with low fluorine (≤0.15%) and chlorine (≤0.13%), with compositions between annite and siderophyllite (fig. 5a).

Biotite microphenocrysts (α, β very dark sepia-brown, γ pale honey-yellow) are rare (< 0.1 %), rounded and corroded, apparently partly resorbed anhedra, up to 700 x 380 μm across (pl. 1). They are iron-rich (Mg# 8.4–18.7) with high tetrahedrally coordinated Al^{iv} (2.44–2.59 cations per formula unit), balanced by substitution of small amounts of Ti (TiO_2 ≤ 1.54%) and Al^{vi} into the octahedral sites. MnO (≤0.54%) and CaO (≤0.28%) are low.

Rare small ragged biotite is present in the groundmass of some samples. Analyses (from PHN) have similar Mg# (9.0–13.4) and Al^{iv} (2.35–2.50 cations/formula unit) to the microphenocrysts but lower TiO_2 (0.53–0.77%) (fig. 5b) and slightly higher MnO (0.60–1.62%) and CaO (≤0.57%).

TABLE 5
Representative mineral analyses: magnetite

Sample	CPJ32	PHS	CPJ33	CPJ41
Analysis	R1/3	R14a/1	m4	R11/2
SiO_2	0.33	0.30	0.33	0.30
TiO_2	4.72	2.24	6.24	1.81
ZrO_2	–	0.08	–	0.06
Al_2O_3	3.17	1.29	3.00	1.87
Cr_2O_3	0.02	0.03	–	0.01
FeO_t	84.98	89.20	82.43	90.04
MnO	0.44	0.59	0.66	0.42
ZnO	0.02	–	0.25	–
MgO	0.19	0.05	0.15	0.03
CaO	0.01	–	0.02	0.01
Total	93.89	93.78	93.09	94.54
cations calculated on the basis of Z = 3, (O) = 4				
Ti	0.135	0.064	0.180	0.052
Zr	–	0.002	–	0.001
Al	0.142	0.058	0.136	0.083
Cr	0.001	0.001	–	–
Fe^{III}	1.588	1.809	1.504	1.811
Fe^{II}	1.109	1.044	1.142	1.037
Mn	0.014	0.019	0.022	0.013
Zn	0.001	–	0.007	–
Mg	0.011	0.003	0.009	0.002
Ca	0.001	–	0.001	–
end-members (mole %)				
$Fe^{II}_2TiO_4$	13.47	6.59	18.00	5.26
$Fe^{II}Al_2O_4$	4.47	0.68	2.98	2.63
$Fe^{II}Fe^{III}_2O_4$	79.41	90.46	75.21	90.56
other	2.65	2.27	3.81	1.55

Fayalite and magnetite microphenocrysts commonly exhibit a narrow (5–10 μm) discontinuous reaction rim of granular biotite (pleochroic from deep orange-brown to almost opaque), surrounded by a concentration of green amphibole and pyroxene which passes into the groundmass (pls 3, 4). The biotite rims are low in TiO_2 (≤0.9%), relatively high in MnO (0.9–1.69%) and similar to groundmass biotite. A biotite inclusion within a magnetite phenocryst in CPJ33 has exceptionally low Mg# (0.70) and relatively high TiO_2 (1.81%).

Resorption of the biotite microphenocrysts suggests disequilibrium with the melt at emplacement. However, they are probably not xenocrysts derived from the granitic country rock, as the phonolite lacks other granite-derived xenocrysts such as quartz or plagioclase. Furthermore, biotites from the Poimena and Little Mount Horror plutons have typically higher Mg# and TiO_2 (2.88–5.55%)(Groves 1977, McClenaghan & Williams 1982). Elsewhere in eastern Tasmania, some alkali feldspar granites contain very iron-rich, low Ti biotites, but these have generally lower tetrahedral Al and contain much more F (0.6–4.2%) (Groves 1977, J. L. Everard unpublished data).

TABLE 6
Representative mineral analyses: biotite

Sample	CPJ32	PHS	CPJ32	CPJ32	CPJ33	PHN
Analysis	R2	R3/1	R3/3	R6/9	R1/2	R5/3
Type	pheno	pheno	rim on mt	rim on fa	incl in mt	gmass
SiO_2	33.24	32.70	33.01	33.01	32.82	32.31
TiO_2	1.66	1.30	0.69	0.35	1.81	0.65
ZrO_2	na	na	0.02	0.08	na	0.03
Al_2O_3	14.44	13.98	11.79	10.32	10.13	11.45
Cr_2O_3	–	0.02	na	na	–	0.02
V_2O_3	0.02	–	na	na	–	na
FeO_t	33.08	36.68	38.84	38.19	40.83	36.99
MnO	0.30	0.51	0.69	1.01	0.54	0.60
ZnO	0.12	0.14	na	na	0.02	na
NiO	0.07	–	na	na	na	–
MgO	4.12	1.89	1.10	1.85	0.16	2.06
CaO	–	0.02	0.04	0.14	0.07	0.08
Na_2O	0.70	0.61	0.75	0.54	0.24	0.43
K_2O	8.46	7.67	7.95	7.71	7.75	7.67
SrO	–	0.08	na	na	–	na
BaO	0.65	0.47	na	na	–	na
F	0.08	0.09	0.01	0.08	0.14	0.15
Cl	0.13	0.11	0.04	0.04	0.01	0.08
O=(F,Cl)	–0.06	–0.06	–0.05	–0.05	–0.06	–0.08
Total	97.06	96.21	95.05	93.28	94.48	92.44
atoms on the basis of (O) = 20, (OH, F, Cl) = 4						
Si	5.414	5.456	5.660	5.764	5.712	5.650
Al^{iv}	2.586	2.544	2.340	2.123	2.079	2.350
Al^{vi}	0.186	0.205	0.037	–	–	0.011
Cr	–	0.002	na	na	–	0.003
V	0.002	–	na	na	–	na
Ti	0.204	0.163	0.089	0.046	0.237	0.085
Zr	na	na	0.001	0.006	na	0.002
Fe as Fe^{II}	4.506	5.118	5.554	5.576	5.944	5.410
Mn	0.041	0.073	0.010	0.149	0.080	0.088
Zn	0.014	0.017	na	na	0.003	na
Ni	0.009	–	na	na	na	–
Mg	1.001	0.470	0.281	0.482	0.042	0.537
Ca	–	0.004	0.008	0.026	0.013	0.015
Na	0.222	0.198	0.247	0.183	0.081	0.146
K	1.758	1.633	1.735	1.716	1.721	1.712
Sr	–	0.008	na	na	–	na
Ba	0.042	0.031	na	na	–	na
F	0.042	0.047	0.053	0.047	0.076	0.085
Cl	0.035	0.032	0.011	0.013	0.004	0.022
(OH)	3.923	3.922	3.936	3.940	3.920	3.893
cation total	15.985	15.920	16.052	16.071	15.912	16.009
Mg#	18.18	8.41	4.82	7.95	0.70	9.03

na – not analysed; pheno – phenocryst; incl – inclusion; gmass – groundmass; mt – magnetite; fa – fayalite.

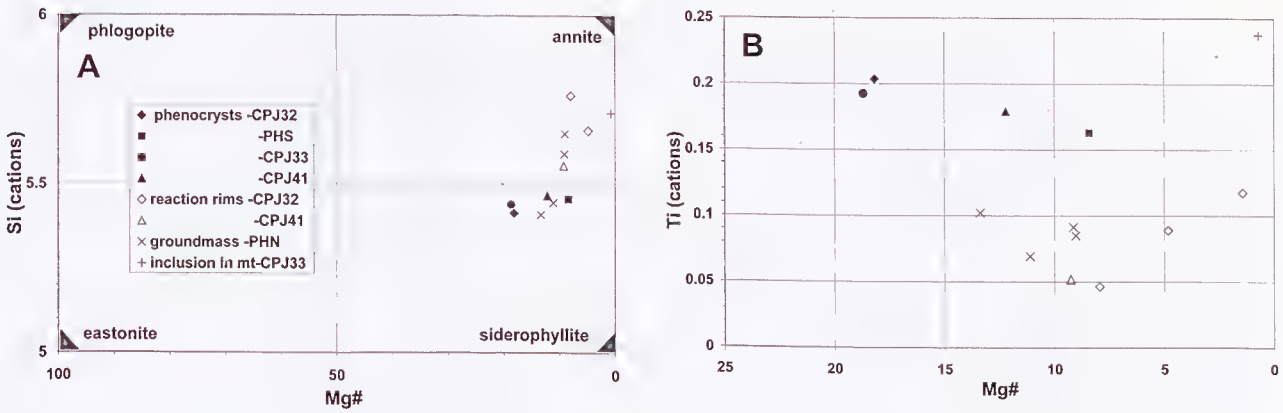

FIG. 5 — Electron microprobe analyses of biotite. (A) Si cations against Mg#, ideal end-member compositions also shown. (B) Ti cations against Mg#.

The biotite microphenocrysts are probably cognate products of fractionating phonolitic magma at depth, and disequilibrium at emplacement may be due to lower pressure. In some samples, biotite re-appeared later as a groundmass phase, probably because crystallisation of sodic amphiboles and pyroxenes had increased K/Na in the residual liquid just prior to solidification.

Feldspars

Both X-ray diffraction and electron microprobe data indicate that two alkali felspars (sanidine and anorthoclase) are present. Simple Carlsbad twinning is ubiquitous and very fine, multiple twinning common, but cross-hatched twinning was not observed. Undulose extinction indicating compositional zoning is common. In some samples, feldspar is turbid and partly altered to fine-grained sericite (pl. 3).

Most of the analysed feldspars (table 7, fig. 6) are anorthoclase ($Or_{10.0-37.6}$) with small amounts of CaO (up to 8.6 mole % anorthite in solid solution). Some have significant BaO (≤2.51%) and SrO (≤1.31%), corresponding to 4.5 mole % celsian (Ba-feldspar) and 3.4 mole % Sr-feldspar, respectively. The remaining analyses are sanidine ($Or_{62.8-91.1}$) with very low CaO, BaO and SrO. All analyses contain minor iron (0.15 - 0.31 % as FeO).

The groundmass of CPJ41 contains small grains of near-stoichiometric celsian, and a grain intermediate between celsian and K-feldspar. Celsian is rare in igneous rocks, and mostly occurs in hydrothermal or contact-metamorphic manganese deposits. Here, it is probably a very late-stage deuteric mineral. Some feldspars plot very close to the albite or K-feldspar end-members, but the analyses are less satisfactory, with high totals and/or significant cation deficiencies. These may have crystallised or been altered during late-stage hydrothermal processes.

Pyroxenes

Small, well-formed, elongate to acicular prisms (typically 20–100 to rarely 400 μm long x 5–20 μm across) of pale yellow to green clinopyroxene are abundant (pl. 6). Analyses (table 8) are recalculated to four cations and Fe distributed to Fe^{III} and Fe^{II} to ensure charge balance (6 oxygens). Although all these pyroxenes are iron-rich with low TiO_2 (≤0.43%) and little or no tetrahedrally coordinated Al, they fall into two groups. The nomenclature follows Morimoto (1988).

Those from CPJ32, and a few from PHN and CPJ33, are relatively calcic (CaO 13.06–19.27%) and are hedenbergites or relatively calcic aegirine-augites (fig. 7). In CPJ32, their pleochroism is α deep green, β pale yellow-green, γ pale yellow-brown.

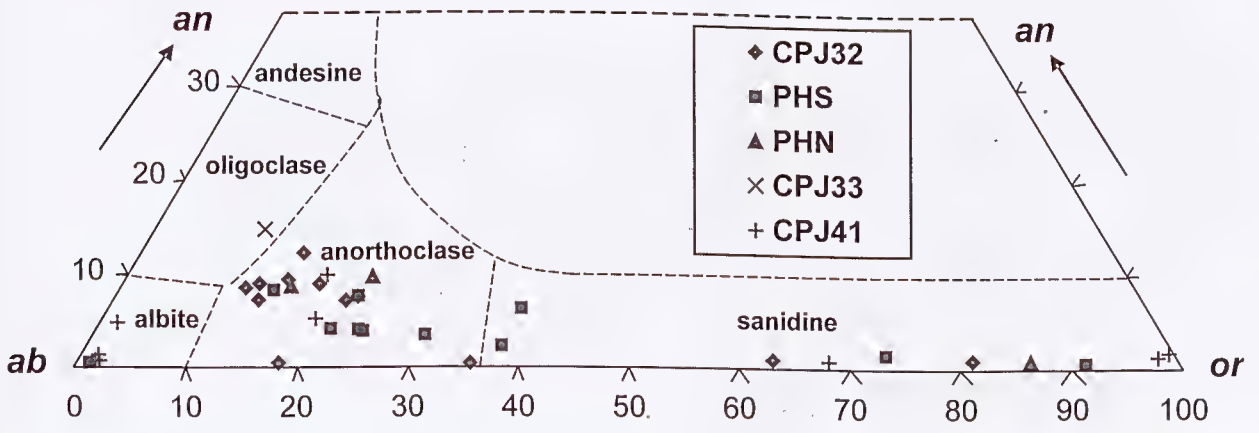

FIG. 6 — Electron microprobe analyses of feldspars, plotted in the system $NaAlSi_3O_8$ (Ab)–$CaAl_2Si_2O_8$ (An)–$KAlSi_3O_8$ (Or). Small amounts of Ba and Sr included with An; celsian (Ba feldspar) analyses not plotted.

TABLE 7
Representative mineral analyses: feldspars, feldspathoids and analcime

Sample	CPJ32	PHS	PHN	CPJ32	PHS	PHN	CPJ41	CPJ32	PHS	CPJ33
Analysis	R1/4	R11/2	R4/3	R9/a	R8/1	R6/7	e1	R11/5	R12/4	R1/6
mineral	anorthoclase			sanidine			celsian	nepheline	sodalite	analcime
SiO_2	66.04	64.18	63.71	65.52	63.96	63.75	31.50	43.39	37.41	56.57
TiO_2	0.02	0.02	–	0.02	–	–	–	–	–	–
Al_2O_3	21.65	19.81	20.03	19.55	18.95	18.29	25.98	32.60	31.49	23.12
FeO	0.28	0.24	0.27	0.15	0.31	0.11	0.25	0.18	0.23	0.06
MgO	–	–	–	–	–	–	0.01	–	–	0.02
CaO	1.28	0.45	0.56	0.05	–	–	0.19	–	0.00	–
Na_2O	8.47	6.46	7.71	4.15	0.98	1.51	0.10	14.89	24.54	13.01
K_2O	2.03	6.46	3.81	10.79	15.69	14.60	0.05	6.48	0.10	0.08
P_2O_5	–	na	na	0.02	–	na	na	na	na	na
SrO	–	0.40	0.76	0.01	–	–	0.04	–	–	–
BaO	1.02	1.48	2.51	0.13	0.13	0.28	40.00	0.01	0.05	–
SO_3	na	na	na	na	na	na	na	na	0.40	na
Cl	–	na	na	–	0.06	na	na	na	6.86	na
O=Cl	–	na	na	–	–0.01	na	na	na	–1.55	na
TOTAL	100.80	99.49	99.36	100.39	100.06	98.53	98.11	97.55	99.55	92.87
atoms on the basis of (O) =										
	8	8	8	8	8	8	8	4	12.5	6
Si	2.911	2.929	2.913	2.964	2.963	2.986	2.013	1.064	3.026	2.035
Ti	0.001	0.001	–	0.001	–	–	–	–	–	–
Al	1.125	1.066	1.079	1.043	1.035	1.001	1.957	0.942	3.001	0.980
Fe	0.010	0.009	0.010	0.006	0.012	0.004	0.013	0.004	0.015	0.002
Mg	–	–	–	–	–	–	0.001	–	–	0.001
Ca	0.061	0.022	0.028	0.002	–	–	0.013	–	0.001	–
Na	0.724	0.571	0.683	0.364	0.088	0.137	0.012	0.708	3.848	0.907
K	0.114	0.376	0.222	0.623	0.927	0.872	0.004	0.203	0.011	0.004
Sr	–	0.011	0.020	–	–	–	0.001	–	–	–
Ba	0.018	0.026	0.045	0.002	0.002	0.005	1.002	–	0.002	–
P	–	na	na	0.001	–	na	na	na	na	na
S	na	na	na	na	na	na	na	na	0.024	na
Cl	–	na	na	–	0.004	na	na	na	0.940	na
cation total	4.963	5.011	5.000	5.006	5.027	5.014	5.017	2.920	9.903	3.930
end-members (mole %)										
an	6.6	2.2	2.8	0.2	–	–	1.2	ne 71.7		
ab	79.0	56.8	68.4	36.7	8.6	13.5	1.2	ks 20.5		
or	12.4	37.4	22.3	62.8	91.1	86.0	0.4	Q 7.8		
Sr feldspar	–	1.1	2.0	–	–	–	0.1			
celsian	1.9	2.6	4.5	0.2	0.2	0.5	97.0			

TABLE 8
Representative mineral analyses: pyroxenes

Sample	CPJ32	PHN	PHN	CPJ33	PHS	CPJ33
Analysis	R6/1	R7/2	R4/5	R7/3	R2/3	R2/4
Mineral	Hedenbergite		Aegirine-augite		Aegirine	
SiO_2	46.90	48.05	49.35	50.64	52.05	51.49
TiO_2	0.32	0.12	0.16	0.41	0.20	0.34
ZrO_2	0.35	0.28	0.51	1.19	0.46	2.11
Al_2O_3	1.99	1.42	2.23	1.20	3.88	1.03
Cr_2O_3	0.03	-	0.02	-	0.01	-
FeO_t	24.72	24.90	26.58	27.70	25.38	27.57
MnO	1.02	1.03	0.90	0.63	0.57	0.32
NiO	-	0.03	-	-	-	0.04
MgO	1.75	2.14	0.50	0.01	0.17	0.29
CaO	19.01	19.15	13.16	6.56	2.19	2.92
Na_2O	2.21	2.06	5.59	9.37	12.01	11.40
K_2O	0.15	0.02	0.02	-	0.05	0.03
Total	98.54	99.19	99.00	97.79	96.98	97.55
Cations calculated on the basis of Z = 4, (O) = 6						
Si	1.899	1.934	1.953	1.986	1.989	1.998
Al^{iv}	0.095	0.066	0.047	0.014	0.011	0.002
Al^{vi}	-	0.001	0.057	0.042	0.164	0.046
Ti	0.001	0.004	0.005	0.012	0.006	0.001
Zr	0.007	0.006	0.001	0.023	0.009	0.040
Cr	0.001	-	0.001	-	0.000	-
Fe^{III}	0.253	0.209	0.389	0.615	0.711	0.716
Fe^{II}	0.584	0.629	0.491	0.293	0.100	0.179
Mn	0.035	0.035	0.030	0.021	0.018	0.011
Ni	-	0.001	-	-	-	0.001
Mg	0.105	0.128	0.029	0.006	0.001	0.017
Ca	0.829	0.826	0.558	0.276	0.090	0.122
Na	0.174	0.161	0.429	0.713	0.890	0.858
K	0.008	0.001	0.000	-	0.002	0.001
Mg#	15.30	16.92	5.64	1.90	9.01	8.66

The remaining analyses, including all from PHN and CPJ41, are sodic pyroxenes with low CaO (≤7.12%). Most are aegirines, but a few are sodic aegirine-augites. Crystallographic orientation is difficult due to the small grain size, but in PHS pleochroism is approximately α pale green, β and γ pale greenish yellow.

MnO (≤1.19%) ranges to higher values in hedenbergite and calcic aegirine-augite, whereas Al_2O_3 (1.03–3.88%) ranges higher in aegirine, implying some solid solution towards jadeite. ZrO_2 is variable but sometimes relatively high (0.28–0.54% in hedenbergite, 0.10–2.11% in aegirine) and does not correlate with other elements, grain size or morphology.

An apparent slight excess of Si (≤2.027 cations per formula unit) in some aegirine analyses may result from small amounts of unanalysed elements. In particular, Nb is relatively high in the whole rock (169–174 ppm, see below) and can enter sodic pyroxenes, as Nickel & Mark (1965) report 1.04% Nb_2O_5 in aegirine-augite (and 0.14% in arfvedsonite) in a paragneiss at Seal Lake, Labrador.

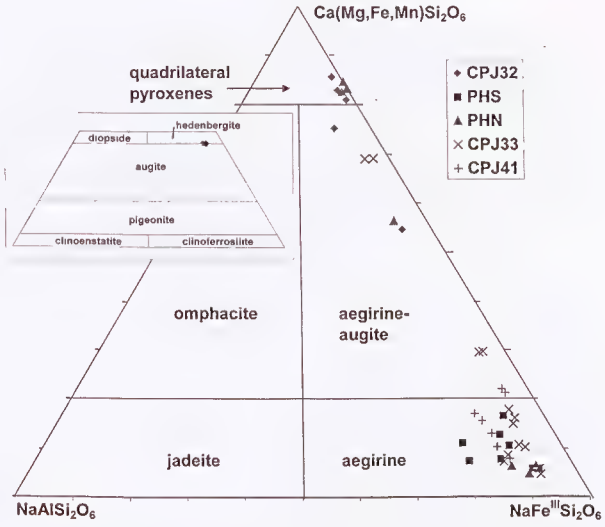

FIG. 7 — Electron microprobe analyses of pyroxenes projected on to the plane $NaAlSi_2O_6$ (jadeite)–$NaFe^{III}Si_2O_6$ (acmite)–$Ca(Mg,Fe,Mn)Si_2O_6$ (quadrilateral clinopyroxene). Inset shows hedenbergites plotted on to the pyroxene quadrilateral (diopside-hedenbergite-clinoenstatite-clinoferrosilite). Nomenclature after Morimoto (1988).

Amphiboles

Sodic amphibole is common in the groundmass as ragged prisms (mostly ≤100 μm long) (pl. 5) and more rarely as subhedral to euhedral pseudohexagonal sections (≤200 μm across) (pl. 6) or glomerocrystic clots. In PHS, an amphibole rhomb (200 x 100 μm) encloses a fayalite grain (70 μm).

Analyses (table 9) were converted to the amphibole formula $AB_2C_5T_8O_{22}(OH,F,Cl)_2$ by the method of J. C. Schumacher (in Leake 1997, appendix 2). For all of these amphiboles, estimates of minimum Fe^{III} are given by the "16CAT" formulae, in which the cations are recalculated to sum to 16, implying full occupancy of the A sites, and Fe distributed between Fe^{III} and Fe^{II} to maintain charge balance. They fall into two distinct populations.

Those from CPJ32 and a few from CPJ33 are iron-rich calcic amphiboles with substantial substitution of Al for Si in the tetrahedral (T) sites. They also have low $Mg/(Mg+Fe^{II})$, and since $Fe^{III} > Al$ in the C sites most fall into the hastingsite field (fig. 8). Analysis R7/5 falls into the ferroedenite field because of its slightly higher Si. Optically, the hastingsite in CPJ32 is length slow with distinctive pleochroism (α pale straw yellow-brown, β deep khaki green to olive-green, γ blue-green).

The remaining analyses, including all those from PHS, PHN and CPJ41, have much higher SiO_2 and Na_2O and very low Al_2O_3 and CaO. They are sodic amphiboles, because the B sites are largely occupied by Na. Because of their low tetrahedral Al and high $Mg/Mg+Fe^{II}$ and Fe^{III} relative to octahedral Al, they are classified as arfvedsonite (fig. 8), and several lie close to the end-member $(Na,K).Na_2.Fe_4^{II}Fe^{III}.Si_8O_{22}(OH,F)_2$. Optically, the arfvedsonite in PHS is length fast and strongly coloured (α very dark blue-green, β pale greenish- to olive-brown, γ dark grey-green).

TABLE 9
Representative mineral analyses: amphiboles

Sample		CPJ32	CPJ33	CPJ32	PHS	CPJ33	CPJ41
Analysis		R2/3	R4/1	R7/5	R7/2	R2/2	R1/7
Mineral		Hastingsite		Edenite	Arfvedsonite		
SiO_2		38.66	39.05	40.58	49.03	48.19	47.94
TiO_2		0.67	0.69	0.52	0.04	0.51	0.14
ZrO_2		0.28	0.52	0.33	0.04	0.13	2.08
Al_2O_3		9.11	8.43	8.09	1.04	1.45	1.77
Cr_2O_3		0.04	0.01	-	0.04	-	0.04
FeO		30.49	32.18	31.05	31.87	32.17	32.69
MnO		0.77	0.74	0.78	1.83	1.68	1.64
NiO		-	-	-	-	-	0.03
MgO		2.47	1.61	1.91	2.21	0.87	0.73
CaO		9.96	9.97	8.84	1.29	0.76	0.83
SrO		-	-	-	0.21	-	0.06
Na_2O		3.18	3.21	3.51	6.57	7.70	7.56
K_2O		1.24	1.42	1.44	2.92	2.07	2.15
BaO		-	-	0.09	-	-	0.04
F		0.07	0.09	0.07	0.23	0.22	0.25
Cl		0.06	0.05	0.06	-	0.02	0.01
O=(F,Cl)		-0.04	-0.05	-0.04	-0.01	-0.01	-0.11
Total		96.96	97.93	97.24	97.23	95.67	97.86
atoms on the basis of $AB_2C_5T_8O_{22}(OH,F)_2$ (16CAT formulae)							
Si	T	6.291	6.348	6.605	7.859	7.841	7.720
Al^{iv}	T	1.709	1.615	1.395	0.141	0.159	0.280
Al^{vi}	C	0.038	-	0.156	0.056	0.119	0.056
Cr	C	0.005	0.002	-	0.005	-	0.005
Ti	C	0.082	0.084	0.064	0.005	0.063	0.017
Zr	C	0.022	0.041	0.026	0.003	0.010	0.164
Fe^{III}	C	0.720	0.744	0.466	0.704	0.752	0.659
Fe^{II}	C	3.429	3.630	3.761	3.568	3.624	3.744
Ni	C	-	-	-	-	-	0.004
Mg	C	0.600	0.390	0.464	0.529	0.212	0.176
Mn	C	0.104	0.102	0.063	0.130	0.221	0.176
Mn	B	0.002	-	0.045	0.119	0.011	0.048
Ca	B	1.736	1.737	1.542	0.222	0.132	0.143
Sr	B	-	-	-	0.020	-	0.005
Na	B	0.262	0.307	0.413	1.640	1.857	1.804
Na	A	0.742	0.705	0.695	0.402	0.571	0.555
K	A	0.258	0.295	0.299	0.598	0.429	0.442
Ba	A	-	-	0.006	-	-	0.002
F		0.035	0.045	0.037	0.116	0.113	0.129
Cl		0.016	0.015	0.015	-	0.005	0.003
OH		1.949	1.941	1.957	1.884	1.883	1.868
Mg#		14.89	9.70	10.98	12.91	5.52	4.49

Arfvedsonite is lower in TiO_2 and higher in MnO (≤2.95%) and K_2O (≤3.10%) than hastingsite. All are low in Ba, Sr, F (≤0.25%) and Cl (≤0.06%). As in pyroxenes, ZrO_2 is very variable but sometimes considerable (up to 2.08% in arfvedsonite).

For some analyses, the total occupancy of the T and C sites is slightly less than 13, due to an excess of cations that must be allocated to the A and B sites (i.e., Ca, Na, Ba and Sr) relative to all other cations. This cannot be corrected by any assumption regarding Fe^{III}/Fe^{II}, and suggests an analytical problem. It is possible that there are small amounts of additional, unanalysed elements in the C sites, particularly REE or Nb.

The formulae can be projected on to a ternary diagram (fig. 8) depicting the three mutually coupled substitutions Si ↔ Al in the T sites, (Mg, Fe^{II}, Mn) ↔ (Al, Fe^{III}) in the C sites, and Na ↔ Ca in the B sites. The amphiboles lie fairly close to the end members of the join between hastingsite/pargasite and arfvedsonite/eckermannite, in which the first and third of the above substitutions are coupled.

Apatite

Accessory apatite is present as small laths (≤250 x 20 μm), acicular prisms (pl. 6) and hexagonal cross-sections (rarely ≤100 μm but mostly ≤15 μm) in the groundmass and as inclusions in fayalite and magnetite microphenocrysts.

Typical analyses (table 10) are near-stoichiometric, with mostly small amounts of iron (≤1.29% as FeO), SrO (≤0.94%), BaO (≤0.96%), Na_2O (≤0.53%) and light rare earth elements (LREE) (≤1.65% La_2O_3 + Ce_2O_3). They are relatively low in F (one analysis 1.88%, rest ≤ 1.18%) and Cl (≤0.37%) and are mostly hydroxyapatites.

Small apatite grains from CPJ41 and PHS, however, have large amounts of SrO (≤25.74%) and LREE (≤12.22%). In CPJ41 they accompany celsian and may be a late stage hydrothermal mineral.

Nepheline, Sodalite and Analcime

The feldspathoidal material consists of an irregularly polygonal aggregate of colourless anhedra, each typically 25–150 μm across. Some is weakly birefringent and sometimes slightly turbid, and has optical properties consistent with nepheline. The remainder, with slightly higher relief, is clear and isotropic (pl. 3), and probably consists of sodalite and analcime, as indicated by X-ray diffraction. The more altered samples (CPJ33, PHN) lack nepheline and sodalite, and analcime is more abundant.

Because of their fine grain size, "clean" near-stoichiometric microprobe analyses of these minerals (table 7) were difficult to obtain, and some are probably mixtures of two or more Na-Al silicates and other minerals. In addition, the analyses are usually deficient in Na relative to the ideal formulae, probably due to volatilisation in the electron beam. Small amounts of iron (usually <0.5% as FeO) are invariably present.

Reasonably stoichiometric analyses of nepheline were obtained from CPJ32, PHS and CPJ41. They contain appreciable K_2O (4.67–6.69%) suggesting approximately 15–20 mole % $KAlSiO_4$ in solid solution, and "excess silica" corresponding to 10–15% solid solution towards alkali feldspar. Near-stoichiometric sodalite ($Na_4Al_3Si_3O_8Cl$) was

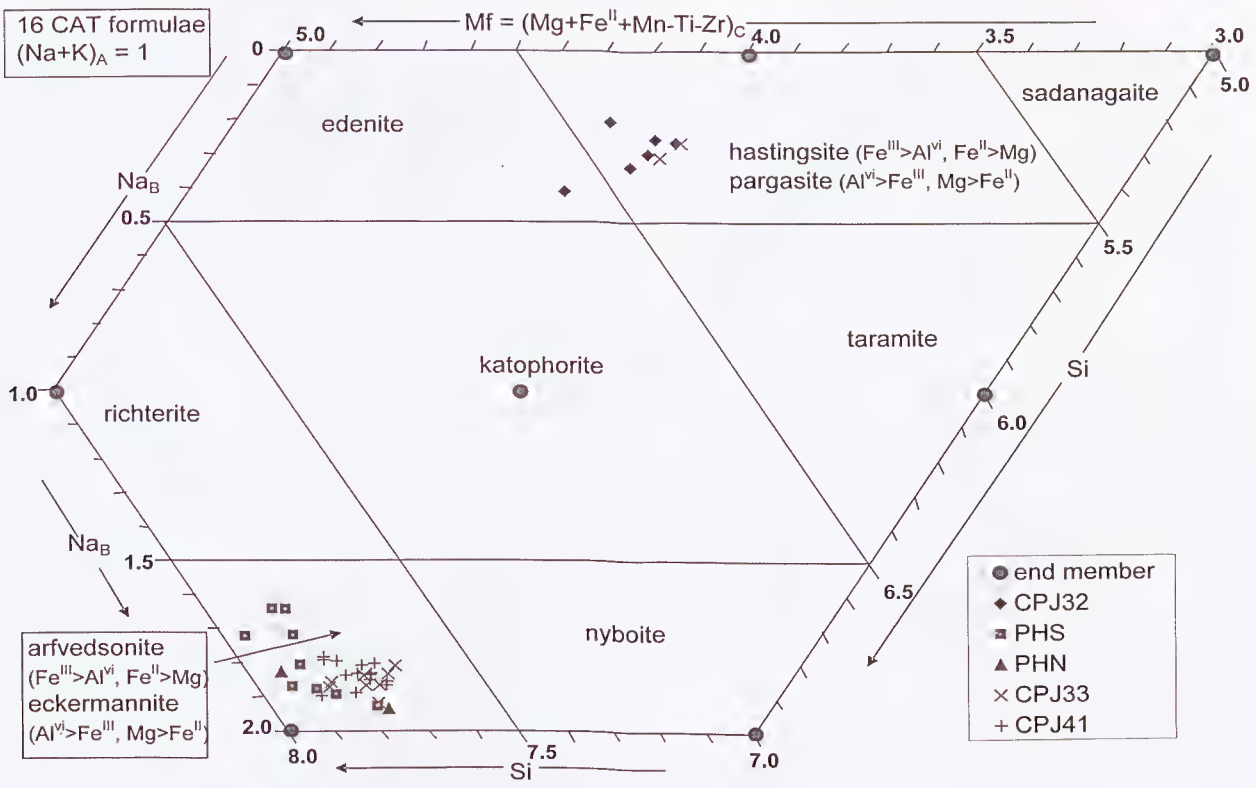

FIG. 8 — Electron microprobe analyses of amphiboles (16 CAT, minimum Fe^{III} formulae) projected on to the system edenite-richterite-arfvedsonite/eckermannite-nyboite-taramite-hastingsite/pargasite, showing coupled substitutions and ideal end-member compositions. Nomenclature consistent with Leake et al. *(1997). See text for further discussion.*

analysed from CPJ32 and PHS. In contrast to nepheline, K_2O is negligible.

Possible analcime analyses, from four samples, are mostly less stoichiometric. Those from CPJ32 and PHS contain significant iron and/or K_2O, and some have excess alkalis suggesting contamination by sodalite.

DISCUSSION

Phenocrysts

The rare fayalite, biotite and magnetite phenocrysts probably represent near-liquidus phases that crystallised from the phonolitic magma at depth. They may have buffered fO_2 by reactions of the form

$$[1a]\ 3Fe_2SiO_4 + O_2 = 2Fe_3O_4 + 3SiO_2$$

This is the well-known quartz-fayalite-magnetite buffer, but its T-fO_2 calibration is not directly applicable, as SiO_2 is a low-activity component in the melt, rather than a mineral phase. Alternatively, it could be rewritten as

$$[1b]\ 6Fe_2SiO_4 + 3(Na,K)AlSiO_4 + 2O_2 = 4Fe_3O_4 + 3(Na,K)AlSi_3O_8$$

where nepheline, kalsilite (K-nepheline) and probably alkali feldspar are components in the melt, rather than mineral phases. Although alkali feldspar occurs as phenocrysts in the phonolite, they grade down into the groundmass and probably crystallised later than the other phenocrysts.

The strong resorption of biotite and fayalite phenocrysts may in part be due to adiabatic decompression, but the general absence of these minerals in the groundmass suggests that they were not stable at the lower pressures and temperatures during final emplacement and cooling of the dyke. Fayalite and magnetite are frequently surrounded by a reaction rim of biotite, which may be represented by reactions of the form:

$$[2a]\ 6Fe_2SiO_4 + 4KAlSiO_4 + 2SiO_2 + 4H_2O = 4KFe^{II}{}_3AlSi_3O_{10}(OH)_2$$

$$[3a]\ 2Fe_3O_4 + 2KAlSiO_4 + 4SiO_2 + 2H_2O = 2KFe^{II}{}_3AlSi_3O_{10}(OH)_2 + O_2$$

or

$$[2b]\ 6\,Fe_2SiO_4 + 3KAlSiO_4 + KAlSi_3O_8 + 4H_2O = 4KFe^{II}{}_3AlSi_3O_{10}(OH)_2$$

$$[3b]\ 2Fe_3O_4 + 2KAlSi_3O_8 + 2H_2O = 2KFe^{II}{}_3AlSi_3O_{10}(OH)_2 + O_2$$

It is clear from reactions [2] and [3], which intersect with [1] (fig. 9), that increasing fH_2O (or decreasing temperature) will favour biotite relative to fayalite and magnetite respectively. From [3], lower fO_2 will also favour biotite relative to magnetite. The experiments of Wones & Eugster (1965) place [3b] for pure annite (Fe-biotite) at about 680° C at 103.5 MPa, or about 710°C at 207 MPa, for oxygen fugacities controlled by the quartz-fayalite-magnetite buffer [1a].

TABLE 10
Representative mineral analyses: apatite

Sample	CPJ41	CPJ41
Analysis	a5	a7
SiO_2	0.33	2.79
ThO_2	0.01	0.68
La_2O_3	0.40	5.02
Ce_2O_3	0.64	5.92
Pr_2O_3	0.13	0.37
Nd_2O_3	0.24	0.91
Sm_2O_3	–	0.02
Y_2O_3	0.08	0.04
FeO	0.46	0.65
MnO	0.15	0.19
MgO	0.02	0.01
CaO	52.72	20.52
SrO	1.16	25.74
BaO	–	0.81
Na_2O	0.27	0.64
P_2O_5	40.62	31.70
As_2O_5	0.04	0.01
SO_3	0.01	0.02
F	1.03	2.03
Cl	0.32	0.01
O = (F, Cl)	–0.51	–0.86
TOTAL	98.13	97.23
Atoms on the basis of (O) = 12, (OH,F,Cl) = 1		
P	2.954	2.838
As	0.002	0.001
S	0.001	0.001
Si	0.028	0.296
Th	–	0.016
La	0.013	0.196
Ce	0.020	0.229
Pr	0.004	0.014
Nd	0.008	0.035
Sm	–	0.001
Y	0.003	0.002
Fe^{II}	0.033	0.057
Mn	0.011	0.017
Mg	0.002	0.001
Ca	4.852	2.324
Sr	0.058	1.578
Ba	–	0.034
Na	0.045	0.131
F	0.279	0.678
Cl	0.047	0.003
(OH)	0.674	0.319
cation total	8.034	7.771

Groundmass

Fergusson (1978) noted that a compositional gap occurs between Ca- and Na- rich pyroxenes within single samples of many felsic alkaline rocks, and attributed this to crystallisation of amphibole, particularly in slowly cooled intrusive rocks. In the Tomahawk phonolite, most pyroxenes are either hedenbergite or aegirine, but the analyses (fig. 7) do not show a clear compositional gap. Those in PHN and CPJ33 have a wide range with some intermediate compositions (aegirine-augite). As both pyroxene and amphibole are groundmass phases, they probably crystallised together rapidly.

However, a large and obvious compositional gap lies between Ca-rich and Na-rich amphiboles (hastingsite and arfvedsonite), even within a thin section (CPJ33; fig. 8). Intermediate sodic-calcic amphiboles near katophorite $Na_A.Na_BCa(Mg,Fe^{II})_4(Al,Fe^{III}).AlSi_7O_{22}(OH,F,Cl)_2$, on the hastingsite-arfvedsonite compositional join, are absent. Katophorite, which contains both Na and Ca in the B sites, is a comparatively rare high temperature amphibole mainly occurring in ultramafic alkaline rocks (Deer *et al.* 1997). There may be a miscibility gap between hastingsite and arfvedsonite at the lower temperatures at which the phonolite groundmass crystallised. As the remaining melt cooled and became further depleted in CaO, this solvus may have been intersected, causing the precipitating amphibole to change suddenly from hastingsite to arfvedsonite.

Arfvedsonite and aegirine may be related by reactions of the form

$$[4]\ 5NaFe^{III}Si_2O_6 + H_2O = Na_3Fe^{II}_4\,Fe^{III}Si_8O_{22}(OH)_2 + Na_2Si_2O_5 + O_2$$

$$[5]\ 18NaFe^{III}Si_2O_6 + 4Fe_3O_4 + 12SiO_2 + 6H_2O = 6Na_3Fe^{II}_4Fe^{III}Si_8O_{22}(OH)_2 + 5O_2$$

where SiO_2 and $Na_2Si_2O_5$ are components in the melt, the latter expressing peralkalinity.

These reactions probably intersect (fig. 9) and define a restricted sector in fO_2-fH_2O space in which both arfvedsonite and aegirine are stable, and magnetite is absent. Clearly, the reduced hydrous phase arfvedsonite is favoured by low fO_2 and high fH_2O (or lower temperature), whereas aegirine is favoured by high fO_2 and low fH_2O.

Marsh (1975) suggested that the stability of acmite (end-member aegirine) in strongly undersaturated liquids is limited by the reaction

$$[6]\ 12NaFe^{III}Si_2O_6 = 4Fe_3O_4 + 6Na_2Si_2O_5 + 12SiO_2 + O_2$$

for which thermodynamic calculations suggested unrealistically high oxygen fugacities (above the hematite-magnetite buffer). This is contrary to petrographic evidence in some nepheline syenites (and the Tomahawk phonolite) and was attributed to inaccurate thermodynamic data (specifically, the free energy of acmite).

Aenigmatite ($Na_2Fe^{II}_5TiSi_6O_{20}$) is common in many peralkaline phonolites and its absence in the Tomahawk River dyke requires comment. Marsh (1975) noted that it typically forms by the reaction of Ti-magnetite with a peralkaline undersaturated liquid. Because of inadequate thermodynamic data he could not define its stability field, but suggested that it lay at low fO_2 and was enlarged by high activity of $Na_2Si_2O_5$ (in melt) and low activity of $NaFeSi_2O_6$ (in pyroxene). High fO_2 and/or aegirine-rich

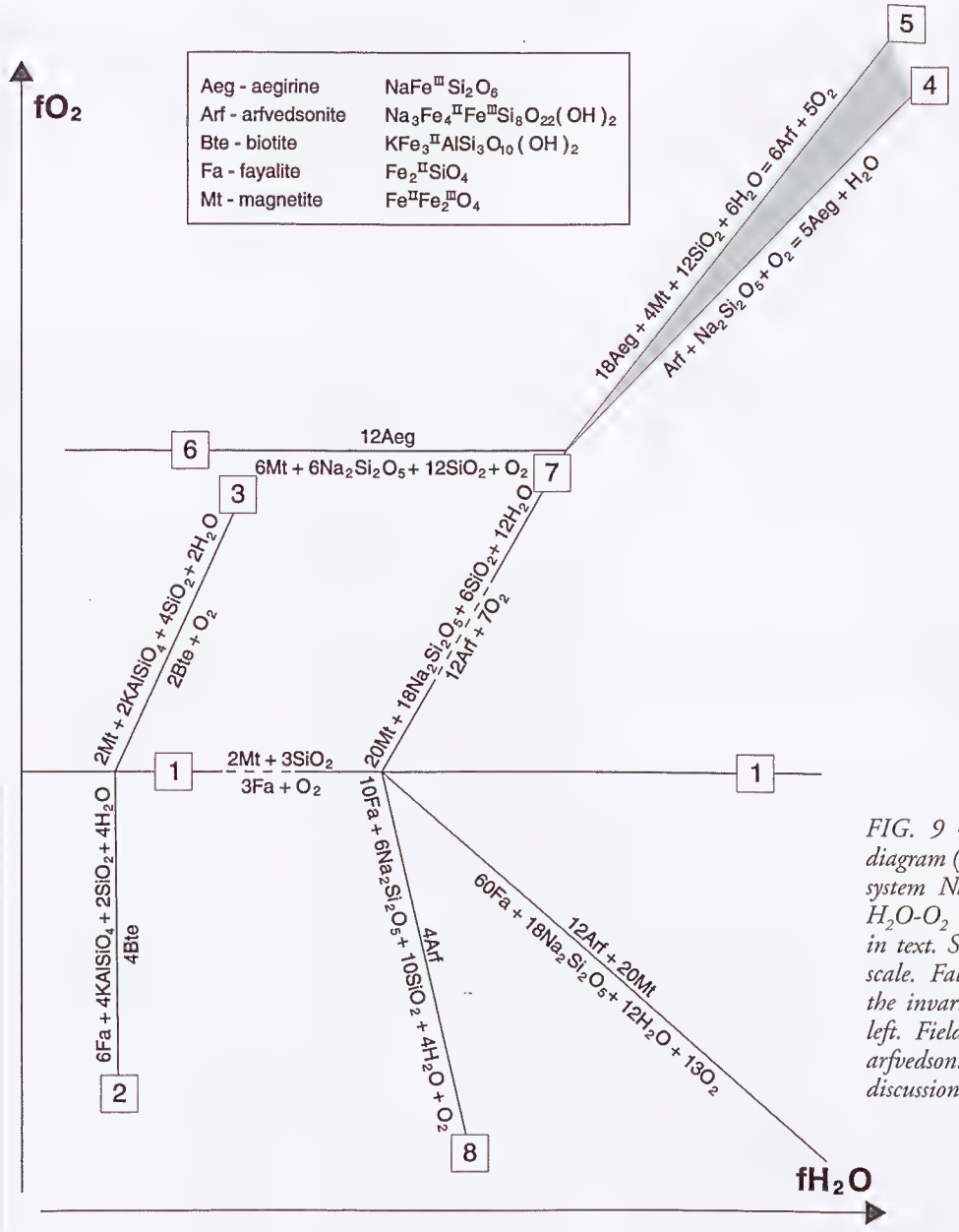
Aeg - aegirine NaFe^{III}Si$_2$O$_6$
Arf - arfvedsonite Na$_3$Fe$_4^{II}$Fe^{III}Si$_8$O$_{22}$(OH)$_2$
Bte - biotite KFe$_3^{II}$AlSi$_3$O$_{10}$(OH)$_2$
Fa - fayalite Fe$_2^{II}$SiO$_4$
Mt - magnetite Fe^{II}Fe$_2^{III}$O$_4$
fO$_2$
fH$_2$O
1
2
3
4
5
6
7
8
2Mt + 3SiO$_2$ = 3Fa + O$_2$
6Fa + 4KAlSiO$_4$ + 2SiO$_2$ + 4H$_2$O = 4Bte
2Mt + 2KAlSiO$_4$ + 4SiO$_2$ + 2H$_2$O = 2Bte + O$_2$
12Aeg = 6Mt + 6Na$_2$Si$_2$O$_5$ + 12SiO$_2$ + O$_2$
18Aeg + 4Mt + 12SiO$_2$ + 6H$_2$O = 6Arf + 5O$_2$
Arf + Na$_2$Si$_2$O$_5$ + O$_2$ = 5Aeg + H$_2$O
20Mt + 18Na$_2$Si$_2$O$_5$ + 6SiO$_2$ + 12H$_2$O = 12Arf + 7O$_2$
10Fa + 6Na$_2$Si$_2$O$_5$ + 10SiO$_2$ + 4H$_2$O + O$_2$ = 4Arf
60Fa + 18Na$_2$Si$_2$O$_5$ + 12H$_2$O + 13O$_2$ = 12Arf + 20Mt

FIG. 9 — Partial Schreinemakers diagram (fO_2-fH_2O, isothermal) for the system Na_2O-(K_2O-Al_2O_3)-FeO-SiO_2-H_2O-O_2 showing reactions mentioned in text. Schematic only with arbitrary scale. Falling temperature will move the invariant points down and to the left. Field of co-existing aegirine and arfvedsonite shaded. See text for further discussion.

pyroxene may explain the absence of aenigmatite in the Tomahawk River dyke. Alternatively, it may result from the very low TiO_2 content (0.05–0.06%, see below) of the dyke. Although low-Ti aenigmatite has been both synthesised and reported in natural rocks, its stability field is restricted to lower fO_2 and pressures than normal aenigmatite (Deer *et al.* 1997 and references therein). In this rock, reaction of magnetite with peralkaline melt instead produced rims of biotite or haloes of aegirine and arfvedsonite, by reactions [3], [6] and/or

[7] $20Fe_3O_4 + 18Na_2Si_2O_5 + 6SiO_2 + 12H_2O = 12Na_3Fe^{II}{}_4Fe^{III}Si_8O_{22}(OH)_2 + 7O_2$

There is also petrographic evidence (pl. 6) for direct reaction of fayalite with peralkaline melt to produce arfvedsonite:

[8] $10Fe_2SiO_4 + 6Na_2Si_2O_5 + 10SiO_2 + 4H_2O + O_2 = 4Na_3Fe^{II}{}_4Fe^{III}Si_8O_{22}(OH)_2$

WHOLE ROCK CHEMISTRY

Analytical Techniques

Two fresh samples, CPJ32 and PHS, were crushed in a steel jaw crusher. Major elements were determined by X-ray fluorescence (XRF) on glass discs, prepared by standard techniques at Mineral Resources Tasmania (MRT) laboratories, Hobart. FeO/Fe_2O_3 was determined by titration and CO_2 by gravimetric methods. H_2O+ was calculated from loss-on-ignition after adjusting for FeO, CO_2 and SO_3.

Four separate determinations were made of many trace elements. XRF analyses, using standard techniques on pressed pellets, were done at both MRT and the University of Tasmania. Each sample was also analysed by inductively coupled plasma mass spectroscopy (ICP-MS) at the University. Small (5–10 mm) chips remaining from the initial jaw crushing were ground in agate and digested by two techniques: HF-HNO_3 digestion in Savillex® teflon vessels on a hotplate at 130°–150°C and 1 atmosphere, and

the PicoTrace® HF/H_2SO_4–$HClO_4$ digestion system at ≤2000 kPa and ≤180°C. Full details of procedures are given by Yu *et al.* (2001) and data by Everard (2004).

Although the ICP-MS data mostly have better precision and lower detection limits than XRF, errors may arise from incomplete digestion of resistant minerals. Data obtained using the more intensive PicoTrace® digestion system are generally preferred, as values for several elements (REE, Y, Zr, Hf and Sn) exceed those obtained by Savillex® digestion, but are similar to XRF data where available.

For Cr, V and Ba, the university XRF data are preferred because of contamination or digestion problems with ICP-MS. W and As were below XRF detection limits (10 ppm) at MRT. For Li and Be, which are difficult to determine, the average of two ICP-MS determinations, rounded to the nearest ppm, are quoted. The remaining trace element data in table 11 were determined by PicoTrace® digestion and ICP-MS.

Major Elements

Both analyses are phonolites according to the total alkali-silica diagram of Le Bas *et al.* (1986) (fig. 10) and the CIPW-normative classification of Johnson & Duggan (1989) (DI > 75; *An* < 50 mol %, and *ne* > 10 %).

The high (>1) Agpaitic Index (table 11) indicates a peralkaline composition (molar (Na_2O+K_2O) > molar Al_2O_3). Mineralogically, this is expressed by the presence of sodic amphiboles, sodic pyroxenes and sodalite and the absence of calcic plagioclase.

Compared with the average phonolite of Le Maitre (1976), and those in eastern Australia (table 11) and elsewhere, the Tomahawk River phonolite is exceptionally depleted in TiO_2, MgO and CaO and has unusually high Na_2O/K_2O. Of the eastern Australian examples quoted, only the Cretaceous (72 Ma) Baralaba plug (Sutherland *et al.* 1996) is also peralkaline, although less strongly so, and more depleted in MgO, CaO and also P_2O_5.

When CIPW-normative components *or*, *ab* and *ne* are calculated and plotted as weight % on to the $NaAlSiO_4$-$KAlSiO_4$-SiO_2 system (fig. 11), the analyses plot very near the feldspar-nepheline temperature minima as determined at atmospheric pressure (Schairer 1950) and 98 MPa (0.98 kb) water pressure (Hamilton & McKenzie 1965). This suggests that, like many other phonolites, compositions were largely controlled by crystal-liquid equilibrium processes at relatively low pressures. However, the minima in this system are relatively insensitive to pressure, and the Tomahawk River phonolite has other significant components, particularly the Na-bearing component *ac* (acmite) which accounts for its peralkalinity and high Na_2O/K_2O.

Bailey (1976) reviewed experimental work relevant to peralkaline feldspathoidal rocks. Although the effect of acmite (end-member aegirine) on the K-bearing system is not well determined, Schairer & Bowen (1956) found that excess Na_2O (i.e., peralkalinity) at 1 atmosphere extends the albite-nepheline cotectic from 1063°C to a eutectic with $Na_2Si_2O_5$ at 732°C. Bailey & Schairer (1966) found that the phase relations in system Na_2O-Al_2O_3-Fe_2O_3-SiO_2 at 1 atmosphere largely reflect the incongruent melting of acmite (to hematite and liquid). Crystallisation of albite, nepheline and acmite from a sodium silicate *(ns)*-normative liquid leads to a eutectic with $Na_2Si_2O_5$ at 715° ± 5°C. This matches the late groundmass crystallisation of aegirine in the Tomahawk River phonolite. Nolan (1966) found that the minimum (715°C at 98 MPa) in the join albite-nepheline-acmite coexists with magnetite and a very iron-rich liquid, but that the addition of minor diopside greatly enlarges the stability field of pyroxene.

Trace Elements

In common with most phonolites, the Tomahawk River dyke is strongly depleted in trace elements (Ni, Cr, Sc, V, Co) that are compatible in early crystallising ferromagnesian minerals. Both high field strength elements (HFSE)(Nb, Zr, La, Ce) and Rb are high, as found in many phonolites and intermediate-silicic Cainozoic and Mesozoic volcanic rocks from eastern Australia (e.g., Ewart *et al.* 1985, Sutherland *et al.* 1996).

Published analyses of phonolites (table 11 and reference list) show extreme variability in Sr (e.g., 5–3000 ppm) and Ba (e.g., 2–1645 ppm). The Tomahawk River dyke is relatively high in Sr (430, 570 ppm) and especially Ba (1040, 1300 ppm).

The chondrite-normalised REE plots (fig. 12) have distinctive concave patterns, with strong light REE (LREE) enrichment, relative middle REE (MREE) depletion, and a flat to slightly positive slope in heavy REE (HREE). Both analyses have very slight positive Eu anomalies, in contrast to the negative Eu anomaly of the Mt Wilson phonolite in Victoria (Ewart *et al.* 1985). Only a few published phonolite REE data display negative Eu anomalies, and those rocks, like the Mt Wilson phonolite, are commonly also low in Sr and Ba (e.g., Weaver 1990, Ablay *et al.* 1998). At Cantal, Massif Central (France), Wilson *et al.* (1995) distinguished aphyric "Type A" phonolites with low Sr, Ba and negative Eu anomalies from porphyritic "Type B" phonolites lacking these features.

Mantle-normalised spidergrams (fig. 13) illustrate the very strong depletions in TiO_2 and P_2O_5, whereas tetravalent trace elements (Zr, Hf, Sn) together with Pb, Mo, Sb and Li are enriched relative to comparable REE. These features presumably reflect fractionation processes rather than characteristics of the mantle source: Ti and P have clearly strongly partitioned into a fractionating phase,

---

Key to Table 11 (opposite)

[a] atomic $100Mg/(Mg+Fe^{II})$
[b] atomic $100Mg/(Mg+Fe^{total})$
[c] agpaitic (peralkaline) index: molar $(Na_2O + K_2O)/Al_2O_3$

[1] mean phonolite, n = 340 (Le Maitre, 1976)
[2] "phonolite" [trachyte], 5.92 Ma, sample 7809/3, Mt Wilson, Trentham, Vic (Ewart *et al.*, 1985)
[3] "phonolite" [trachyte], Jurassic, sample 7809/10, Coleraine, W Vic (Ewart *et al.*, 1985)
[4] phonolite, 169 Ma, sample 7809/25, Pinnacle Mt, via Mullaley, NSW (Ewart *et al.*, 1985)
[5] nepheline syenite plug, 72 Ma, Mt Ramsay, via Baralaba, Qld (Sutherland *et al.*, 1996)
[6] phonolite, <2.8 Ma, Phonolite Hill, McBride province, N Qld (Stephenson *et al.*, 1980)

TABLE 11
Whole-rock analyses

	Tomahawk River		World Av	East Australian phonolites and similar rocks				
Field No.	CPJ32	PHS	1	2	3	4	5	6
SiO_2 (%)	56.23	56.75	56.19	59.39	59.04	56.57	61.80	54.34
TiO_2	0.06	0.05	0.62	0.13	0.10	0.14	0.12	0.14
Al_2O_3	18.99	19.01	19.04	18.36	18.61	19.51	18.20	19.46
Fe_2O_3	3.27	3.86	2.79	3.78	2.67	3.54	3.10	4.15
FeO	3.01	2.24	2.03	1.93	2.57	2.34	1.10	1.55
MnO	0.19	0.20	0.17	0.13	0.19	0.17	0.14	0.17
MgO	0.26	0.17	1.07	0.35	0.31	0.37	0.10	0.98
CaO	1.01	0.83	2.72	1.25	1.36	1.72	0.50	1.89
Na_2O	10.46	10.32	7.79	7.51	6.80	8.08	8.30	8.18
K_2O	4.03	3.95	5.24	5.46	5.68	5.40	4.90	4.46
P_2O_5	0.25	0.19	0.18	0.08	0.04	0.16	0.01	0.29
SO_3	0.09	0.02	nd	nd	nd	nd	nd	nd
CO_2	0.02	0.11	0.08	-	0.19	0.27	<0.10	0.14
H_2O+	1.56	1.32	1.57	0.70	1.75	0.97	1.21	1.34
H_2O-	nd	nd	0.37	0.24	0.70	0.68	0.38	1.60
Total	99.42	99.01	99.41	99.31	100.01	99.92	99.96	98.71
FeO^{total}	5.95	5.71	4.54	5.33	4.97	5.53	3.89	5.28
Mg# [a]	13.20	11.92	48.44	24.43	17.79	21.99	13.95	52.99
mg# [b]	7.14	5.04	29.58	10.48	10.01	10.66	4.38	24.85
AI [c]	1.136	1.118	0.971	0.995	0.931	0.981	1.042	0.940
Li (ppm)	32	50						
Be	7	9						
Sc	3.99	1.26		0.97				
V	15.8	<1.5		10	15	15	2	
Cr	14.1	3.3		3	2		<10	34
Co	4.36	1.04						
Ni	7.27	0.64		4	5	3	<10	8
Cu	12.3	6.0		10	19	12	<5	13
Zn	193	219		255	148	171		125
Ga	30.2	32.4					41	27
Rb	127	131		261	241	126	195	36
Sr	572	434		41	20	129	12	848
Y	22.4	24.7		43	45	25	125	20
Zr	758	917		1710	842	932	1485	965
Nb	169	194		283	228	145	210	236
Mo	10.4	6.0						
Sn	6.13	7.20						
Sb	0.24	0.27		0.64				
Cs	3.17	3.20		8.4				
Ba	1304	1041		40	19	174	120	128
La	86.8	99.0		137			141	66
Ce	136.9	149.2		224	251	138	270	116
Pr	13.2	13.8					32	
Nd	38.9	40.2		58			94	
Sm	5.69	5.84		8.3			17	
Eu	1.82	1.78		0.85				
Gd	4.28	4.35					16	
Tb	0.70	0.72		1.12				
Dy	4.07	4.38					17	
Ho	0.81	0.87		1.44				
Er	2.39	2.65						
Tm	0.39	0.42		0.63				
Yb	2.49	2.72		4.63			5	
Lu	0.40	0.43		0.68				
Hf	14.9	17.7		36.6			18	
Ta	11.5	13.0		20.5				
Tl	0.60	0.68						
Pb	20.2	17.6		25	23	15	27	12
Bi	0.09	0.10						
Th	20.4	27.7		58	46	19	30	21
U	5.74	7.53		8.9			11	2

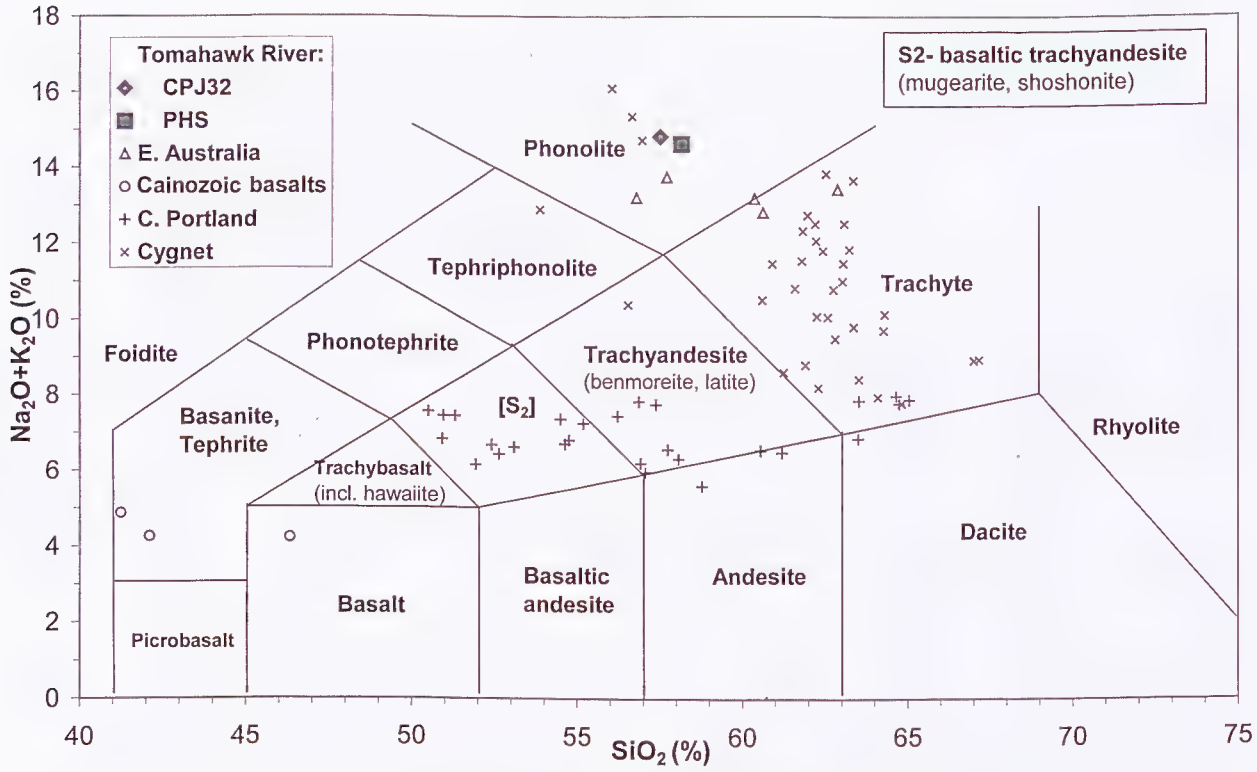

FIG. 10 — Whole-rock analyses of the Tomahawk phonolite plotted on the total alkali-silica diagram, showing volcanic rock nomenclature of Le Bas et al. *(1986). Data from other eastern Australian phonolites and trachytes (table 9), local Cainozoic basalts and Cape Portland appinites (J. L. Everard unpublished data) and Cygnet syenites (Taheri & Bottrill 1999) shown for comparison. All data recalculated to 100% anhydrous.*

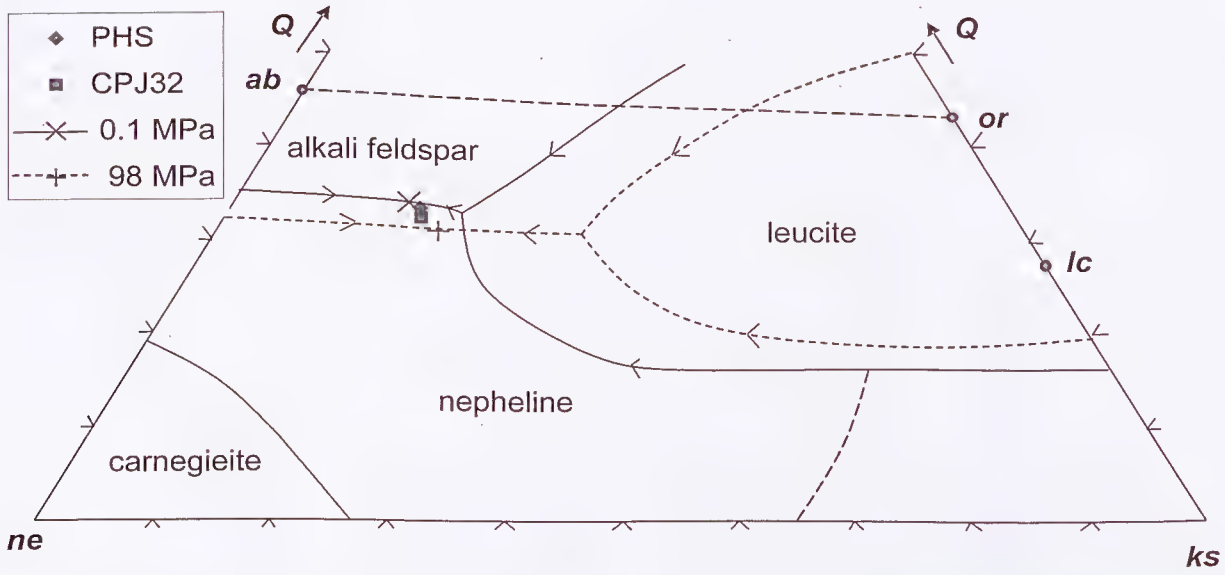

FIG. 11 — Whole-rock analyses of the Tomahawk phonolite projected on to part of the system $NaAlSiO_4$-$KAlSiO_4$-SiO_2, showing experimentally determined phase relations at 0.1 MPa (Schairer 1950) and 98 MPa (Hamilton & McKenzie 1965).

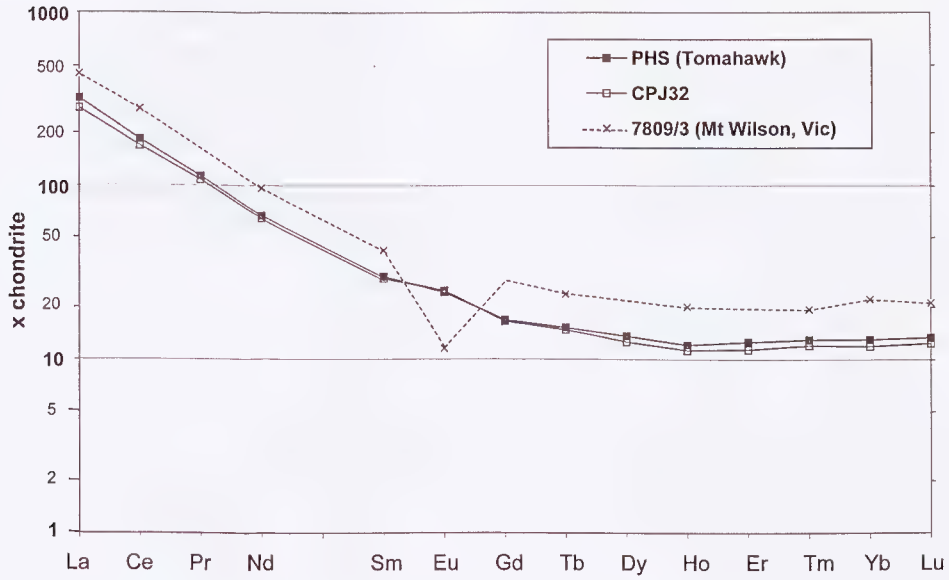

FIG. 12 — Chondrite normalized rare-earth plot for Tomahawk phonolite; data for Mt Wilson phonolite, Victoria (table 9 and Ewart et al. 1985) also plotted (with Gd interpolated) for comparison. Chondrite normalization factors after Boynton (1984).

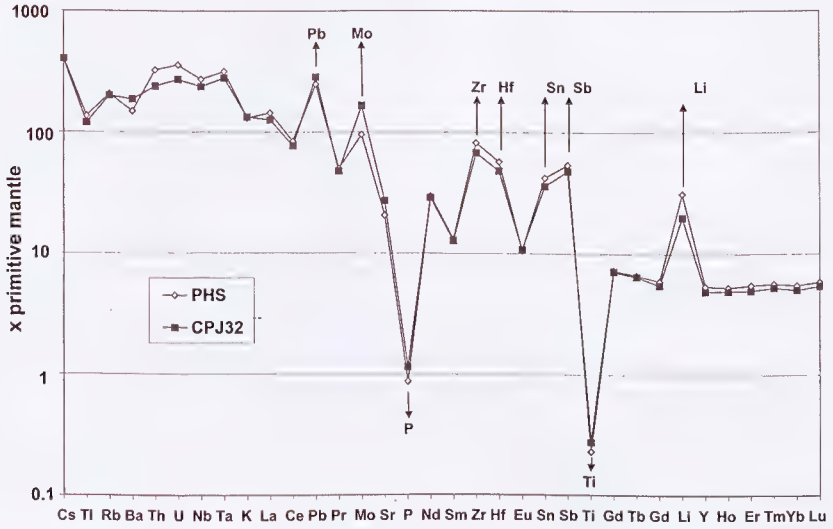

FIG. 13 — Primitive mantle (Sun & McDonough 1989) normalized trace element spider-diagram for Tomahawk phonolite analyses.

whereas REE (especially MREE and HREE) and Sr have been weakly compatible.

Although the two analyses are very similar, PHS generally has slightly lower levels of compatible trace elements (and also TiO_2, MgO and CaO) and higher levels of incompatible elements, indicating that it is more evolved than CPJ32.

Petrogenesis

Although Bailey (1974) maintained that large volumes of phonolitic magma are generated by partial melting in the lower continental crust, most workers ascribe phonolites to the extreme fractionation of silica-undersaturated mafic magmas, such as alkali basalt, basanite or nephelinite. In many studies this is supported by quantitative models of fractional crystallisation and/or direct observation of upward changes in chemical composition within a lava pile or tephra sequence (e.g., Garcia *et al.* 1986, Kyle 1981, Kyle *et al.* 1992, Le Roex 1990, Price *et al.* 1985, Thompson *et al.* 2001, Weaver 1990, Wörner & Schmincke 1984b). Wilson *et al.* (1995) and Ablay *et al.* (1998) suggested crustal assimilation combined with fractional crystallisation (AFC processes) may also occur.

Although lherzolite-bearing olivine nephelinite lavas occur 2–4 km east of the Tomahawk River dyke (Baillie *et al.* 1978, J. L. Everard, unpublished data; figs 1, 2), they are almost certainly outliers of the Miocene (16 Ma) Ringarooma volcanism (McClenaghan *et al.* 1982) and are thus unrelated. In the absence of any potentially parental mafic or intermediate rocks, a discussion of the petrogenesis of the Tomahawk River phonolite is speculative. However, some qualitative comments can be made, particularly by comparing its geochemistry with some of the above examples.

The high HFSE and Rb are generally consistent with strong crystal fractionation, but the lack of Sr or Ba depletion or negative Eu anomalies implies that neither alkali feldspar nor plagioclase were major fractionating phases. This suggests an already strongly undersaturated parental basanite or nephelinite with low normative feldspar. The very low levels of compatible elements (MgO, Ni, Cr etc.) suggest dominant olivine, pyroxene and/or amphibole fractionation left a residual felsic liquid that approached the feldspar-nepheline minimum. Strong depletion of P suggests removal of apatite, consistent with apatite inclusions in magnetite and fayalite microphenocrysts.

Fractionation of kaersutitic amphibole from a mafic precursor could account for the concave REE patterns, as MREE are strongly partitioned into amphibole (Sisson 1994), and together with titanomagnetite fractionation may partly account for Ti depletion. Additionally, as noted by Ablay *et al.* (1978), kaersutite has a low Na:Al ratio and its removal will delay feldspar crystallisation and drive the melt towards peralkaline compositions.

REGIONAL SIGNIFICANCE AND CONCLUSION

In Tasmania, the Cretaceous was mainly a prolonged period of non-deposition or erosion, and surface environments are rarely preserved. Only localised and relatively minor Cretaceous igneous rocks, mainly intrusions, are known. All are appreciably older than the phonolite, and compositionally dissimilar to it (fig. 10).

Cretaceous appinitic rocks occur in northeast Tasmania at Cape Portland, about 30 km to the northeast of Tomahawk River, as irregular plug-like intrusions of porphyrite, dykes of lamprophyre and flow remnants of andesite (Jennings & Sutherland 1969). Sutherland & Corbett (1974) reported minimum ages ranging from 91 ± 1 Ma (K/Ar) to 103 ± 23 Ma (Rb/Sr), and McDougall & Green (in McClenaghan *et al.* 1982) obtained K/Ar ages of between 102.3 ± 2.6 and 101.3 ± 2.6 Ma from hornblende separates. Small lamprophyre dykes also crop out on Waterhouse Island (Baillie *et al.* 1978), north of Great Musselroe Bay, Cod Bay and George Rocks (Baillie 1984). Drilling at Cuckoo Creek, behind Great Musselroe Bay, encountered similar dykes, one of which yielded a K/Ar whole rock age of 98.7 ± 0.6 Ma (Baillie 1986).

Cretaceous syenites intrude both Late Carboniferous-Permian beds and Jurassic dolerite in the Cygnet-Kettering area of southern Tasmania (Ford 1983). Although mainly oversaturated, they include some silica-undersaturated dykes. K/Ar dating of mineral separates indicate an age of 100.5 ± 0.8 Ma (Evernden & Richards 1962, McDougall & Leggo 1965).

The younger (8 to > 58 Ma) Tasmanian Cainozoic basalts contain some relatively evolved nepheline mugearites and mafic nepheline benmoreites (Mg# 43-53; D. I. 53-58; Sutherland *et al.* 1989), but none approach the Tomahawk rock (Mg# 13.2, D. I. 82.8) in this respect.

The Tomahawk River dyke represents a new, albeit very minor, phase of igneous activity for Tasmania. However, some indirect evidence for other Late Cretaceous magmatism exists in the area. This comes from fission-track dating of distinctive pale yellow-brown zircon megacrysts (5 grains, 71.3 ± 5.9 Ma) found with other younger zircon megacryst suites (42–53 ± 2–4 Ma) in an alluvial sub-basaltic deposit at Grays Hill, near Branxholm (Australian Museum unpublished data, Geotrack International Report #169, June 1989). The older zircons lie within error of the Ar-Ar dating of the Tomahawk phonolite.

The 75–81 Ma age of the Tomahawk phonolite overlaps with the main period of the opening of the Tasman Sea, which spans Anomalies 34 to 24 (Gaina *et al.* 1998), corresponding to about 84 to 52 Ma (Cande & Kent 1995). Rifting and spreading commenced after 84 Ma, along the Tasman margin, off northeastern Tasmania (Duddy & Green 1992, Sutherland 1994, Royer & Rollet 1997, O'Sullivan *et al.* 2000, Norvick & Smith 2001).

More locally, Cretaceous rifting formed the Boobyalla Sub-basin, a southeasterly extension of the Bass Basin that extends on-shore near the mouth of the Ringarooma River, about 15 km ENE of the Tomahawk dyke (fig. 1; Moore *et al.* 1984, Luskin *et al.* 1989). Geophysical evidence suggests that, in this area, the sub-basin is 600–800 m thick and bounded by rotational normal faults (Leaman 1973, Leaman & Symonds 1975). Two drill holes penetrated a non-marine sequence of dolerite-boulder to granule-conglomerate and poorly sorted ferruginous sandstone of mainly Late Cretaceous biostratigraphic age. Angiosperm pollen at the base of the deepest hole (491 m) indicates an age probably no older than Turonian (89–91 Ma). Thus the Boobyalla Sub-basin appears to have been initiated in the Late Cretaceous, considerably later than the remainder of Bass Basin (Luskin *et al.* 1989) but prior to the opening of the Tasman Sea and the Tomahawk phonolitic magmatism.

Sharples & Klootwijk (1981) showed that Ordovician Gordon Group Limestone at Ida Bay, in far southern Tasmania, was completely remagnetised in the Late Cretaceous or Early Cainozoic, even though conodont colour indices indicate that the limestone had not been heated beyond 100°C. This was interpreted as further evidence for a prolonged episode of increased heat flow and widespread remagnetisation in southeastern Australia at this time, possibly related to the rifting prior to opening of Tasman Sea.

Thus, like many other alkaline rocks from continental settings, the Tomahawk River phonolite may be related to rifting and increased heat flow associated with continental break-up.

The Tomahawk alkaline activity does not correlate with any published Late Cretaceous intraplate basaltic activity in eastern Victoria, on the northern side of the intervening Gippsland Basin. Eastern Victorian basaltic intrusions and associated contact metamorphic activity are recorded between 85–95 Ma (McKenzie *et al.* 1984, Price *et al.* 1988, Duddy & Green 1992), but mark an earlier rift-related episode in relation to the initial Tasman spreading period and the Tomahawk magmatism. Phonolitic intrusions appear within some basalt provinces in eastern Victoria, but are not dated and may relate to the older Mesozoic phonolites at Gallows Hill, near Mansfield (~ 156 ± 20 Ma, recalculated from McDougall & Wellman 1976). Proven Late Cretaceous phonolitic magmatism, as at Tomahawk, is rare in eastern Australia. However, a comparative example forms the Mount Ramsay nepheline syenite, near Baralaba, central Queensland (72 Ma; table 11), which may relate to a central volcano plume trace (Sutherland *et al.* 1996).

ACKNOWLEDGEMENTS

The dating work was undertaken as a joint project between the Australian Museum Geodiversity Research Centre and the CSIRO Division of Petroleum Resources (Bentley, Perth, WA). The Ar-Ar data presented in this study were undertaken at the Western Australian Argon Isotope Facility, operated by a consortium of Curtin University and University of Western Australia.

Dr Jo-Anne Wartho (Curtin University) and Andrew Todd (CSIRO Petroleum) are thanked for assistance during K-Ar and ^{40}Ar-^{39}Ar analyses. R. S. Bottrill, G. R. Green, L. M. Hay, A. J. Hollick, S. Heawood, R. G. Richardson, J. Taheri and R. N. Woolley at Mineral Resources Tasmania are thanked for use of equipment, technical assistance and support. D. Steele and P. Robinson (University of Tasmania) assisted with electron microprobe and performed ICPMS analyses respectively. We also thank Prof. A. J. Crawford and an anonymous reviewer for their advice on the manuscript.

REFERENCES

ABLAY, G.J., CARROLL, M.R., PALMER, M.R., MARTI, J. & SPARKS, R.S.J., 1998: Basanite-phonolite lineages of the Teide-Pico Viejo Volcanic Complex, Canary Islands. *Journal of Petrology* 39: 905–936.

ANON., 1970: Catalogue of the minerals of Tasmania. *Geological Survey Record* 9, Tasmania Department of Mines.

BAILEY, D.K., 1974: Origin of alkaline magmas as a result of anatexis: (b) melting in the deep crust. *In* Sorensen, H. (Ed.): *The Alkaline Rocks.* John Wiley & Sons, London: 436–442.

BAILEY, D.K., 1976: Applications of experiments to alkaline rocks. *In* Bailey, D. K. & Macdonald, R. (Eds): *The Evolution of Crystalline Rocks.* Academic Press, London: 419–469.

BAILEY, D.K. & SCHAIRER, J.F., 1965: The system Na_2O-Al_2O_3-Fe_2O_3-SiO_2 at 1 atmosphere, and the petrogenesis of alkaline rocks. *Journal of Petrology* 7: 114–170.

BAILLIE, P.W., 1972: The structure of the granitic rocks of the Little Mt Horror area. *Tasmania Department of Mines Technical Reports* 15: 32–36.

BAILLIE, P.W., 1984: Geological Atlas 1:50,000 Series. Sheet 8516S (25). Eddystone. Tasmania Department of Mines, Hobart.

BAILLIE, P.W., 1986: Geological Survey Explanatory Report. Sheet 8516S (25). Eddystone. Tasmania Department of Mines, Hobart.

BAILLIE, P.W., TURNER, N.J. & COX, S.F., 1978: Geological Atlas 1:50,000 Series. Sheet 8416S (24). Boobyalla. Tasmania Department of Mines, Hobart.

BONHOMME, M.G., THUIZAT, R., PINAULT, Y., CLAUER, N., WENDLING, R. & WINKLER, R., 1975: *Méthode de datation potassium-argon. Appareillage et technique.* University of Strasbourg, 53pp.

BOYNTON, W.V., 1984: Geochemistry of the rare earth elements: meteorite studies. *In* Henderson, P. (Ed.): *Rare earth element geochemistry.* Elsevier, Amsterdam: 63–114.

CANDE, S.C. & KENT, D.V., 1995: Revised calibration of the geomagnetic polarity time scale for the Late Cretaceous and Cenozoic. *Journal of Geophysical Research* 100: 6093–6095.

DEER, W.A., HOWIE, R.A. & ZUSSMAN, J., 1997: *Rock-forming minerals. Volume 2B, second edition. Double-chain silicates.* The Geological Society, London, 764 pp.

DUDDY, I.R. & GREEN, P.F., 1992: Tectonic development of the Gippsland Basin and environs: identification of key episodes using apatite fission track analysis (AFTA). *In* Barton, C. (Ed.) *Energy, Economics and Environmemt: Gippsland Basin Symposium, 22-23 June 1992.* Australasian Institute of Mining and Metallurgy, Melbourne: 111–120.

EDWARDS, A.B., 1947: Alkali hybrid rocks of Port Cygnet, Tasmania. *Proceedings of the Royal Society of Victoria* 58: 81–115.

EVERARD, J.L., 2004: A ground magnetometer survey and compilation of field, petrographic and geochemical data from the Tomahawk River phonolite dyke, northeast Tasmania. *Tasmanian Geological Survey Record.*

EVERNDEN, J.F. & RICHARDS, J.R., 1962: Potassium-argon ages in eastern Australia. *Journal of the Geological Society of Australia* 9: 1–37.

EWART, A., CHAPPELL, B.W. & LE MAITRE, R.W., 1985: Aspects of the mineralogy and geochemistry of the intermediate-silicic Cainozoic volcanic rocks of eastern Australia; part 1: introduction and geochemistry. *Australian Journal of Earth Sciences* 32: 359–382.

FERGUSSON, A.K., 1978: The crystallization of pyroxenes and amphiboles in some igneous rocks and the presence of a pyroxene compositional gap. *Contributions to Mineralogy and Petrology* 67: 11–15.

FORD, R.J., 1983: The alkaline rocks of Port Cygnet, Tasmania. Unpublished Ph.D. thesis, University of Tasmania.

GAINA, C., MÜLLER, D.R., ROYER, J.-Y., STOCK, J., HARDEBECK, J. & SYMONDS, P., 1998: The tectonic history of the Tasman Sea: a puzzle with 13 pieces. *Journal of Geophysical Research* 103: 12413–21433.

GARCIA, M.O., FREY, F.A. & GROOMS, D.G., 1986: Petrology of volcanic rocks from Kaula Island, Hawaii. *Contributions to Mineralogy and Petrology* 94: 461–471.

GROVES, D.I., 1977: The geology, geochemistry and mineralization of the Blue Tier Batholith. *Geological Survey of Tasmania Bulletin* 53. Tasmania Department of Mines, Hobart.

HAMILTON, D.L. & MCKENZIE, W.S., 1965: Phase equilibria studies in the system $NaAlSiO_4$ (nepheline) - $KAlSiO_4$ (kalsilite) - SiO_2 (quartz). *Mineralogical Magazine* 34: 214–231.

HEINRICHS H. & HERRMANN, A.G., 1990: *Praktikum der Analytischen Geochemie.* Springer-Verlag, Berlin-Heidelberg, 669 pp.

HESS, J.C. & LIPPOLT, H.J., 1994: Compilation of K-Ar measurements on HD-B1 standard biotite 1994 status report. Phanerozoic Time Scale. G. S. Odin, Paris. *Bulletin of Liaison and Information, IUGS Subcommission of Geochronology* 12: 19–23.

JENNINGS, D.J. & SUTHERLAND, F.L., 1969: Geology of the Cape Portland area, with special reference to the Mesozoic(?) appinitic rocks. *Tasmania Department of Mines Technical Reports* 13: 45–81.

JOHNSON, R.W. & DUGGAN, M.B., 1989: Rock classification and analytical data bases. *In* Johnson, R.W. (Comp. & Ed.): *Intraplate Volcanism in Eastern Australia and New Zealand.* Cambridge University Press, Cambridge: 12–13.

KELLER, J., 1983: Potassic lavas in the orogenic volcanism of the Mediterranean area. *Journal of Volcanology and Geothermal Research* 18: 321–335.

KNUTSON, J. (Ed.), 1989: East Australian Volcanic Geology. *In* Johnson, R.W. (Comp. & Ed.): *Intraplate Volcanism in Eastern Australia and New Zealand.* Cambridge University Press, Cambridge: 89–115.

KYLE, P.R., 1981: Mineralogy and petrology of a basanite to phonolite sequence at Hut Point Peninsula, Antarctica, based on core from Dry Valley Drilling Project Drillholes 1, 2 and 3. *Journal of Petrology* 22: 451 - 500.

KYLE, P.R., MOORE, J.A. & THIRLWALL, M.F., 1992: Petrological evolution of anorthoclase phonolite lavas at Mt Erebus, Ross Island, Antarctica. *Journal of Petrology* 33: 849–875.

LEAKE, B.E. (Comp.), 1997: Nomenclature of amphiboles: Report of the Subcommittee on Amphiboles of the International Mineralogical Association, Commission on New Miner-

als and Mineral Names. *American Mineralogist* 82: 1019–1037.

LEAMAN, D.E., 1973: Summary of geophysical work, Gladstone area. *Tasmania Department of Mines Technical Reports* 16: 89–96.

LEAMAN, D.E. & SYMONDS, P.A., 1975: Gravity survey of north-eastern Tasmania. *Geological Survey of Tasmania Paper 2.* Tasmania Department of Mines, Hobart.

LE BAS, M.J., LE MAITRE, R.W., STRECKEISEN, A. & ZANETTIN, B., 1986: A chemical classification of volcanic rocks based on the total alkali silica diagram. *Journal of Petrology* 27: 745–750.

LE MAITRE, R.W., 1976: The chemical variability of some common igneous rocks. *Journal of Petrology* 17: 589–637.

LE ROEX, A.P., CLIFF, R.A. & ADLER, B.J. I., 1990: Tristan da Cunha, South Atlantic: geochemistry and petrogenesis of a basanite-phonolite lava series. *Journal of Petrology* 31: 779–812.

LIPPARD, S.J., 1973: The petrology of phonolites from the Kenya Rift. *Lithos* 6: 217–234.

LUDWIG, K.R., 2001: Isoplot/Ex rev. 2.49, a Geochronological Toolkit for Microsoft Excel. *Berkeley Geochronology Centre Special Publication 1a.*

LUSKIN, A., HOBDAY, D.K. & BAILLIE, P.W., 1989: Boobyalla Sub-basin. *In* Burrett, C.F. & Martin, E.L. (Eds): *Geology and Mineral Resources of Tasmania.* Geological Society of Australia Inc., Special Publication 15: 356–358.

MCCLENAGHAN, M.P. & WILLIAMS, P.R., 1982: Distribution and characterisation of granitoid intrusions in the Blue Tier area. *Geological Survey Paper 4.* Tasmania Department of Mines, Hobart.

MCCLENAGHAN, M.P., TURNER, N.J., BAILLIE, P.W., BROWN, A.V., WILLIAMS, P.R. & MOORE, W.R., 1982: Geology of the Ringarooma- Boobyalla area. *Geological Survey of Tasmania Bulletin* 61. Tasmania Department of Mines, Hobart.

MCDOUGALL, I. & HARRISON, T.M., 1999: *Geochronology and Thermochronology by the $^{40}Ar/^{39}Ar$ method* (2nd Edition). Oxford University Press, New York, 269 pp.

MCDOUGALL, I. & LEGGO, P.J., 1965: Isotopic age determination on granitic rocks from Tasmania. *Journal of the Geological Society of Australia* 12: 295–332.

MCDOUGALL, I. & ROKSANDIC, Z., 1974: Total fusion $^{40}Ar/^{39}Ar$ ages using HIFAR reactor. *Journal of the Geological Society of Australia* 21: 81–89.

MCDOUGALL, I. & WELLMAN, P., 1976: Potassium-argon ages for some Australian Mesozoic igneous rocks. *Journal of the Geological Society of Australia* 23: 1–9.

MCKENZIE, D.A., NOTT, R.J. & BOLGER, P.F., 1984: Radiometric age determinations. *Geological Survey of Victoria Report* 74 (unpublished).

MACKENZIE, D.E., BLACK, L.P. & SUN, S.-S., 1988: Origin of alkali feldspar granites associated with the Poimena granite, northeastern Tasmania. *Geochimica et Cosmochimica Acta* 54: 2313–2322.

MARSH, J.S., 1975: Aenigmatite stability in silica- undersaturated rocks. *Contributions to Mineralogy and Petrology* 50: 135–144.

MOORE, W.R., BAILLIE, P.W., FORSYTH, S.M., HUDSPETH, J.W., RICHARDSON, R.G. & TURNER, N.J., 1984: Boobyalla Sub-basin: a Cretaceous onshore extension of the southern edge of the Bass Basin. *APEA Journal* 24: 110–117.

MORIMOTO, N., 1988: Nomenclature of pyroxenes. *American Mineralogist* 73: 1123–1133.

NICKEL, E.H. & MARK, E., 1965: Arfvedsonite and aegirine-augite from Seal Lake, Labrador. *Canadian Mineralogist* 8: 185–197.

NOLAN, J., 1966: Melting relations in the system $NaAlSi_3O_8$-$NaAlSiO_4$- $NaFeSi_2O_6$-$CaMgSi_2O_6$-H_2O and their bearing on the genesis of alkaline undersaturated rocks. *Quarterly Journal of the Geological Society* 112: 119–157.

NORVICK, M.S. & SMITH, M.A., 2001: Mapping the plate tectonic reconstruction of southern and southeastern Australia and implications for petroleum systems. *APPEA Journal* 41: 15–34.

O'SULLIVAN, P.B., MITCHELL, M.M., O'SULLIVAN, A.J., KOHN, B.P. & GLEADOW, A.J.W., 2000: Thermotectonic history of the Bassian Rise, Australia: implications for the breakup of eastern Gondwana along Australia's southeastern margins. *Earth and Planetary Science Letters* 182: 31–47.

PRICE, R.C., JOHNSON, R.W., GRAY, C.M. & FREY, F.A., 1985: Geochemistry of phonolites and trachytes from the summit region of Mt Kenya. *Contributions to Mineralogy and Petrology* 89: 394–409.

PRICE, R.C., GRAY, C.M., NICHOLLS, I.A. & DAY, A., 1988: Cainozoic volcanic rocks. *In* Douglas, J.G. & Ferguson, J.A. (Eds): *Geology of Victoria.* Geological Society of Australia, Victorian Division. Melbourne: 439–451.

QUILTY, P.G. & WHELLER, G.E., 2000: Heard Island and the McDonald Islands: a window into the Kerguelen plateau. *Papers and Proceedings of the Royal Society of Tasmania* 122(2): 1–12.

ROYER, J-Y. & ROLLET, N., 1997: Plate-tectonic setting of the Tasmanian region. *Australian Journal of Earth Sciences* 44: 543–560.

SCHAIRER, J.F., 1950: The alkali feldspar join in the system $NaAlSiO_4$-$KAlSiO_4$ -SiO_2. *Journal of Geology* 58: 512–517.

SCHAIRER, J.F. & BOWEN, N.L., 1956: The system Na_2O-Al_2O_3-SiO_2. *American Journal of Science* 254: 129–195.

SHARPLES, C. & KLOOTWIJK, C.T., 1981: Palaeomagnetic results from the Gordon Subgroup of Tasmania: further evidence for a late Cretaceous magnetic overprint in southeastern Australia. *Papers and Proceedings of the Royal Society of Tasmania* 115: 85–91.

SIMKIN, T. & SMITH, J.V., 1970: Minor element distribution in olivine. *Journal of Geology* 78: 304–325.

SISSON, T.W., 1994: Hornblende-melt trace-element partitioning measured by ion microprobe. *Chemical Geology* 117: 331–344.

SORENSEN, H. (Ed.), 1974: *The Alkaline Rocks.* John Wiley & Sons, London. 622 pp.

STEIGER, R.H. & JÄGER, E., 1977: Subcommission on Geochronology: convention on the use of decay constants in geo- and cosmochronology. *Earth and Planetary Science Letters* 36: 359–362.

STEPHENSON, P.J., GRIFFIN, T.J. & SUTHERLAND, F.L., 1980: Cainozoic volcanism in northeastern Australia. *In* Henderson, R. A. & Stephenson, P.J. (Eds) *The Geology and Geophysics of Northeastern Australia.* Geological Society of Australia, Queensland Division: 349–374.

SUN, S.-S. & MCDONOUGH, W.F., 1989: Chemical and isotopic systematics of oceanic basalts: implications for mantle composition and processes. *In* Saunders, A. D. & Norry, M. J. (Eds) *Magmatism in the Ocean Basins.* Geological Society of London Special Publication 42: 313–346.

SUTHERLAND, F.L., 1976: Cainozoic volcanic rocks. *In* Leaman, D.E. Geological Survey Explanatory Report. Sheet 82 (8312S). Hobart. Tasmania Department of Mines, Hobart: 35–36.

SUTHERLAND, F.L., 1994: Tasman Sea evolution and hotspot trails. *In* Van der Lingen, G.J., Swanson, K.M. & Muir, R.J. (Eds): *Evolution of the Tasman Sea Basin.* A.A. Balkema, Rotterdam: 35–51.

SUTHERLAND, F.L. & CORBETT, E.B., 1974: The extent of Upper Mesozoic igneous activity in relation to lamprophyric intrusions in Tasmania. *Papers and Proceedings of the Royal Society of Tasmania* 107: 175–190.

SUTHERLAND, F.L., EWART, A., RAYNOR, L.R., HOLLIS, J.D. & MCDONOUGH, W.D., 1989: Tertiary basaltic magmas and the Tasmanian lithosphere. *In* Burrett, C.F. & Martin, E.L. (Eds): *Geology and Mineral Resources of Tasmania.* Geological Society of Australia Special Publication 15: 386–398.

SUTHERLAND, F.L., ROBERTSON, A.D., BARRON, B.J. & POGSON, R.E., 1996: The Rockhampton plume and its late Mesozoic trace? *In* Mesozoic Geology of the Eastern Australian Plate, Mesozoic 96 Conference, 23 - 26 September, Brisbane. *Geological Society of Australia Extended Abstracts* 43: 519–527.

TAHERI, J. & BOTTRILL, R., 1999: Porphyry and sedimentary-hosted gold deposits near Cygnet: new styles of gold mineralisation in Tasmania. *Tasmanian Geological Survey Record* 1999/01.

THOMPSON, G.M., SMITH, I.E.M. & MALPAS, J.G., 2001: Origin of oceanic phonolites by crystal fractionation and the problem of the Daly gap: an example from Rarotonga. *Contributions to Mineralogy and Petrology* 142: 336–346.

WEAVER, B.L., 1990: Geochemistry of highly under-saturated oceanic island basalt suites from the South Atlantic Ocean: Fernando de Noronha and Trinidade islands. *Contributions to Mineralogy and Petrology* 105: 502–515.

WILSON, M., DOWNES, H. & CEBRIA, J., 1995: Contrasting fractionation trends in coexisting continental alkaline magma series; Cantal, Massif Central, France. *Journal of Petrology* 36: 1723–1753.

WONES, D.R. & EUGSTER, H.P., 1965: Stability of biotite: experiment, theory and application. *American Mineralogist* 50: 1228–1272.

WÖRNER, G. & SCHMINCKE, H.-U., 1984a: Mineralogical and chemical zonation of the Laacher See tephra sequence (East Eifel, W. Germany). *Journal of Petrology* 25: 805–835.

WÖRNER, G. & SCHMINCKE, H.-U., 1984b: Petrogenesis of the zoned Laacher See tephra. *Journal of Petrology* 25: 836 –851.

YOUNG, G.C. & LAURIE, J.R., (Eds), 1996: *An Australian Phanerozoic Timescale.* Oxford University Press, Melbourne, 279 pp.

YU Z., ROBINSON P. & MCGOLDRICK P., 2001: An evaluation of methods for the chemical decomposition of geological materials for trace element determination using ICP-MS. *Geostandards Newsletter, the Journal of Geostandards and Geoanalysis* 25: 199–217.

(accepted 2 February 2004)

LAXMANNIA MORRISII KEIGHERY (ANTHERICACEAE) A SYNONYM OF *L. SQUARROSA* LINDL., NOT A NATIVE OF TASMANIA

by D. I. Morris

(with two plates)

MORRIS, D. I., 2004 (29:x): *Laxmannia morrisii* Keighery (Anthericaceae) a synonym of *L. squarrosa* Lindl., not a native of Tasmania. *Papers and Proceedings of the Royal Society of Tasmania* 138: 35–36. ISSN 0080-4703. Tasmanian Herbarium, Private Bag 4, Hobart, Tasmania 7001, Australia.

Laxmannia morrisii Keighery is a synonym of *Laxmannia squarrosa* Lindl. The type specimen of *L. morrisii* was mistakenly believed to have been collected in Tasmania but was later found to be part of a collection from Western Australia.

Key Words: Liliaceae, Anthericaceae, *Laxmannia*.

INTRODUCTION

In the course of preparation of the account of the Liliaceae for Part 4B of *The Student's Flora of Tasmania* (Curtis & Morris 1994), an unmounted specimen of a *Laxmannia* was found in the collection at the Tasmanian Herbarium (HO) (pl. 1). Accompanying the specimen was a note in the handwriting of Dr Winifred Curtis giving the collection details "W.D.J. Snug Plains or Middlesex Plains ? Jan 1960". "W.D.J." referred to Professor William D. Jackson. A later addition to the note indicated that Professor Jackson thought that it may have been collected at Snug Plains, probably near Grey Mountain.

The *Laxmannia* was not *L. orientalis* Keighery, the only known Tasmanian species, and did not agree with the description of any species of the genus from southeastern Australia. Searches in the Grey Mountain area failed to find more of the plant and the matter was set aside awaiting clarification.

In 1999 when Mr G. J. Keighery, the author of the account of *Laxmannia* in the *Flora of Australia,* vol. 45 (Keighery 1987), was in Hobart he was shown the unidentified specimen. He requested a loan and subsequently published the new species *L. morrisii* Keighery based on this single specimen (Keighery 2002).

In 2003 some unmounted specimens collected by E. Kalmborg from Western Australia in 1938 were incorporated into HO. Two specimens with a label bearing the information "Camp 2 1/2 miles North of Mt Ross, 18.10.38. Tallanalla District" closely resembled *L. morrisii* (pl. 2). I examined the specimens and using Keighery's key and description in the *Flora of Australia* determined them as *L. squarrosa*

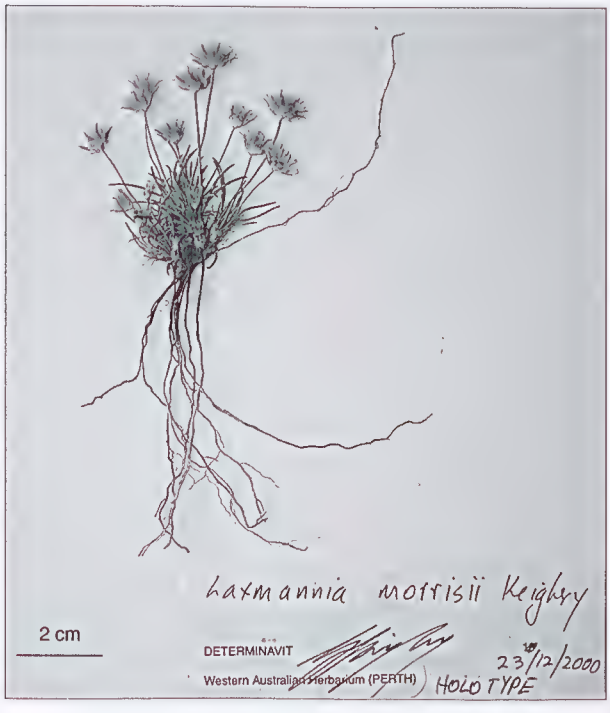

PLATE 1 — Laxmannia morrisii *HO 446141.*

PLATE 2 — Laxmannia squarrosa *HO 326387.*

Lindl. The specimens were identical in all characters with the *L. morrisii*. In his original description of *L. morrisii* in *Nuytsia* Keighery had noted that "The plant is superficially very similar in appearance to some forest populations of *Laxmannia squarrosa*" (Keighery 2002: 378).

DISCUSSION

There appears to be little doubt that the Western Australian specimens and the *L. morrisii* specimen are part of the same collection by E. Kalmborg. It would seem that at some stage, perhaps in 1960, the *L. morrisii* specimen became separated from the two others in the folder and was mistakenly taken to be a collection by Professor Jackson who, when asked many years later, had no clear recollection of having made the collection. Consequently, *L. morrisii* is to be regarded as a synonym of *L. squarrosa* and should be deleted from the *Census of the Vascular Plants of Tasmania*, and the type details in *Australian Plant Name Index* must be corrected.

ACKNOWLEDGEMENTS

I acknowledge with gratitude the contribution of Alex Buchanan, who drew my attention to the Kalmborg collection, and that of Lyn Cave, who produced the photographs.

REFERENCES

CURTIS, W. M. & MORRIS, D. I., [1994] 1995: *The Student's Flora of Tasmania, Part 4B*. St David's Park Publishing, Hobart, Tasmania.

KEIGHERY, G.J., 1987: *Laxmannia. Flora of Australia* 45: 254–264. Australian Government Publishing Service, Canberra.

KEIGHERY, G.J., 2002: A new species of *Laxmannia* (Anthericaceae) from Tasmania and a new subspecies from Western Australia. *Nuytsia* 14(3): 375–380.

(accepted 22 March 2004)

CHARACTERISTICS AND DYNAMICS OF THE SAND DUNE VEGETATION AT NORTH BAY, TASMANIA

by J. B. Kirkpatrick, T. Leaman, A. Pennington and T. Pollard

(with four tables, five text-figures and nine plates)

KIRKPATRICK, J. B., LEAMAN, T., PENNINGTON, A. & POLLARD, T., 2004 (29:x): Characteristics and dynamics of the sand dune vegetation at North Bay, Tasmania. *Papers and Proceedings of the Royal Society of Tasmania* 138: 37–45. ISSN 0080-4703. School of Geography and Environmental Studies, University of Tasmania, Private Bag 78, Hobart, Tasmania 7001, Australia (JBK*, TL, AP, TP). *Author for correspondence.

The vegetation of the coastal sand dunes at North Bay on the Forestier Peninsula was surveyed in 80 quadrats along seven transects. A total of six plant communities was identified; four from the back dunes and two from the fore dunes. The back dunes were dominated by *Banksia marginata* Cav. and the fore dunes by *Spinifex sericeus* R.Br.and *Acacia sophorae* (Labill.) R.Br. Size class analysis of age classes of the back dune vegetation indicated an eventual senescence of the dominant *B. marginata* and a replacement by closed canopy trees from wet eucalypt forest, such as *Notelaea ligustrina* Vent. Two communities were found to be of high conservation significance: a *S. sericeus* grassland from the fore dune and a closed-forest community from the back dunes. Both communities are in a relatively undisturbed state, although the *S. sericeus* grassland has been invaded by exotic herbs. For these significant communities to remain intact, weeds and human activity must be controlled on the fore dunes and fire excluded from the back dunes.

Key Words: *Banksia*, sand dune vegetation, conservation, management, succession, Tasmania.

INTRODUCTION

The coastal sand dune vegetation of Tasmania has close affinities with the coastal sand dune vegetation of the humid temperate parts of southeastern Australia (Kirkpatrick 1993, Clarke 1994). This vegetation has been relatively well-described, both for the State as a whole (Harris 1991, Kirkpatrick 1993, Kirkpatrick & Harris 1995, 1999), and for particular areas (Bowden & Kirkpatrick 1974, Chladil & Kirkpatrick 1989, Harris & Kirkpatrick 1996). However, the two detailed studies of succession in Tasmanian coastal sand dune vegetation (Bowden & Kirkpatrick 1974, Chladil & Kirkpatrick 1989) relate to dune systems that have been subject to a high degree of disturbance from either clearance and stock grazing, or the invasion of marram grass (*Ammophila arenaria* (L.) Link).

North Bay (42°52'S 147°56'E), located on the northern end of the Forestier Peninsula, southeast Tasmania, has one of the few coastal sand dune systems in eastern Tasmania that has not been strongly disturbed by people and has not been invaded by marram grass. Blowouts have been substantial between the 1940s and the present (pls 1, 2), possibly caused by rising sea levels (Komar *et al.* 1991, Healy 1996, Nicholls & Leatherman 1996). The patterns of fires on aerial photographs indicate that two lagoons, Swan Lagoon and Top Lagoon, and their outlet to the sea, have provided a barrier to the movement of fire from adjacent dry eucalypt forest into the dune system (fig. 1, pl. 1). Only two parts of the coastal dune system have been burned since 1946, one between 1966 and 1975, probably in 1967, and one between 1975 and 1986, possibly in 1983. The 1946 photograph clearly shows the effects of fire on a more substantial part of the dune (pl. 1). This may have occurred in the fire year of 1939. Within the area that was not burnt in these fires, there is evidence of an older fire which burned all but a small part of the dune system on which trees of species with aerial parts that are normally killed by fire are substantial enough in size to suggest a century without its incidence. This fire possibly occurred in the fire year of 1898. These four distinct fire ages (putatively 1898, 1939, 1967, 1983) provided us with an opportunity to infer the nature and dynamics of long-term succession in eastern Tasmanian back dune systems. We also describe the zonation patterns on the relatively undisturbed fore dunes and discuss the conservation management needs of the system.

METHODS

A total of 80 5 x 5 m quadrats were surveyed along seven transects, located orthogonally to the line of the dunes (fig. 1). Quadrats were located contiguously in each transect. All species of vascular plant within each quadrat were recorded, using the following cover scale: 1 = < 1%, 2 = 1–5%,

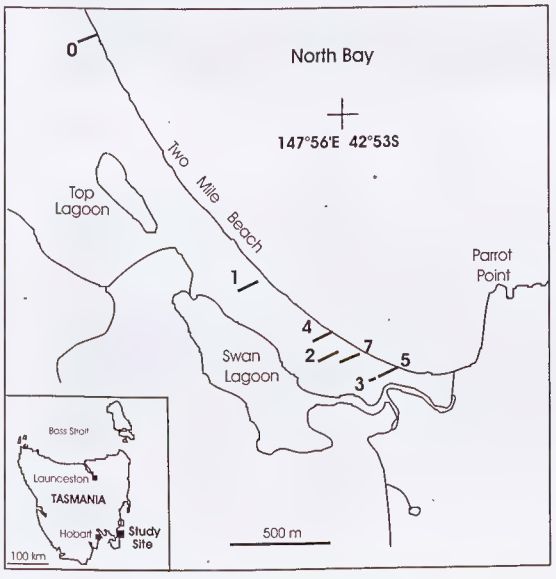

FIG. 1 — Location of North Bay showing the position of the seven transects along the dune system. Transect 6 is the fore dune portion of transect 0.

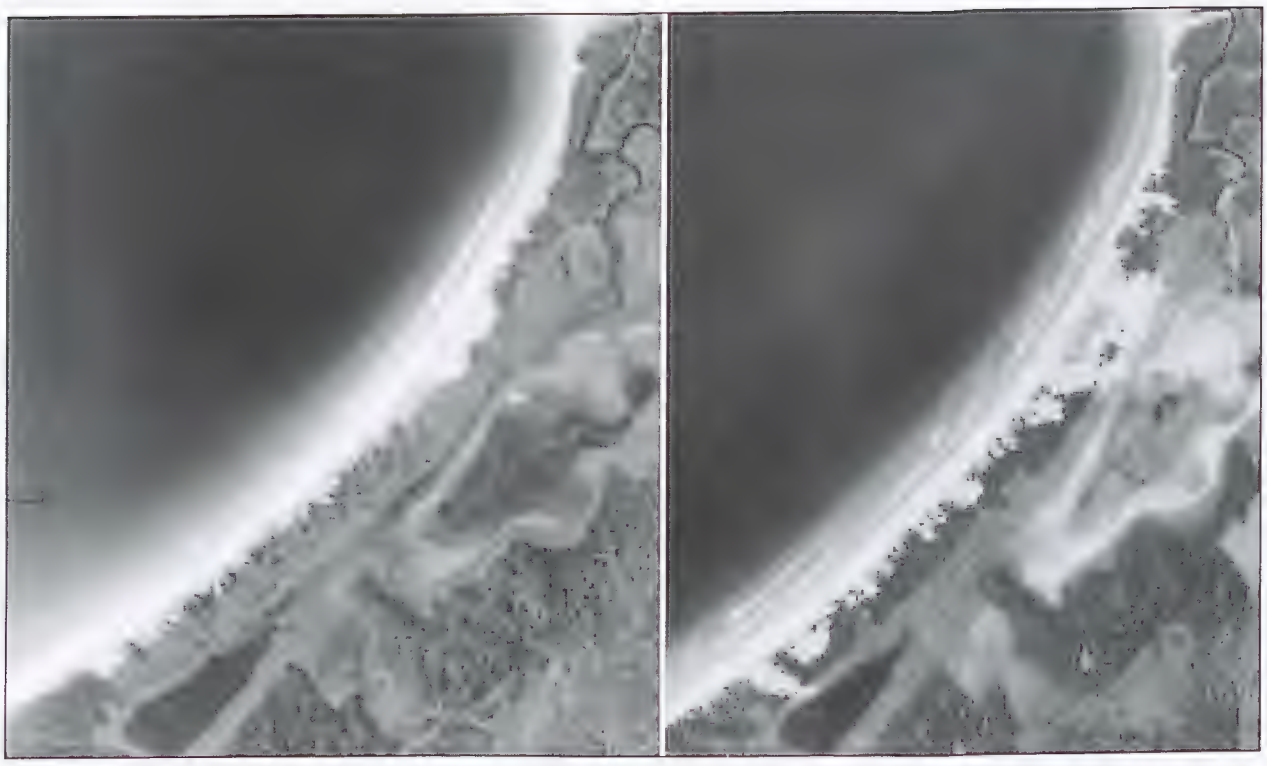

PLATE 1

The dune system in 1946 (left) and 2000 (right). The eastern end of the beach is at the top of the photographs. Note the unburned section between the beach and the dune outlet in 1946, and the transgression of sand between the two dates.

PLATE 2

The major blowout on North Bay Beach. Note Leptospermum lanigerum *in foreground.*

PLATE 3

Spinifex sericeus *grassland on the beach berm.* Cakile *spp. occur to the seaward of* S. sericeus. *Note the receding foredune.*

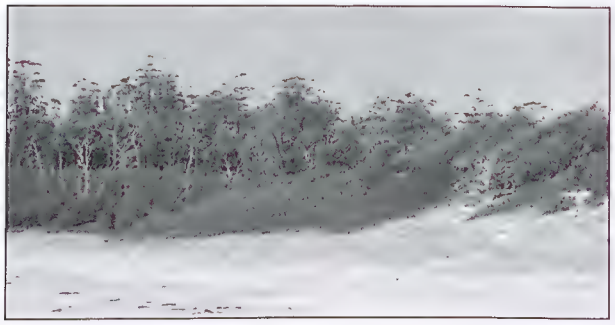

PLATE 4

Spinifex hirsutus *grassland with* Acacia sophorae *heath on the seaward slope of the fore dune at the eastern end of the beach. The live eucalypts in the background are not on the sand dune system.*

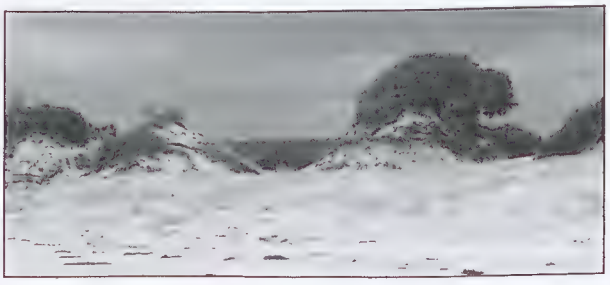

PLATE 5

Exposed Banksia marginata *roots provide evidence of retreat of the line of the foredune. Note the fossil soil horizon exposed by the retreat.* Spinifex sericeus *grassland in the foreground.*

3 = 5–25%, 4 = 25–50%, 5 = 50–75%, 6 = 75–100%. A species was considered to be present if any of its aerial organs were found overhanging the quadrat. Species nomenclature follows Buchanan (1999).

Within each quadrat the location and circumference at breast height (1.3 m) of each stem of all trees were recorded and the basal area calculated. Where a tree had more than one stem, the area of each stem at breast height was calculated. These figures were added to give the basal area for the individual. The height and number of branch whorls of all seedlings of *Banksia marginata* Cav. were also noted. The slope of the quadrat was measured using a clinometer and the soil noted as grey or yellow sand.

The quadrats were ordinated, using the default options for global non-metric multidimensional scaling in DECODA (Minchin 1994). The cover codes were used as input. The scores for dimensions 1 to 4 were used as the input to a classification of quadrats which used Ward's agglomerative method with Euclidean distance in Minitab 13 for Windows. One-way ANOVA was used to test for significant differentiation between ages of back dune forest in the ordination scores and species richness.

RESULTS AND DISCUSSION

Beach Berm and Fore Dune Vegetation

Two of the six communities selected from the dendrogram were located on the seaward side of the fore dunes. These were 4 and 6 (tables 1, 2). Community 4 was a *Spinifex sericeus* R.Br. – (*Austrofestuca littoralis* (Labill.) E. Alexeev) tussock grassland (pl. 3), in which *S. sericeus* was the dominant species, constituting 13.93% of the plant cover and occurring in all the quadrats (tables 1, 2). Other common taxa in the community were *Cakile* spp., with a cover of 1.1% occurring in 30% of surveyed quadrats, *Correa alba* Andrews (0.5% cover in 20% of the quadrats), *Pteridium esculentum* (Forst. f.) Cockayne and *Isolepis nodosa* (Rottb.) R.Br. (both with 0.2% cover and in 20% of the quadrats).

Acacia sophorae (Labill.) R.Br. shrubland occurred where the seaward slope of the foredune was stable (pl. 4). *A. sophorae* was present in all quadrats in group 6 and constituted more than half the plant cover (tables 1, 2). *S. sericeus* and *Carpobrotus rossii* (Haw.) Schwantes were the next most frequent species occurring in 40% of the quadrats, with 13.1% and 0.4% cover respectively (tables 1, 2). A herb that is absent from secure reserves in Tasmania, *Calystegia soldanella* (L.) R.Br., also occurs in the community.

While typical sequences of species on the seaward side of the dunes are shown in figures 2 and 3, it must be noted that the prevailing condition of the dunes was retreat (pls 1, 2), with root systems of *B. marginata* being exposed in many places (pl. 5). The exposure of a palaeosol has given the opportunity for soil-stored seed of a heath plant, *Aotus ericoides* (Vent.) G.Don, to germinate and establish (pl. 6). This species was not observed on any part of the back dune, and may indicate more frequent fire than at present in the eighteenth or nineteenth centuries, as it is usually a component of heath or heathy understories to eucalypt woodland/forest.

The presence of the original native sand-binders (e.g., *S. sericeus* and *A. littoralis*), and the relatively low abundance of introduced species, is a distinct feature of the fore dune vegetation at North Bay. Many Tasmanian beaches, especially those of the north and east coasts, have been invaded by the exotic species *A. arenaria* and *Euphorbia paralias* L., which have displaced many of the native sand-binding species (Kirkpatrick & Harris 1999). The fore dune vegetation at North Bay has high conservation significance, as it is one of the last beaches on the Tasmanian east coast where the native sand-binders still retain dominance. However, individuals of *E. paralias* have been uprooted by the owners of most of the dunes, and were observed and removed in the course of our data collection.

Succession on the Back Dunes

Four age classes were evident in the back dune vegetation at North Bay. The 1983 age class (0, table 3) still had charcoal on dead large individuals of *B. marginata*, and had numerous *B. marginata* seedlings and shrubs, with whorl counts that varied from 1 to 42 (fig. 4).

The quadrats in this age class all belonged to community one (table 4). *P. esculentum* is the species with the most cover in this community. The relatively open conditions favoured a high species richness, consisting mostly of herbs and grasses (tables 1, 2, 3).

The vegetation of the area of the back dunes that was probably burned in both 1939 and 1967 (1, table 3) was a tangled *B. marginata* closed-scrub interspersed with small patches of *P. esculentum* fernland. The quadrats fell in communities 2, 3 and 5 (table 4), indicating that variation in the vegetation of the back dunes as a whole was not responding only to time since fire. *Leucopogon lanceolatus, Leptospermum scoparium* and *L. lanigerum* were relatively abundant as small trees at this site (table 3). There was a very small basal area of dead stems compared with the older sites, and quadrat species richness was the lowest of all four age classes (table 3). The numerous individuals of *B. marginata* generally have relatively small basal areas (fig. 5), and there are no seedlings.

The quadrats in the area probably last burned in 1939 (age class 2, table 3) supported a *B. marginata* open forest with a scattered layer of small trees of *Monotoca glauca* (Labill.) Druce, in turn overlaying a dense bracken understorey. There was a large proportion of dead stems of *B. marginata*, and a small area near the wetland where *Acacia melanoxylon* R.Br. occurred. The quadrats mostly fell into group 3, but there were some in groups 1 and 2 (table 4). There is a wide range of basal area classes of *B. marginata* in the stand, but few fall in the smaller classes (fig. 5), and there are no seedlings.

A late stage in succession in the back dune vegetation is evident in the area possibly last burned in the fire year of 1898 (age class 3, table 3), where many *B. marginata* individuals are dead or dying (pl. 7). The mean basal area of dead stems of *B. marginata* is approximately two-thirds of the mean basal area of live stems (table 3). Large and healthy individuals of *Notelaea ligustrina* Vent., *Pittosporum bicolor* Hook., *Olearia argophylla* (Labill.) Benth. and *Coprosma quadrifida* (Labill.) Robinson (table 3) appear to be in the process of forming a closed-canopy forest (pl. 7). However, no seedlings of any tree species were found in the quadrats. Dense and tall bracken occurs everywhere except directly under the densest parts of the tree canopies (pl. 8). This dense cover may inhibit tree establishment. There is some evidence that the above species have established adjacent

TABLE 1
Mean percentage cover of species by communities defined by floristic composition

	Community					
Species	1	2	3	4	5	6
Atriplex cinerea	–	–	–	0.05	–	–
Austrofestuca littoralis	–	–	–	0.1	–	–
Cakile spp.*	–	–	–	1.1	–	–
Calystegia soldanella	–	–	–	0.05	–	–
*Euphorbia paralias**	–	–	–	0.05	–	–
Spinifex sericeus	–	0.2	–	13.925	–	13.1
Correa alba	–	0.2	–	0.5	–	–
Rhagodia candolleana	5	–	–	0.05	–	–
Acacia sophorae	–	1.267	–	–	–	56.1
Carpobrotus rossii	–	0.333	–	–	–	0.4
Isolepis spp.	–	0.2	0.071	0.2	–	–
Pelargonium australe	–	0.067	0.071	0.15	–	–
Actites megalocarpa	–	0.2	0.071	0.15	0.063	0.2
Pteridium esculentum	38.727	17.2	9.357	0.2	29.656	0.2
Leucopogon parviflorus	1.909	5.167	1.357	0.05	–	–
Austrodanthonia setacea	4.909	–	0.071	–	–	0.2
Acacia melanoxylon	–	2.5	–	–	–	–
Carex appressa	–	0.067	–	–	–	–
Deyeuxia spp.	–	0.067	–	–	–	–
Dichelachne crinita	–	0.133	–	–	–	–
Olearia phlogopappa	–	0.2	–	–	–	–
Picris spp.*	–	0.067	–	–	–	–
*Acetosella vulgaris**	0.273	0.067	–	–	–	–
Leptinella reptans	0.091	0.067	–	–	–	–
Senecio minimus	0.727	0.133	–	–	–	–
Wahlenbergia spp.	1.909	0.067	–	–	–	–
*Leontodon taraxacoides**	–	0.067	0.071	–	–	–
Lobelia alata	–	0.133	0.143	–	–	–
Solanum laciniatum	–	0.067	0.214	–	–	–
Dianella tasmanica	0.636	0.067	–	–	0.063	–
Leptospermum scoparium	–	1.4	0.357	–	0.125	–
Senecio spp.	–	0.133	0.357	–	0.375	–
Agrostis billardierei	0.182	0.4	0.714	–	0.25	–
Banksia marginata	10.5	13.567	51.893	–	12.938	–
Dichondra repens	1.091	0.2	0.357	–	0.063	–
Lomandra longifolia	8	0.067	0.429	–	4.344	–
Olearia lirata	10.318	0.133	5.571	–	2.469	–
Oxalis perennans	2.182	0.067	0.143	–	0.063	–
Coprosma quadrifida	–	–	–	–	11.406	–
Goodenia lanata	–	–	–	–	0.063	–
Laginifera stipitata	–	–	–	–	0.063	–
Notelaea ligustrina	–	–	–	–	15.938	–
Olearia argophylla	–	–	–	–	7.188	–
Pittosporum bicolor	–	–	–	–	16.75	–
Selliera radicans	–	–	–	–	0.063	–
Acacia verticillata	1.636	–	–	–	0.188	–
Hydrocotyle hirta	–	–	0.357	–	0.688	–
Leucopogon lanceolatus	–	–	7.143	–	1.125	–
Monotoca glauca	–	–	10.857	–	2.125	–
Polystichum proliferum	–	–	0.357	–	4.594	–
Viola hederacea	–	–	0.071	–	0.125	–
Ehrharta stipoides	0.818	–	0.071	–	0.063	–
Acaena novae–zelandiae	0.091	–	–	–	–	–
Aira sp.*	3.455	–	–	–	–	–
Astroloma humifusum	0.818	–	–	–	–	–

* exotic taxon.

TABLE 2
Percentage frequency of species by communities defined by floristic composition

Species	Community 1	2	3	4	5	6
Atriplex cinerea	–	–	–	5	–	–
Austrofestuca littoralis	–	–	–	10	–	–
Cakile spp.*	–	–	–	30	–	–
Calystegia soldanella	–	–	–	5	–	–
*Euphorbia paralias**	–	–	–	5	–	–
Spinifex sericeus	–	6.67	–	100	–	40
Correa alba	–	6.67	–	20	–	–
Rhagodia candolleana	63.64	–	–	5	–	–
Acacia sophorae	–	20	–	–	–	100
Carpobrotus rossii	–	20	–	–	–	40
Isolepis spp.	–	20	7.14	20	–	–
Pelargonium australe	–	6.67	7.14	15	–	–
Actites megalocarpa	–	6.67	7.14	15	6.25	20
Pteridium esculentum	100	100	42.86	20	100	20
Leucopogon parviflorus	45.45	60	21.43	5	–	–
Austrodanthonia setacea	72.73	–	7.14	–	–	20
Acacia melanoxylon	–	6.67	–	–	–	–
Carex appressa	–	6.67	–	–	–	–
Deyeuxia spp.	–	6.67	–	–	–	–
Dichelachne crinita	–	13.33	–	–	–	–
Olearia phlogopappa	–	6.67	–	–	–	–
Picris spp.*	–	6.67	–	–	–	–
*Acetosella vulgaris**	9.09	6.67	–	–	–	–
Leptinella reptans	9.09	6.67	–	–	–	–
Senecio minimus	36.36	13.33	–	–	–	–
Wahlenbergia spp.	45.45	6.67	–	–	–	–
*Leontodon taraxacoides**	–	6.67	7.14	–	–	–
Lobelia alata	–	13.33	14.29	–	–	–
Solanum laciniatum	–	6.67	7.14	–	–	–
Dianella tasmanica	27.27	6.67	–	–	6.25	–
Leptospermum scoparium	–	20	21.43	–	12.5	–
Senecio spp.	–	13.33	21.43	–	37.5	–
Agrostis billardierei	18.18	13.33	28.57	–	25	–
Banksia marginata	100	86.67	100	–	93.75	–
Dichondra repens	72.73	20	21.43	–	6.25	–
Lomandra longifolia	90.91	6.67	28.57	–	56.25	–
Olearia lirata	63.64	13.33	21.43	–	18.75	–
Oxalis perennans	54.55	6.67	14.29	–	6.25	–
Coprosma quadrifida	–	–	–	–	75	–
Goodenia lanata	–	–	–	–	6.25	–
Laginifera stipitata	–	–	–	–	6.25	–
Notelaea ligustrina	–	–	–	–	37.5	–
Olearia argophylla	–	–	–	–	18.75	–
Pittosporum bicolor	–	–	–	–	37.5	–
Selliera radicans	–	–	–	–	6.25	–
Acacia verticillata	18.18	–	–	–	6.25	–
Hydrocotyle hirta	–	–	35.71	–	56.25	–
Leucopogon lanceolatus	–	–	14.29	–	12.5	–
Monotoca glauca	–	–	50	–	25	–
Polystichum proliferum	–	–	21.43	–	31.25	–
Viola hederacea	–	–	7.14	–	12.5	–
Ehrharta stipoides	45.45	–	7.14	–	6.25	–
Acaena novae–zelandiae	9.09	–	–	–	–	–
Aira sp.*	72.73	–	–	–	–	–
Astroloma humifusum	45.45	–	–	–	–	–

* Exotic taxon.

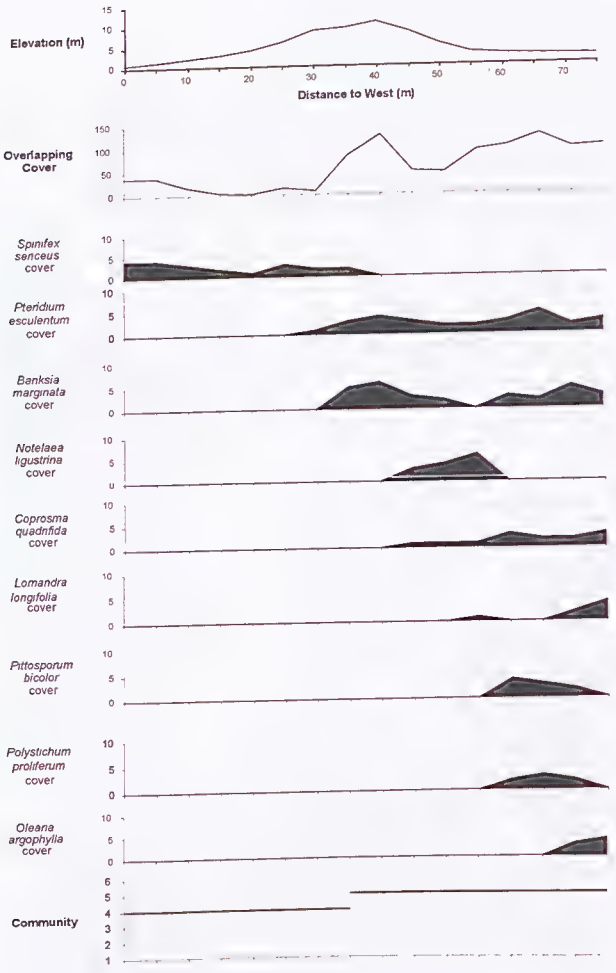

FIG. 2 — Topography, overlapping cover and species cover code value for plant species at transects 3 and 5.

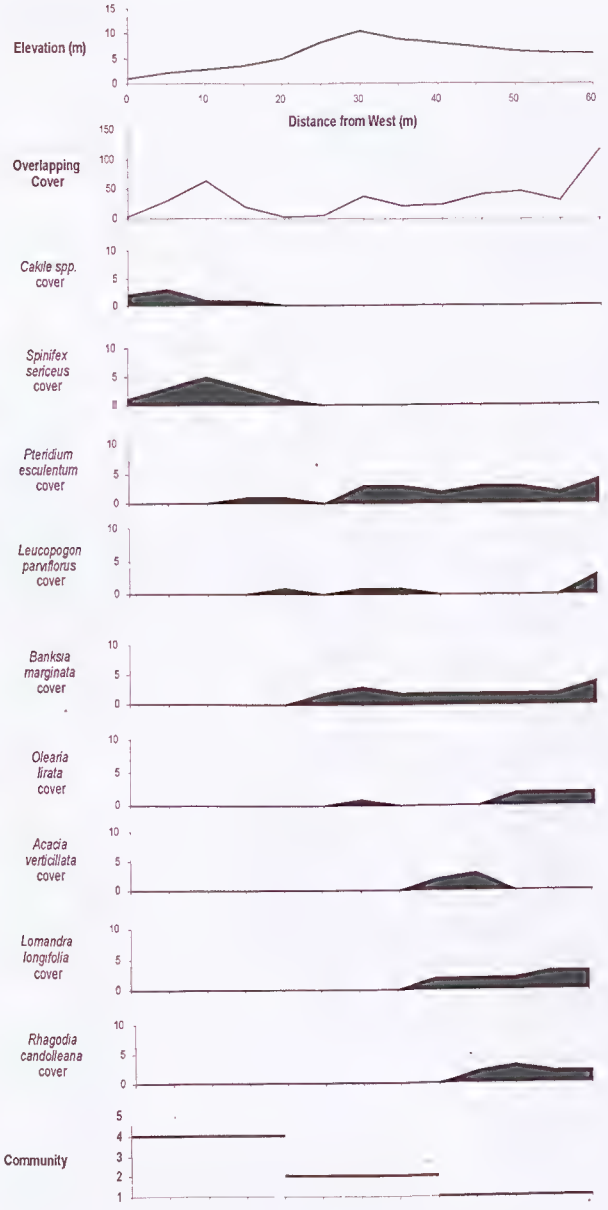

FIG. 3 — Topography, overlapping cover and species cover code value for plant species at transect 6.

to the trunks of individuals of *B. marginata* (pl. 8). This may relate to a high likelihood of bird-dispersed species being found under perching trees, or to the relative lack of shoot competition where the *B. marginata* roots inhibit bracken growth.

Between the *B. marginata* scrub and forest and the wetland herbfields to the rear, there is a zone of low closed forest dominated by *A. melanoxylon* and a zone of closed scrub dominated by *Leptospermum lanigerum* (Aiton) Smith. The large blowout dune shown in plate 2 has partly buried both these zones and large areas of *B. marginata* forest. Only *L. lanigerum* has been able to survive this burial, protruding anomalously from the top of the tallest dune in the system (pl. 2).

At the eastern end of the back dunes there are several large dead eucalypts (pl. 9). The canopies of these eucalypts are visible in the 1946 photograph. As the area has not been burned since 1946, we assume that the eucalypts died of old age.

CONSERVATION AND MANAGEMENT

The *S. sericeus* grassland has the higher conservation significance of the two communities on the fore dunes at North Bay. Despite being well-reserved in Tasmania (Kirkpatrick & Harris 1995), it does not occupy a large area, due to its displacement by exotic species such as *A. arenaria* and *E. paralias* and destruction by off-road vehicles. The unreserved herb *C. soldanella* also occurs in the fore dune vegetation. The *S. sericeus* grassland at North Bay is of high conservation significance not only in terms of the vegetation it contains, but also for the local beach-nesting birds such as the Hooded Plover (*Thinornis rubricollis* Mathews, 1912). The Hooded Plover uses the open vegetation above the high tide mark for nesting sites. On beaches where introduced species, especially *A. arenaria,* have established, the vegetation is transformed from an open grassland to a closed, much more dense one

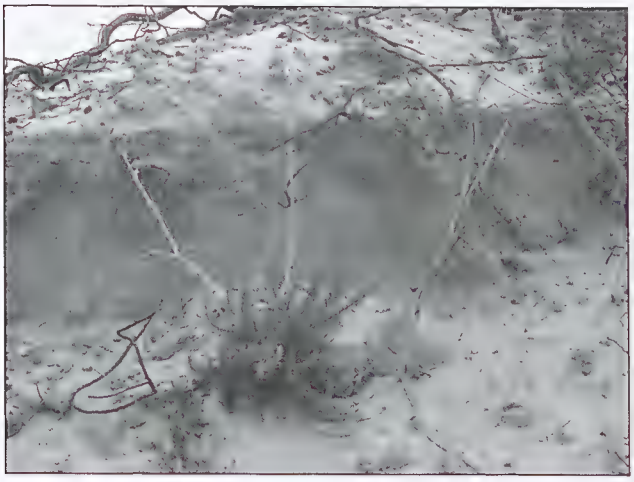

PLATE 6
Aotus ericoides, *still attached to the exposed fossil soil horizon within the truncated fore dune.*

PLATE 7
Closed canopy trees, including Notelaea ligustrina *and* Pittosporum bicolor *among senescing* Banksia marginata.

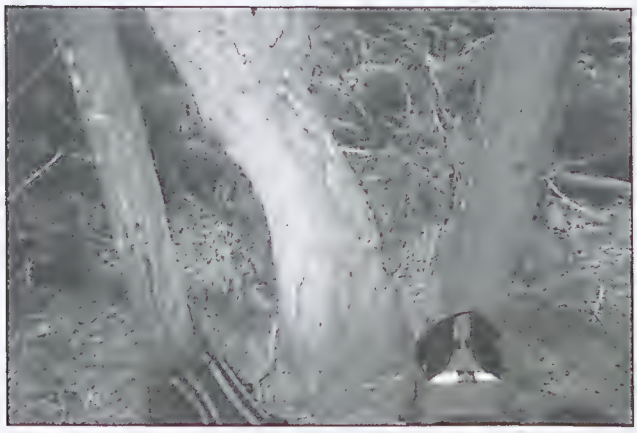

PLATE 8
Two Pittosporum bicolor *trunks on either side of a dead* Banksia marginata.

PLATE 9
Dead eucalypt at the eastern end of the back dune system.

where the Hooded Plover, and other beach-nesting birds, are prevented from establishing their nests. These birds prefer the open vegetation where they nest among natural debris and, occasionally, in *C. rossii*. Thus it is imperative that the integrity of the fore dune vegetation be maintained, through the prevention of weed establishment and the continued exclusion of off-road vehicles. Both *A. arenaria* and *E. paralias* are spread by ocean currents and collectively are the most serious threats to coastal biodiversity in Tasmania. Landowners and users of the beach at North Bay need to be vigilant to prevent the establishment of these exotic species. Monitoring of the fore dune vegetation must be constant in order to recognise the arrival of exotic species and remove them before they can become established.

The vegetation of the long-unburned part of the back dune system is not replicated in eastern Tasmania, although a form of peat-forming rainforest is known from long-unburned coastal dunes in southwest Tasmania (Jarman *et al.* 1991). Thus, although we have some indication in the vegetation (pls 6, 9) that the dune system may have been burned more frequently in the past, continued exclusion of fire seems the best management option to maintain overall diversity in Tasmania's coastal vegetation, while obviously potentially leading to the local depletion of some disturbance-requiring coastal species.

The area of closed-forest, behind the dunes at North Bay and the *B. marginata* sand dune scrub/forest community, are important features of the back dune vegetation. *B. marginata* sand dune scrub is poorly-reserved in Tasmania (Kirkpatrick & Harris 1995), while closed forests dominated by *N. ligustrina* occupy only a small area of Tasmania, but are widely distributed, usually confined to deep, south-facing rocky gullies in the driest parts of the State, where there is topographic protection from the northwest; the direction followed by most fire fronts in Tasmania.

While the exclusion of fire is the major management requirement for the back dune vegetation, there is also a possibility of invasion of the dunes from a population of Montpellier Broom (*Genista monspessulana* (L.) L.Johnson) currently established behind Lagoon Bay, about 1 km from the eastern end of North Bay. Eradication of this stand would remove this possibility.

A major cause of loss of the back dune vegetation has been burial by sand blown from the beach in a large number of blowouts. It may be worth attempting to stabilise the blowouts at the eastern end of the beach, where the closed forest is currently being overwhelmed, although general stabilisation is probably both inappropriate and futile. Given the low degree of anthropogenic disturbance of the dune system, the blowouts seem most likely to be attributable to

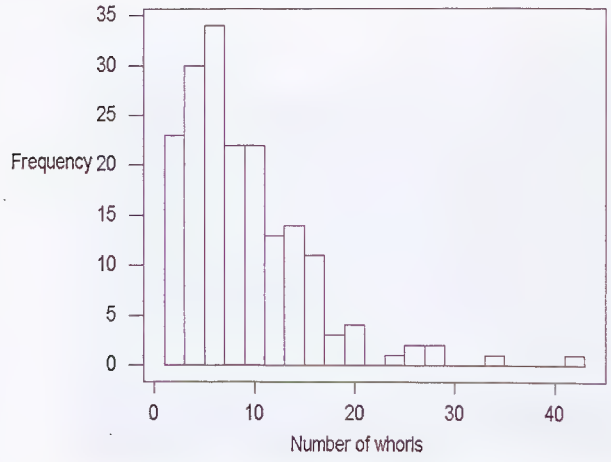

FIG. 4 — Number of whorls counted on seedlings at site 0.

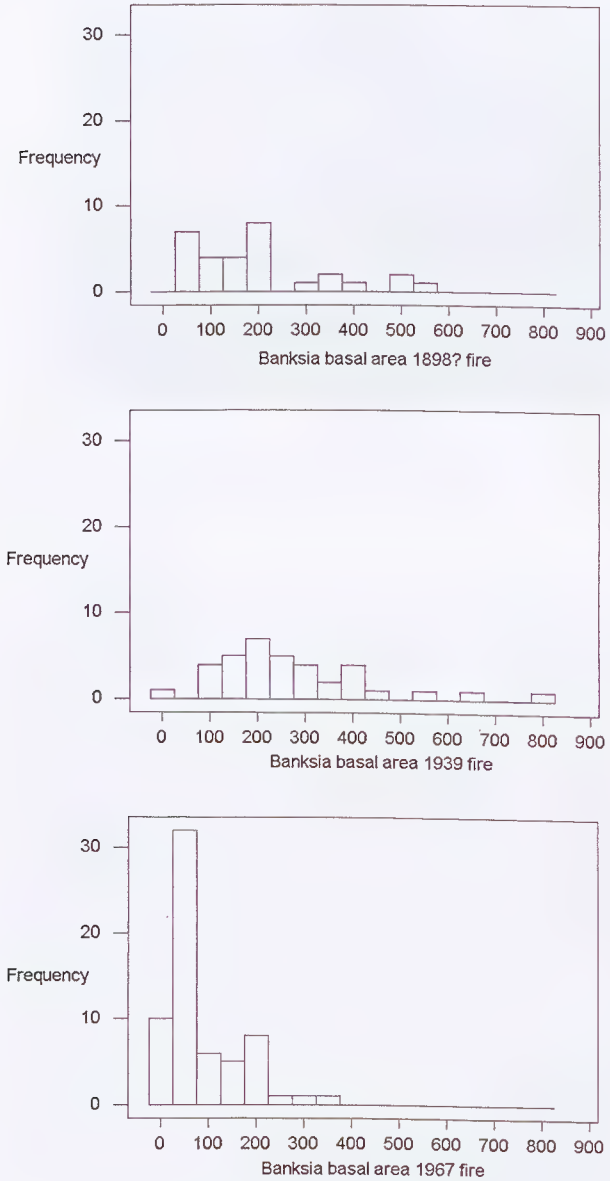

FIG. 5 — Size class distributions of banksias at varying ages since last fire. Figures are cm²/25 m².

TABLE 3
Means for basal area variables, ordination scores, and species richness for the four age classes of back dune vegetation.

	Age Class*			
	0	1	2	3
	n = 10	n = 10	n = 10	n = 15
Live basal area (cm²/25 m²)				
Acacia melanoxylon	0	0	80	0
Banksia marginata	0	528	1138	386
Cassinia aculeata	0	17	0	0
Coprosma quadrifida	0	0	0	34
Leptospermum lanigerum	0	6	0	0
Leptospermum scoparium	0	51	0	0
Leucopogon lanceolatus	0	57	7	0
Monotoca glauca	0	10	21	15
Notelaea ligustrina	0	0	0	60
Olearia argophylla	0	0	0	48
Olearia lirata	0	0	0	1
Pittosporum bicolor	0	0	0	108
Total basal area	0	669	1246	652
Dead basal area (cm²/25 m²)				
Acacia melanoxylon	0	0	19	0
Banksia marginata	579	1	432	243
Cassinia aculeata	0	4	0	0
Olearia argophylla	0	0	0	33
Leucopogon lanceolatus	0	32	0	0
Monotoca glauca	0	0	0	7
Total basal area	579	37	455	283
Floristics and richness				
Ordination score axis 1	0.84	0.74	0.84	0.61 NS
Ordination score axis 2	0.11	-0.18	-0.43	0.30 ***
Ordination score axis 3	-0.14	0.16	-0.21	0.34 ***
Ordination score axis 4	-0.41	0.43	0.16	-0.14 ***
Species richness	10.9	5.7	8.5	6.4 **

* 0 = youngest, 3 = oldest.
NS = P > 0.05, ** = P < 0.01, *** = P < 0.001

the recent accelerated rise in sea level (Cazenave *et al.* 2003), a phenomenon not controllable by local action.

ACKNOWLEDGEMENTS

We thank those members of the 2003 Vegetation Management class at the University of Tasmania who helped us collect the data used in this paper, and Tom and Cynthia Dunbabin for allowing us access to their property. The aerial photographs are used with the kind permission of the Department of Primary Industries, Water and Environment

REFERENCES

BOWDEN, A.R. & KIRKPATRICK, J.R., 1974: The vegetation of the Rheban Spit, Tasmania. *Papers and Proceedings of the Royal Society of Tasmania* 108: 199–210.

BUCHANAN, A.M., 1999: *A Census of the Vascular Plants of Tasmania.* Tasmanian Museum and Art Gallery, Hobart.

CAZENAVE, A., CABANES, C., DOMINH, K., GENNERO, M.C. & LE PROVOST, C., 2003: Present day sea level change: observations and causes. *Space Science Reviews* 108: 131–144.

CHLADIL, M. & KIRKPATRICK, J.B., 1989: A transect study of the sand dune vegetation of Bakers Beach, Tasmania. *Papers and Proceedings of the Royal Society of Tasmania* 123: 247–256.

CLARKE, P.J., 1994: Coastal dune vegetation. *In* Groves, R.H. (Ed.): *Australian Vegetation.* 2nd edn. Cambridge University Press, Cambridge: 501–521.

HARRIS, S., 1991: Coastal vegetation. *In* Kirkpatrick, J.B. (Ed.): *Tasmanian Native Bush: a Management Handbook.* Tasmanian Environment Centre, Hobart: 128–147.

HARRIS, S. & KIRKPATRICK, J.B., 1996: The coastal vegetation of northeast Tasmania. *Records of the Queen Victoria Museum, Launceston* 103: 121–131.

HEALY, T., 1996: Sea level rise and impacts on nearshore sedimentation: an overview. *Geologische Rundschau* 85: 546–553.

JARMAN, S.J., BROWN, M.J. & KANTVILAS, G., 1991: *Floristic and Ecological Studies in Tasmanian Rainforest.* Tasmanian NRCP Report No. 3.

KIRKPATRICK, J.B., 1993: Dry coastal ecosystems of southeastern Australia. *In* E. van der Maarel (Ed.): *Ecosystems of the World 2B: Dry Coastal Ecosystems – Africa, America, Asia and Oceania.* Elsevier, Amsterdam: 273–288.

KIRKPATRICK, J.B. & HARRIS, S., 1995: *The Conservation of Tasmanian Dry Coastal Vascular Plant Communities.* Department of Environment and Land Management, Hobart.

KIRKPATRICK, J.B. & HARRIS, S., 1999: Coastal, heath and wetland vegetation. *In* Reid, J.B., Hill, R.S., Brown, M.J. & Hovendon, M. (Eds): *Vegetation of Tasmania.* Australian Biological Resources Study, Canberra: 304-332.

KOMAR, P.D., LANFREDI, N., BABA, M., DEAN, R.G., DYER, K., HEALY, T., IBE, A.C., TERWINDT, J.H.J. & THOM, B.G., 1991: The response of beaches to sea-level changes – a review of predictive models. *Journal of Coastal Research* 7: 895–921.

MINCHIN, P.R., 1994: *DECODA: Database for Ecological Community Data. Version 2.04.* Research School of Pacific Studies, ANU, Canberra.

NICHOLLS, R.J. & LEATHERMAN, S.P., 1996: Adapting to sea-level rise: relative sea-level trends to 2100 for the United States. *Coastal Management* 24: 301–324.

(accepted 31 May 2004)

VEGETATION PATTERNS ASSOCIATED WITH A LARGE ROCK PLATE IN THE MEEHAN RANGE, TASMANIA

by Kevin E. Leeson and J. B. Kirkpatrick

(with two tables, one plate and three text-figures)

LEESON, K. E. & KIRKPATRICK, J. B., 2004 (29:x): Vegetation patterns associated with a large rock plate in the Meehan Range, Tasmania. *Papers and Proceedings of the Royal Society of Tasmania* 138: 47-52. ISSN 0080-4703. School of Geography & Environmental Studies, University of Tasmania, Private Bag 78, Hobart, Tasmania 7001, Australia. (KEL*, JBK). *Author for correspondence.

Rock outcrops provide unusual environmental conditions, often being the habitats of disjunct populations or rare species. A large rock plate on Mt Direction, within the Meehan Range, southeastern Tasmania, supports an open-heath of unusual floristic composition, and contains the only known population of *Ozothamnus reflexifolius* Leeson & Rozefelds. Four floristic communities occur on and around the plate, forming a sequence from the open-heath on the plate itself to tall woodland with a dense understorey of small trees where rock and bare ground cover are low. Patterns of moisture availability, related to soil depth, aspect, slope and topographic position seem to best explain the floristic, structural and species richness patterns in the area.

Key Words: rock outcrop, skeletal soils, *Ozothamnus reflexifolius*, Tasmania.

INTRODUCTION

Rock plates and the skeletal soils that surround them provide an extreme habitat for vascular plant species within any region (e.g., Kruckerberg & Rabinowitz 1985, Baskin & Baskin 1988, Mishio 1992, Medail & Verlaque 1997, Porembski & Barthlott 2000, Poot & Lambers 2003). Complex patterns of shedding and accumulation of moisture in response to variations in topography and soil depth can induce high local heterogeneity in the vegetation, which often contains disjunct populations of common species, and rare local endemics (Prober & Austin 1990, Prober 1992, Coates 1996, Coates *et al.* 1999, Maisels *et al.* 2000, Wolf *et al.* 2000, Schonswetter *et al.* 2003). While shallow or absent soils induce moisture stress, they also provide a barrier to fire, allowing rare fire-sensitive species to survive in fire-prone landscapes (Coates 1996, Coates *et al.* 1999, Clarke 2002, Leeson & Kirkpatrick 2004). The vegetation of the rock plates of Tasmania has been classified by Gilfedder *et al.* (1997). However, one of the most biologically interesting rock plates in Tasmania, the sole location of the shrub species, *Ozothamnus reflexifolius* Leeson & Rozefelds, was not sampled in that study.

The present paper provides a description of the vegetation of this rock plate and directly adjacent areas, and relates variation in species composition to environmental variables.

THE STUDY AREA

The study area, located in southeastern Tasmania is centred on an unusually large dolerite rock plate (fig. 1). It is approximately 2 ha in area and is divided by an occasional winter creek. Slopes within the study area vary from gentle to 60°. Altitude varies from 200 to 340 m above sea level and aspect ranges from northwesterly through to southwesterly.

Rainfall is less than 600 mm per annum and is generally distributed evenly throughout the year. Annual potential evaporation is approximately 1250 mm. Application of the environmental lapse rate for Mt Wellington (Nunez & Colhoun 1986) indicates that the mean daily maximum temperature of the warmest month is approximately 18°C, while the mean daily minimum temperature of the coolest month is approximately 2.2°C.

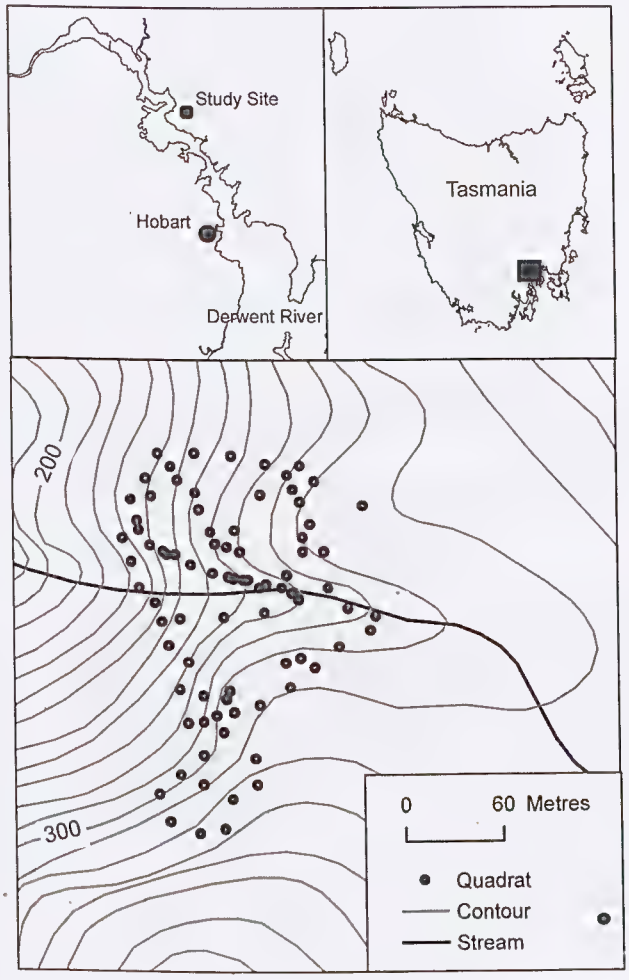

FIG. 1 — Location map, and topography and quadrat locations at the study area.

Soils occurring on the surface of the rock plate are shallow, stony clay-loams containing relatively high levels of organic matter. A gradational change into a shallow duplex clay-loam over a thin reddish-brown clay horizon occurs away from the rock plate. In contrast, these soils contain very little organic matter. Deeper duplex red-brown clay-loam soils are found most distant from the rock plate. The pH of all soils is typically within the range 5.5–6.0.

METHODS

Eighty-three 5 x 5 m quadrats were placed within the study area (fig. 1). Quadrat sampling size was determined by utilising the techniques described by Wiegert (1962). All vascular plant species present within quadrats were recorded and their percentage cover estimated by the one observer within the following Braun-Blanquet cover classes: 1 = 0–0.5%, 2 = 0.5–5%, 3 = 5–25%, 4 = 25–50%, 5 = 50–75%, 6 = >75%. Bare ground, rock and litter were also scored within each quadrat and assigned a relevant cover score. Geocoordinates for all quadrats were recorded during September 2001 with a Garmin GPS12 receiver. Altitude, slope and aspect for each quadrat were also recorded.

All data were entered into the ecological community database, DECODA (Minchin 1994) and an initial sorting of presence-absence data for all 83 quadrats was performed by the polythetic divisive classificatory program, TWINSPAN (Hill 1979). The resulting table was resorted and communities discriminated based on co-occurrence of species.

Global non-metric multidimensional scaling was used to perform an ordination of all 83 quadrats using a Bray-Curtis (1957) dissimilarity matrix (fig. 2). Ten starting configurations were used in two dimensions, using a maximum of 100 repetitions. A stress ratio stopping value of 0.99 and a minimum stress stopping value of 0.01 was applied. Depending on the data structure, ANOVA, the Kruskal-Wallis H test or Chi-squared were used to test the significance of variation in environmental and vegetation variables between groups. Results were taken to be significant if $P < 0.05$. Multiple regression or generalised linear modelling (GLM) were used to develop explanations of variation in the ordination axis scores and species richness.

Nomenclature for all species follows Buchanan (1999).

RESULTS

Four communities were discriminated from the sorted table. Community 1 is characterised by the presence of *Ozothamnus reflexifolius* and a relatively high frequency of *Acianthus caudatus* R.Br., *Allocasuarina verticillata* Labill., *Austrostipa rudis* (Sprengel) S.W.L. Jacobs & J. Everett, *Carex breviculmis* R.Br., *Epacris acuminata* Benth., *Poa rodwayi* Vickery and *Schoenus apogon* Roemer & Schultes. Other species present in this community included *Acacia mearnsii* De Wild., *Astroloma humifusum* (Cav.) R.Br., *Austrodanthonia caespitosa* (Gaudich.) H.P. Linder, *Cheilanthes austrotenuifolia* Quirk & Chambers, *Correa reflexa* (Labill.) Vent., *Dodonaea viscosa* Jacq., *Hibbertia riparia* (R.Br. ex DC.) Hoogl., *Lepidosperma gunnii* Boeck., *Lomandra longifolia* Labill., *Ozothamnus scutellifolius* Hook.f., *Pelargonium inodorum* Willd., *Plantago varia* R.Br., *Themeda triandra* Forsskal and *Thysanotus patersonii* R.Br. (table 1). The quadrats in this community largely fell within the open-heath on the rock plate (pl. 1) and have greater mean species richness than all other communities (table 2).

Community 2 has a high frequency of *Ozothamnus reflexifolius, Allocasuarina verticillata, Astroloma humifusum, Dodonaea viscosa, Lepidosperma gunnii* and *Poa rodwayi.* Additional species recorded are similar to community 1 except for the absence of *Epacris acuminata* and *Pelargonium inodorum.* Species present in this community but absent in community 1 included *Bossiaea prostrata* R.Br., *Bursaria spinosa* Cav., *Eucalyptus globulus* Labill., *Oxalis perennans* Haw. and *Pimelea nivea* Labill. (table 1). The quadrats in this community largely occurred in *Allocasuarina verticillata* low open-forest (pl. 1). The community has lower mean species richness than community 1 and higher mean species richness than community 4 (table 2).

Community 3 had high frequencies of *Allocasuarina verticillata, Astroloma humifusum, Dodonaea viscosa, Lomandra longifolia* and *Poa rodwayi.* These species co-occur in communities 2 and 3 in similar proportions. However, species absent from community 3 but present in communities 1 and 2 include *Ozothamnus reflexifolius, Austrodanthonia caespitosa, Carex breviculmis, Hibbertia riparia, Schoenus apogon, Themeda triandra* and *Thysanotus patersonii.* Species present here but absent from the first two communities include *Acacia melanoxylon* R.Br. in W.T.Aiton, *Allocasuarina verticillata, Asplenium flabellifolium* Cav., *Bedfordia linearis* (Labill.) DC., *Eucalyptus pulchella* Desf. and *Pimelea humilis* R.Br. (table 1). The quadrats in community 3 occur in vegetation in which large emergent *Eucalyptus globulus* occur above a smaller tree layer consisting of *Acacia mearnsii, Acacia melanoxylon, Allocasuarina verticillata, Eucalyptus pulchella, Eucalyptus viminalis* and *Exocarpos cupressiformis* (pl. 1). This community has lower mean species richness than community 1 (table 2).

Community 4 is similar to the other three communities in having a high frequency of *Allocasuarina verticillata, Astroloma humifusum* and *Lomandra longifolia.* Overall, species composition of this community is similar to community 3, except for the presence of *Acaena novae-zelandiae* Kirk and *Austrodanthonia caespitosa* and the absence of *Acacia verticillata, Acacia melanoxylon, Eucalyptus pulchella* and *Pimelea nivea* (table 1). The quadrats in this community largely fall within *A. verticillata* woodland (pl. 1). The community has lower mean species richness than communities 1 and 2.

The four communities occupy largely distinct sections of ordination space (fig. 3), with all communities being statistically distinct on axis 1, and community 3 being distinct from all other communities on axis 2 (table 2).

The environmental variable that most strongly differentiated the communities as a whole was rock cover (table 2). The scores on ordination axis 1 were also most strongly differentiated by this variable (simplified so that classes 4, 5 and 6 of rock cover were merged, GLM, $P < 0.001$). Aspect was significant as a covariate ($P < 0.05$) in the rock cover GLM model for axis 1. A model with the same explanatory components was obtained for mean species richness, which covaried with the ordination score on axis 1 (table 2). Axis 2 of the ordination was very weakly explained by a regression model consisting of altitude and slope (mds2 = 1.44 - 0.0131 Slope - 0.00229 Altitude, $P < 0.05$, R-Sq = 8.9%).

TABLE 1
Percentage frequency of taxa in communities

Species	Community			
	1	2	3	4
Acianthus caudatus	91.67	3.23	18.75	16.67
Austrostipa rudis	83.33	25.81	6.25	4.17
Epacris acuminata	75	-	12.5	4.17
Carex breviculmis	66.67	19.35	-	-
Schoenus apogon	66.67	16.13	-	-
Lepidosperma gunnii	58.33	54.84	18.75	41.67
Themeda triandra	50	12.9	-	-
Cheilanthes austrotenuifolia	50	25.81	18.75	37.5
Austrodanthonia caespitosa	33.33	19.35	-	4.17
Hibbertia riparia	33.33	3.23	-	-
Thysanotus patersonii	25	6.45	-	-
Plantago varia	25	3.23	12.5	4.17
Pelargonium inodorum	8.33	-	-	-
Ozothamnus scutellifolius	8.33	6.45	6.25	8.33
Ozothamnus reflexifolius	100	100	-	-
Pimelea nivea	-	48.39	6.25	-
Bossiaea prostrata	-	3.23	-	-
Poa rodwayi	91.67	100	100	4.17
Dodonaea viscosa	16.67	64.52	87.5	41.67
Lomandra longifolia	33.33	41.94	81.25	66.67
Bursaria spinosa	-	38.71	50	20.83
Eucalyptus pulchella	-	-	37.5	-
Pimelea humilis	-	-	37.5	20.83
Correa reflexa	25	22.58	31.25	8.33
Eucalyptus globulus	-	6.45	25	12.5
Asplenium flabellifolium	-	-	18.75	4.17
Acacia verticillata	-	-	12.5	-
Acacia melanoxylon	-	-	6.25	-
Bedfordia linearis	-	-	6.25	4.17
Allocasuarina verticillata	75	90.32	81.25	95.83
Astroloma humifusum	41.67	58.06	62.5	66.67
Oxalis perennans	-	3.23	37.5	45.83
Acacia mearnsii	8.33	25.81	12.5	41.67
Acaena novae-zelandiae	-	-	-	4.17

Figures in bold are the highest percentage frequencies for taxa.

TABLE 2
Characteristics of communities

	Community				
	1	2	3	4	p
Mean mds 1	1.63A	1.34B	0.85C	0.36D	0.000 (ANOVA)
Mean mds 2	0.48A	0.66A	1.04B	0.57A	0.000 (ANOVA)
Mean species richness	10.67A	8.00B	7.88BC	6.50C	0.000 (ANOVA)
Bare ground > 25% cover (%)	50	67	31	29	0.018 (Chi^2)
Rock > 5% cover (%)	83	58	6	0	0.000 (Chi^2)
Mean elevation (m)	242	260	285	300	0.036 (KW)
Mean slope (°)	17.08A	10.90B	8.75B	11.88AB	0.014 (ANOVA)
Mean aspect (°)	257A	288B	262A	292B	0.007 (ANOVA)

ANOVA = Analysis of variance, KW = Kruskal-Wallis H-test. Values with any letter the same in a row are statistically identical at $p > 0.05$

PLATE 1

Typical views of vegetation types at the study area: ***(A)*** = Allocasuarina verticillata *woodland;* ***(B)*** = Eucalyptus globulus *tall woodland;* ***(C)*** = *rock face vegetation;* ***(D)*** = *open-heath.*

DISCUSSION

Relative degrees of availability of soil moisture seem most consistent with the variation in the vegetation of the study area, with the major axis of floristic variation, and variation in species richness, being strongly related to rock cover and bare ground. This corresponds with a structural change from sparse heath on almost solid rock to tall eucalypt woodland over a dense second stratum of trees where rock cover is negligible. Because soil tends to accumulate more on gentle slopes than on steep slopes, it is not surprising that the rock plate heath is on steeper slopes than most of the other structural communities. The role of aspect in influencing floristic variation is less clear.

Community 1, which occurs in the rockiest situations, has a west-south-west mean aspect, as does the more mesic community 3, while communities 2 and 4 have west-north-west aspects. Given that the strongest and driest winds are northwesterly in southeastern Tasmania, and that insolation is greater on the more northerly slopes, there seems likely to be a moderation of droughtiness related to more southerly aspects. Topographic position is also important for moisture relationships, with the most mesic communities being at the base of the large rock plate.

The rock plate provides the core of the habitat of *Ozothamnus reflexifolius,* only known from this site (Leeson & Rozefelds 2003, Leeson & Kirkpatrick 2004), which even apart from the presence of this species, supports an unusual heath assemblage, not described by Kirkpatrick & Harris (1999) in their statewide conspectus of heath communities, nor by Gilfedder *et al.* (1997) in their classification of Tasmanian rock plate communities. The rock plate with the most similar vegetation to the one described here is on the Lake Leake Road on the seaward slope of the Eastern Tiers, in woodland dominated by *E. pulchella.* This had a Bray-Curtis similarity of only 35% (Leeson and Kirkpatrick 2004). The Mt Direction rock plate is therefore of extremely high conservation significance.

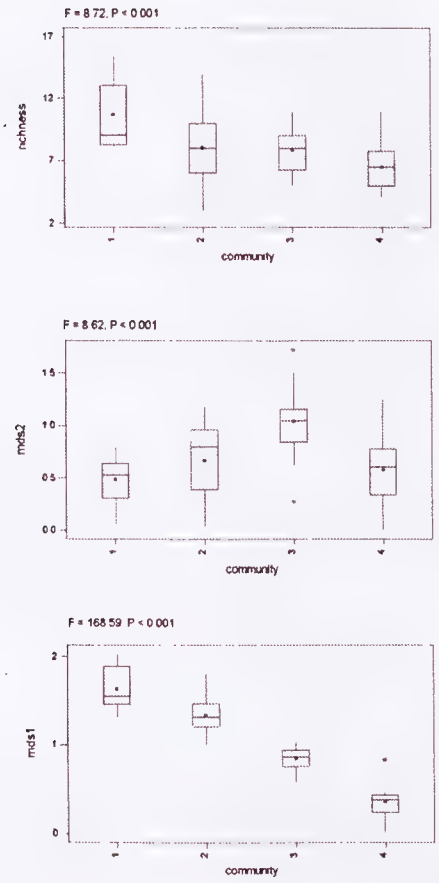

FIG. 2 — Box plots of: mds axis 1 score by community; mds axis 2 score by community; species richness by community. The boxes enclose the 25–75 percentiles, the lines show the ranges and the dots represent the means.

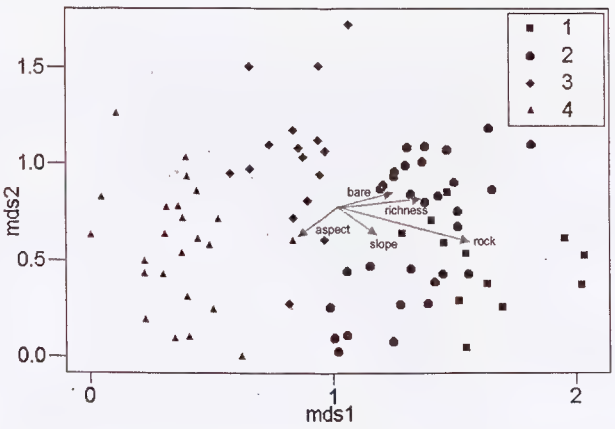

FIG. 4 — Significant vectors in two-dimensional ordination space, showing the distribution of the four communities.

ACKNOWLEDGMENTS

Richard Schahinger from the Threatened Species Unit, Department of Primary Industries, Water and the Environment, Tasmania, is acknowledged for discovery of the population of *Ozothamnus reflexifolius*. Patrick Murray kindly provided assistance with photography and data collection. Mark Fountain, Megan Brown and Michelle Lang from the Royal Tasmanian Botanical Gardens provided advice on various issues and technical support. Mick Russel and Rob Anders kindly provided assistance with GIS applications. Janet Smith assisted with corrections to improve the manuscript.

REFERENCES

BASKIN, J.M. & BASKIN, C.C., 1988: Endemism in rock outcrop plant communities of unglaciated eastern United States: an evaluation of the roles of edaphic, genetic and light factors. *Journal of Biogeography* 15: 829–840.

BRAY, J.R. & CURTIS, J.T., 1957: An ordination of the upland forest communities of southern Wisconsin. *Ecological Monographs* 27: 325–349.

BUCHANAN, A.M., 1999: *A census of the vascular plants of Tasmania and index to* 'The student's flora of Tasmania'. Tasmanian Herbarium Occasional Publication 6, Hobart.

CLARKE, P.J., 2002. Habitat islands in fire-prone vegetation: do landscape features influence community composition? *Journal of Biogeography* 29: 677–684.

COATES, F., 1996: Ecological and biogeographical correlates of rarity in two narrow endemics in Tasmania: *Spyridium microphyllum* (F. Muell. ex Reiseck) Druce and *Spyridium obcordatum* (Hook. f.) W. M. Curtis. Unpubl. PhD thesis. University of Tasmania, Hobart.

COATES, F., KIRKPATRICK, J.B. & MINCHIN, P.R., 1999: Towards an explanation of the causes of the rarity of two Tasmanian *Spyridium* species. *Australian Journal of Ecology* 24: 11–17.

GILFEDDER, L., KIRKPATRICK, J.B. & ZIEGELER, D., 1997: Characteristics and conservation status of rock pavement vegetation in lowland perhumid and subhumid Tasmania. A report to the Australian Heritage Commission from the University of Tasmania. 50 pp.

HILL, M.O., 1979: TWINSPAN: A FORTRAN Program for arranging multivariate data in an ordered two way table by classification of the individual and attributes. Cornell University, New York.

KIRKPATRICK, J.B. & HARRIS, S., 1999. The disappearing heath revisited. Tasmanian Environment Centre, Hobart.

KRUCKERBERG, A.R. & RABINOWITZ, D., 1985: Biological aspects of endemism in higher plants. *Annual Review of Ecology and Systematics* 16: 447–479.

LEESON, K.E. & ROZEFELDS, A.C., 2003: A new endemic *Ozothamnus* species (Asteraceae) from Tasmania, Australia. *Australian Systematic Botany* 16: 317–322.

LEESON, K.E. & KIRKPATRICK, J.B., 2004: Ecological and physiological explanations for the restriction of a Tasmanian species of *Ozothamnus* to a single population. *Australian Journal of Botany* 52: 39–45.

MAISELS, F.G., CHEEK, M. & WILD, C., 2000: Rare plants on Mount Oku summit, Cameroon. *Oryx* 34: 136–140.

MEDAIL, F. & VERLAQUE, R., 1997: Ecological characteristics and rarity of endemic plants from south-eastern France and Corsica: implications for biodiversity conservation. *Biological Conservation* 80: 269–281.

MINCHIN, P.R., 1994: DECODA. Database for ecological community data. Version 2.04. Research School of Pacific Studies, ANU, Canberra.

MISHIO, M., 1992: Adaptations to drought in five woody species co-occurring on shallow soil ridges. *Australian Journal of Plant Physiology* 19: 539–553.

NUNEZ, M. & COLHOUN, E.A., 1986: A note on air temperature lapse rates on Mt Wellington, Tasmania. *Papers and Proceedings of the Royal Society of Tasmania* 120: 11–15.

POOT, P. & LAMBERS, H., 2003: Are trade-offs in allocation pattern and root morphology related to species abundance? A congeneric comparison between rare and common species

in the south-western Australian flora. *Journal of Ecology* 91: 58–67.

POREMBSKI, S. & BARTHLOTT, W., 2000: Granitic and gneissic outcrops (inselbergs) as centers of diversity for desiccation-tolerant vascular plants. *Plant Ecology* 151: 19–28.

PROBER, S.M., 1992: Environmental influences on the distribution of the rare *Eucalyptus paliformis* and the common *E. fraxinoides*. *Australian Journal of Botany* 17: 51–65.

PROBER, S.M. & AUSTIN, M.P., 1990: Habitat peculiarity as a cause of rarity in *Eucalyptus paliformis*. *Australian Journal of Ecology* 16: 189–205.

SCHONSWETTER, P., TRIBSCH, A., SCHNEEWEISS, G.M. & NIKLFELD, H., 2003: Disjunctions in relict alpine plants: phylogeography of *Androsace brevis* and *A. wulfeniana* (Primulaceae). *Botanical Journal of the Linnean Society* 141: 437–446.

WIEGERT, R.G., 1962: The selection of an optimum quadrat size for sampling the standing crop of grasses and forbs. *Ecology* 43: 125–129.

WOLF A.T., HARRISON, S.P., & HAMRICK, J.L., 2000: Influence of habitat patchiness on genetic diversity and spatial structure of a serpentine endemic plant. *Conservation Biology* 14: 454–463.

(accepted 31 May 2004)

A PRELIMINARY CENSUS OF THE MACROFUNGI OF MT WELLINGTON, TASMANIA – THE NON-GILLED BASIDIOMYCOTA

by Genevieve M. Gates and David A. Ratkowsky

(with two appendices)

GATES, G. M. & RATKOWSKY, D. A., 2004 (29:x): A preliminary census of the macrofungi of Mt Wellington, Tasmania – the non-gilled Basidiomycota. *Papers and Proceedings of the Royal Society of Tasmania* 138: 53–59. ISSN 0080–4703. School of Plant Science, University of Tasmania, Private Bag 55, Hobart, Tasmania 7001, Australia (GMG*); School of Agricultural Science, University of Tasmania, Private Bag 54, Hobart, Tasmania 7001, Australia (DAR). *Author for correspondence.

This work is a further contribution towards documenting the macrofungi of Mt Wellington. An earlier publication was confined to 130 named and described species of 'agarics', or gilled fungi. The focus of the present paper is on the non-gilled Basidiomycota with the exception of the sequestrate species, which will be the subject of a separate study. A total of 65 non-gilled species is included here. Further, the acquisition of recent information has added 11 species to the previous list of gilled fungi and enabled two of the names to be revised.
Key Words: Macrofungi, Mt Wellington (Tasmania), non-gilled, Basidiomycota, polypores, boletes, crust fungi, coral fungi, puffballs, stinkhorns, spine fungi, jelly fungi.

INTRODUCTION

A preliminary census of the Mt Wellington 'agarics' identified 130 species of gilled fungi (Ratkowsky & Gates 2002). In this paper, the authors deal with almost all of the remaining previously-named and described Basidiomycota of the macrofungi that were not included in Ratkowsky & Gates (2002). Thus, fungi commonly referred to as 'polypores', 'boletes', 'shelf or crust fungi', 'coral fungi', 'puffballs', 'stinkhorns', 'spine fungi' and 'jelly fungi' are treated here, the exception being sequestrate fungi ('earthballs' or truffle-like fungi), which will be the subject of a separate study. The present work was facilitated by the recent publication of the second part of a comprehensive catalogue and bibliography of Australian fungi (May *et al.* 2003), which completed the listing of all the validly named larger basidiomycetes reported to occur in Australia.

The taxonomy of the larger homobasidiomycetes, which includes the mushrooms and related fungi, was based in the nineteenth century upon the Friesian system with its origins in Persoon (1801). Orders were delimited on the gross morphology of the fruiting bodies and their anatomical features, i.e., whether the fungi were, using informal terms, gilled, poroid, jelly-like, etc. These groupings had the advantage of easy application in the field, making ready recognition the prime factor, ignoring phylogenetic considerations. This became the dominant approach to the classification of homobasidiomycetes until the late 1980s, when attention turned towards the use of DNA to determine phylogenetic relationships. Ratkowsky & Gates (2002) used an old-fashioned concept of Agaricales, which delimited that Order as fungi with gills. Thus, genera such as *Lactarius, Lentinellus* and *Russula* were included in Agaricales, although they are now placed in Russulales (Kirk *et al.* 2001). In contrast, modern studies using nucleotide sequence data show a close affinity of 'puffballs' such as *Bovista* and *Lycoperdon* with the 'agarics' *Agaricus* and *Lepiota* (Moncalvo *et al.* 2002), so that they should all be grouped into Agaricales in a phylogenetic classification. Hence, some of the groupings of genera into Orders in appendices 1 and 2 may appear surprising, these following Kirk *et al.* (2001). One example of this contrast between morphological and phylogenetic classification is that the genera *Clavaria, Clavicorona, Clavulina* and *Ramaria,* all considered informally as 'coral fungi', are found in four different orders in appendix 1.

MATERIALS AND METHODS

The survey zones are those of Ratkowsky & Gates (2002), which includes a map of the survey area, details of the tracks followed and descriptions of the habitats. Fieldwork began on 1 January 1994 and was completed on 31 December 2003. During that time, 249 forays were conducted on Mt Wellington. Material collected was macroscopically described within 24 hours of collection and examined microscopically. Species identification was made by comparison of the detailed macro and micro descriptions with those of published species in the scientific literature. Voucher material for each species has been deposited in the Tasmanian Herbarium (HO) and, wherever sufficient material was available, in the National Herbarium of Victoria (MEL).

RESULTS

The list of non-gilled species in appendix 1 is confined to those taxa that have been validly named and described. This was the approach taken in Ratkowsky & Gates (2002). Hence, the names of the 65 species listed in appendix 1 may be found either in May & Wood (1997) or May *et al.* (2003) or as updated by the interactive catalogue of fungi on the Royal Botanic Gardens Melbourne website (www.rbg.vic.gov.au). The species are arranged alphabetically within each of ten Orders, these conforming to the list given in Kirk *et al.* (2001). Wherever photographs and/or illustrations exist in readily available sources for the species listed in appendix 1, references to these are given.

Four further species of *Mycena* can be added to the list of gilled fungi in Ratkowsky & Gates (2002), and one name change made, as a result of the recent monograph

on that genus by Grgurinovic (2003). In addition, the three species of *Lentinellus* in Tasmania treated by Gates & Ratkowsky (2003) all occur on Mt Wellington and are included in appendix 2, these species having been omitted from Ratkowsky & Gates (2002). A few additional gilled species are included in appendix 2, resulting either from recent collections or from identifications or nomenclatural changes made possible by recent publications.

DISCUSSION

As stressed in Ratkowsky & Gates (2002), the study and documentation of macrofungal species in Australia is in its early stages. Various problems in taxonomy and identification still need to be resolved. Consider, for example, the genus of 'jelly fungi' *Calocera* (Fr. : Fr.) Fr., which produces gregarious, rod-like fruit bodies on wood over a wide range of altitudes on Mt Wellington and in other Tasmanian wet forests. Four *Calocera* species with a Tasmanian type are listed in May *et al.* (2003), viz. *C. australis* McNabb, *C. candida* Lloyd, *C. cuneata* Lloyd, and *C. lutea* (Massee) McNabb. Identifying the specimens to species level is difficult in the absence of a definitive study of the Australian species of the genus, and is beyond the scope of this survey.

The 65 species in appendix 1, the 11 additional gilled species in appendix 2, plus the 130 species of 'agarics' in the appendix of Ratkowsky & Gates (2002), result in a list for Mt Wellington of 206 species. If all the undescribed but recognisable taxa were added to the list, the total would be considerably higher. It is not possible to make an estimate of the total number of macrofungi species on Mt Wellington at the present time. Many additional taxonomic studies will need to be undertaken, especially on species-rich families, before the species count of Mt Wellington macrofungi can be expected to stabilise.

ACKNOWLEDGEMENT

We thank Dr Leif Ryvarden of Oslo, Norway, for identifying many of our polypore collections.

REFERENCES

ARORA, D., 1986: *Mushrooms Demystified.* Second Edition. Ten Speed Press, Berkeley, California. 959 pp.

BERKELEY, M.J., 1859: Fungi, *in* J.D. Hooker, *The Botany of the Antarctic voyage of H.M. discovery ships Erebus and Terror in the years 1839–1843.* Part III. *Flora Tasmaniae.* Vol. 2. *Monocotyledones and Acotyledones.* Lovell Reeve, London: 241–282.

BOUGHER, N.L. & SYME, K., 1998: *Fungi of Southern Australia.* University of Western Australia Press, Nedlands, WA. 391 pp.

COURTECUISSE, R. & DUHEM, B., 1995: *Mushrooms and Toadstools of Britain and Europe.* HarperCollins, London. 480 pp.

CUNNINGHAM, G.H., 1963: The Thelephoraceae of Australia and New Zealand. *Bulletin of the New Zealand Department of Scientific and Industrial Research* 145: 1–359.

CUNNINGHAM, G.H., 1965: Polyporaceae of New Zealand. *Bulletin of the New Zealand Department of Scientific and Industrial Research* 164: 1–304.

FUHRER, B.A., 2001: *A Field Companion to Australian Fungi.* Revised Edition. Bloomings Books, Hawthorn, Victoria. 162 pp.

FUHRER, B.A. & ROBINSON, R., 1992: *Rainforest Fungi of Tasmania and South-2East Australia.* CSIRO, East Melbourne, Victoria. 95 pp.

Gates, G.M. & RATKOWSKY, D.A., 2003: The fungal genus *Lentinellus* in Tasmania. *The Tasmanian Naturalist* 125: 9–13.

GRGURINOVIC, C.A., 1997: *Larger Fungi of South Australia.* The Botanic Gardens of Adelaide and State Herbarium and the Flora and Fauna of South Australia Handbooks Committee, Adelaide. 725 pp.

GRGURINOVIC, C.A., 2003: *The Genus* Mycena *in South-Eastern Australia.* Fungal Diversity Press, Hong Kong. 329 pp.

GRGURINOVIC, C.A. & MALLETT, K. (Eds), 1996: *Fungi of Australia,* Vol. 1A. Australian Biological Resources Study, Canberra. 413 pp.

HONGO, T. & MILLS, A.K., 1988: Five noteworthy larger fungi new to Tasmania, Australia. *Transactions of the Mycological Society of Japan* 29: 351–357.

HOOD, I.A. 1992: *An Illustrated Guide to Fungi on Wood in New Zealand.* Auckland University Press, Auckland, New Zealand. 424 pp.

HOOD, I.A. 2003: *An Introduction to Fungi on Wood in Queensland.* University of New England, Armidale, NSW. 388 pp.

KIRK, P.M., CANNON, P.F., DAVID, J.C. & STALPERS, J.A., 2001: *Dictionary of the Fungi,* 9th edition. CAB International, Wallingford, Oxfordshire. 655 pp.

MACDONALD, R. & WESTERMAN, J., 1979: *A Field Guide to Fungi of South-Eastern Australia.* Nelson, Melbourne. 153 pp.

MALLETT, K. & GRGURINOVIC, C.A. (Eds), 1996: *Fungi of Australia,* Vol. 1B. Australian Biological Resources Study, Canberra. 405 pp.

MARKS, G.C., FUHRER, B.A. & WALTERS, N.E.M. (Huebner, M.L., ed.), 1982: *Tree Diseases in Victoria.* Forests Commission Victoria, Melbourne. 149 pp.

MAY, T.W., MILNE, J., SHINGLES, S. & JONES, R.H., 2003: *Catalogue and Bibliography of Australian Fungi 2. Basidiomycota p.p. & Myxomycota p.p.* (Fungi of Australia, Volume 2B). Australian Biological Resources Study, Canberra. 452 pp.

MAY, T.W. & WOOD, A.E., 1997: *Catalogue and Bibliography of Australian Macrofungi 1. Basidiomycota p.p.* (Fungi of Australia, Volume 2A). Australian Biological Resources Study, Canberra. 348 pp.

MCCANN, I.R., 2003: *Australian Fungi Illustrated.* Macdown Productions, Vermont, Victoria. 128 pp.

MCNABB, R.F.R., 1965: Taxonomic studies in the Dacrymycetaceae. V. *Heterotextus* Lloyd. *New Zealand Journal of Botany* 3: 215–22.

MILLS, A.K., MAY, T.W., FUHRER, B.A., RATKOWSKY, D.A. & RATKOWSKY, A.V., 1997: *Claustula*: the forgotten phalloid. *The Mycologist* 11: 31–35.

MONCALVO, J.-M., VILGALYS, R., REDHEAD, S.A., JOHNSON, J.E., JAMES, T.Y., AIME, M.C., HOFSTETTER, V., VERDUIN, S.J.W., LARSSON, E., BARONI, T.J., THORN, R.G., JACOBSSON, S., CLÉMENÇON, H. & MILLER, O.K., Jr., 2002: One hundred and seventeen clades of euagarics. *Molecular Phylogenetics and Evolution* 23: 357–400.

PERSOON, C.H., 1801. *Synopsis methodica fungorum.* Hendricus Dietrich, Göttingen, Germany. 706 pp.

PETERSEN, R.H., 1988: The clavarioid fungi of New Zealand. *Bulletin of the New Zealand Department of Scientific and Industrial Research* 236: 1–170.

RATKOWSKY, D.A. & GATES, G.M., 2002: A preliminary census of the macrofungi of Mount Wellington, Tasmania – the Agaricales. *Papers and Proceedings of the Royal Society of Tasmania* 136: 89–100.

ROBINSON, R., 2003: *Fungi of the South-West Forests.* Department of Conservation and Land Management, Kensington, Western Australia. 72 pp.

SHEPHERD, C.J. & TOTTERDELL, C.J., 1988: *Mushrooms and Toadstools of Australia.* Inkata Press, Melbourne and Sydney. 162 pp.

VELLINGA, E.C., 2003: *Chlorophyllum* and *Macrolepiota* (Agaricaceae) in Australia. *Australian Systematic Botany* 16: 361–370.

YOUNG, A.M., 2000: *Common Australian Fungi.* Revised Edition. University of New South Wales Press, Sydney. 154 pp.

APPENDIX 1
Species descriptions of Mt Wellington non-gilled Basidiomycetes

[Agaricales]

Clavaria amoena Zoll. & Moritzi – A simple, i.e., unbranched or at most sparingly branched, yellow, robust, club-like coral fungus. Illustrations – Shepherd & Totterdell (1988, p. 127), as *Clavulinopsis amoena*; Fuhrer (2001, p. 88); McCann (2003, p. 85).

Clavaria aurantia Cooke & Massee – Short, slender, simple orange clubs characterise this species, which may be confused with the more robust *Clavaria miniata* (q.v.) or with *Ramariopsis depokensis* (see Bougher & Syme 1998, pp. 336–7), the latter differing in microscopic details. Illustration – Robinson (2003, p. 37), as *Clavulinopsis* aff. *aurantia.*

Clavaria miniata Berk. – Simple clubs characterise this relatively robust orange or red club-like coral fungus. Illustrations – Macdonald & Westerman (1979, p. 101), as *Clavulinopsis miniata*; Young (2000, Plate 5), as *Clavulinopsis miniata*; Fuhrer (2001, p. 89); McCann (2003, p. 85).

Clavaria zollingeri Lév. – This multi-branched, violet or pink-lilac coral fungus may be confused with the similarly-coloured and branched *Ramaria versatilis* Quél. However, the white spores of the genus *Clavaria* distinguish it from the ochre-spored genus *Ramaria.* Illustrations – Fuhrer & Robinson (1992, pp. 62–3); May *et al.* (2003, plate 12).

Fistulina hepatica (Schaeff. : Fr.) Fr. – The 'Beefsteak Fungus' is a cosmopolitan, fleshy, pinkish brown, bracket-forming polypore with an unusual hymenium that is made up of separable tubes. The tubes and pores are bright pink, becoming brown with age. Illustrations – Shepherd & Totterdell (1988, p. 130); Bougher & Syme (1998, pp. 318–9); Fuhrer (2001, p. 116); May *et al.* (2003, plate 15); McCann (2003, p. 82); Robinson (2003, p. 49).

Lycoperdon perlatum Pers. : Pers. – This brown species, with a globose fruit body and prominent sterile base, is usually found on soil. Confusion with *L. pyriforme* (q.v.) is possible, but that species has smaller spores with less definite spines. Illustration – Shepherd & Totterdell (1988, p. 115).

Lycoperdon pyriforme Schaeff. : Pers. – The pear-shaped fruit body, with a greatly reduced sterile base, is usually found on wood. The spores are almost smooth. Illustrations – Fuhrer & Robinson (1992, p. 66); Hood (1992, fig. 26); Young (2000, plate 17); May *et al.* (2003, plate 27); McCann (2003, p. 100).

Macrotyphula juncea (Fr. : Fr.) Berthier – This threadlike fungus is almost inconspicuous amongst the leaves and small twigs on which it grows. The light-coloured, fertile upper portion contrasts with the brown sterile base. Illustrations – Fuhrer (2001, p. 85); McCann (2003, p. 87).

[Boletales]

Boletellus obscurecoccineus (Höhn.) Singer – The deep pink pileus and stipe contrast with the non-bruising yellow tubes and pores. The stipe is long, slender and squamulose. Illustrations – Shepherd & Totterdell (1988, p. 104); Fuhrer & Robinson (1992, p. 60); Bougher & Syme (1998, pp. 304–5); Fuhrer (2001, p. 80); Robinson (2003, p. 33).

Boletus tasmanicus Hongo & A.K. Mills – This medium to large bolete is characterised by its dry, dark reddish brown, finely velvety or finely roughened pileus, yellowish olivaceous tubes with reddish pores, and a subfusoid, reddish brown stipe with faint reticulations. Pores, tubes and stipe bruise blue upon cutting. Illustration – Hongo & Mills (1988, p. 354).

Calostoma fuscum (Berk.) Massee – A puffball in which the peridium is supported by a network composed of strands of gelatinised tissue. The more or less spherical spore sac is protected by a reddish brown, tough, outer cap that falls off at maturity, exposing the thin-walled, orange-mouthed sac. Illustrations – Shepherd & Totterdell (1988, p. 123); Bougher & Syme (1998, pp. 112–3); Fuhrer (2001, p. 94); McCann (2003, p. 102).

Fistulinella mollis Watling – An extremely soft, sticky, bolete with pileus colours varying through a range of creams, buffs and browns. The tubes and pores are usually pink. Illustrations – Bougher & Syme (1998, pp. 306–7); Fuhrer (2001, pp. 79 and 81); McCann (2003, p. 64).

Podoserpula pusio (Berk.) D.A. Reid – The buff-coloured, soft upper surface contrasts with the pink hymenial surface and stipe. An unusual species, having a multi-tiered structure on a central stipe, although it can occur with a shelf-like growth form. Illustrations – Shepherd & Totterdell (1988, p. 130), as *Cantharellus pusio*; Grgurinovic & Mallett (1996, fig. 28); Bougher & Syme (1998, pp. 326–7); Fuhrer (2001, p. 132); McCann (2003, p. 66); Robinson (2003, p. 45).

Scleroderma cepa Pers. : Pers. – The genus is readily recognised and separated from other 'puffballs' and 'earthballs' by its yellow-brown, hard outer peridium and olivaceous to violaceous gleba. Frequently found in soil alongside roads, or in dry sclerophyll environments. Illustrations – Macdonald & Westerman (1979, p. 135), as *S. flavidum*; Shepherd & Totterdell (1988, p. 122), as *S. flavidum*; Grgurinovic & Mallett (1996, fig. 32); May *et al.* (2003, plate 51).

[Cantharellales]

Cantharellus concinnus Berk. – Previously considered an Australian variety of a worldwide species, it is recognised by its apricot-orange colours, funnel shape, and shallow, decurrent lamellae that are often forked or tend to

anastomose. Illustrations – Shepherd & Totterdell (1988, p. 130), as *C. cinnabarina* var. *australiensis*; Fuhrer & Robinson (1992, p. 24), as *C. cibarius* var. *australiensis*; Grgurinovic & Mallett (1996, fig. 46), as *C. cibarius* var. *australiensis*; Bougher & Syme (1998, pp. 312–3), as *C.* aff. *cinnabarina* var. *australiensis*; Young (2000, Plate 4); McCann (2003, p. 65), as *C. cibarius*; Robinson (2003, p. 15), as *C.* aff. *cinnabarina* var. *australiensis*.

Clavulina cristata (Holmsk. : Fr.) J. Schröt. – This is a white or whitish species group with very fine, crested branch tips. The genus *Clavulina* is differentiated from *Clavaria* in having subglobose spores almost completely filled with a guttation drop and 2-spored basidia with incurved sterigmata. Illustration – McCann (2003, p. 86).

Clavulina rugosa (Bull. : Fr.) J. Schröt. – A greyish, branched, sturdy, rugulose species group. Illustrations – Fuhrer (2001, p. 87); McCann (2003, p. 86).

Hydnum repandum L. : Fr. – Pileus very variable with a range of colours from off-white through various shades of buff and brown. The spore-bearing spines may be up to 5 mm long. Illustrations – Shepherd & Totterdell (1988, p. 131); Fuhrer & Robinson (1992, p. 69), a dark form cited as *H.* aff. *repandum*; Grgurinovic & Mallett (1996, fig. 45); Young (2000, plate 8, as *H. crocidens*); Fuhrer (2001, p. 107); May *et al.* (2003, plate 14); McCann (2003, p. 72); Robinson (2003, p. 41).

[Dacrymycetales]

Heterotextus peziziformis (Berk.) Lloyd – A very common unbranched, often top-shaped, yellow 'jelly fungus', found at all altitudes on wet, decaying twigs, branches and logs. Its separation from the almost identical *H. miltinus* (Berk.) McNabb is based on microscopic characters (see McNabb, 1965). Illustrations – Macdonald & Westerman (1979, p. 141); Fuhrer & Robinson (1992, p. 81); Hood (1992, fig. 26); McCann (2003, p. 91), as *H. miltinus*; Robinson (2003, p. 57).

[Hymenochaetales]

Coltricia cinnamomea (Jacq.) Murrill – Recognised by its tough, cinnamon-brown, concentrically zoned pileus with coarse, radiating fibrils and a hymenial surface of small, polygonal pores. Illustrations – Bougher & Syme (1998, pp. 316–7), as *Coltricia oblectans*; Young (2000, plate 21), as *Polyporus oblectans*; May *et al.* (2003, plate 22); McCann (2003, p. 85).

Phellinus wahlbergii (Fr.) D.A. Reid – A concolorous dark brown, chestnut, bay, umber or rusty brown, hard and persisting polypore, it is usually found at the base of dead or dying standing trees. Illustrations – Hood (1992, figs. 56–8); McCann (2003, p. 80).

[Phallales]

Aseroë rubra Labill. – A red, starfish-like stinkhorn that emerges from a 'myco-egg', the fertile area blackish and concentrated near the centre of the arms, which sit on top of a pinkish white sterile column. Illustrations – Shepherd & Totterdell (1988, p. 120); Grgurinovic & Mallett (1996, fig. 23); Grgurinovic (1997, plate 28c); Young (2000, plate 2); Fuhrer (2001, pp. 103); May *et al.* (2003, plate 35); McCann (2003, p. 94).

Beenakia dacostae D.A. Reid – A small, soft, whitish stipitate fungus with the basidia borne on spines. It is often found in dry, sheltered areas in wet forests, such as beneath logs. Despite the spines, the genus is not considered to be related to *Hydnum*. Illustration – Fuhrer & Robinson (1992, p. 63).

Claustula fischeri K.M. Curtis – Characterised by a white 'mycoegg' with violet hues. The endoperidium is a thick gelatinous layer surrounding the white, chambered receptacle enclosing the brown spore mass. Illustration – Mills *et al.* (1997, p. 33).

Geastrum triplex Jungh. – This 'Earthstar' is a form of puffball in which the pinkish or brownish outer peridium splits into 5–8 rays. The inner peridium is a thin, light brown, almost globose sac enclosing the spore-bearing gleba. Illustrations – Macdonald & Westerman (1979, p. 133); Shepherd & Totterdell (1988, p. 116); Fuhrer & Robinson (1992, p. 66), as *G. indicum*; Grgurinovic & Mallett (1996, fig. 31), as *G. indicum*; Fuhrer (2001, p. 95), as *G. indicum*; May *et al.* (2003, plate 25); McCann (2003, p. 96), as *G. indicum*.

Ramaria botrytis (Pers.:Fr.) Ricken var. *holorubella* (G.F. Atk.) Corner – The ochre-coloured spore print of this genus separates it from the white-spored genera *Clavaria* and *Clavulina*. The fruit body of this cauliflower-like species is mainly buff and tan, with pink to vinaceous tips to the branches. Illustration – Fuhrer (2001, p. 92), as *R. holorubella*. The photograph attributed to *R. sinapicolor*, a synonym of *R. lorithamnus*, in Shepherd & Totterdell (1988, p. 129), is probably of *R. botrytis*.

Ramaria lorithamnus (Berk.) R.H. Petersen – The slender, yellow stems of this species distinguish it from others of the genus. Illustrations – Petersen (1988, plate 2–20); McCann (2003, p. 87). The illustration in Shepherd & Totterdell (1988, p. 129), as *R. sinapicolor*, a synonym of *R. lorithamnus*, is a misidentification.

Ramaria ochraceosalmonicolor (Cleland) Corner – Probably the most frequently encountered *Ramaria* in Tasmania with a cauliflower-like habit, this species is very variable in colour, combining various shades of salmon-pink, yellow and orange. In its most typical form, the branches are salmon-pink coloured and the apices yellow-ochre. Illustrations – Macdonald & Westerman (1979, p. 103); Bougher & Syme (1998, pp. 332-3); McCann (2003, p. 87); Robinson (2003, p. 37). The photograph attributed to *R. aurea* in Shepherd & Totterdell (1988, p. 128) is probably of the present species, whereas the one attributed to *R. ochraceosalmonicolor* on the same page may be of some other species.

[Polyporales]

Amauroderma rude (Berk.) Torrend – A brown polypore that may have a central or an excentric stipe, or grow shelf-like from a woody substrate. Fertile surface white, turning red quickly upon injury, eventually becoming black. Illustrations – Marks *et al.* (1982, p. 84); Young (2000, plates 1 and 14); Fuhrer (2001, pp. 113); May *et al.* (2003, plate 18); McCann (2003, p. 74).

Antrodiella citrea (Berk.) Ryvarden – A yellow resupinate polypore, with the brightness of a 'highlighter' pen, sometimes with some shelf development. Illustration – McCann (2003, p. 75), as *A. citra*.

Antrodiella zonata (Berk.) Ryvarden – A polypore with an

apricot-pink, irpicoid (i.e., having broken or irregular spines and grooves) fertile surface, tending to form tiers and cover large areas of the trunks of standing dead trees. The abhymenial surface may have distinct, concentric zones. Previously known by the synonyms *Irpex brevis* or *Irpex zonatus*. Illustrations – Grgurinovic & Mallett (1996, fig. 43); McCann (2003, p. 73).

Aurantiporus pulcherrimus (Rodway) P.K. Buchanan & Hood – A soft, strawberry-red bracket, often but not exclusively found on dead myrtle (*Nothofagus cunninghamii*) in wet forests. Illustrations – Marks *et al.* (1982, p. 87), as *Tyromyces pulcherrimus*; Fuhrer & Robinson (1992, p. 79); McCann (2003, p. 79).

Australoporus tasmanicus (Berk.) P.K. Buchanan & Ryvarden – This bracket fungus is noteworthy for the small area of its usually dark brown abhymenial surface relative to its pale brown, whitish or pinkish hymenial surface. Illustration – Fuhrer & Robinson (1992, p. 76).

Byssomerulius corium (Pers.:Fr.) Parmasto – Whitish, sometimes with pale brown hues, this thin, sheet-forming polypore has varying amounts of development of shelf-like growth and a soft, almost tissue-like texture. Usually on small twigs and branches. Illustrations – Cunningham (1963, plate V, fig. 3), as *Merulius corium*; Hood (1992, fig. 32), as *Meruliopsis corium*.

Fomes hemitephrus (Berk.) Cooke – A common hoof-shaped polypore on wood, whitish in youth, becoming browner with age. The hymenial and abhymenial surfaces are separated internally by a narrow but clearly defined orange zone. It may be confused with *Ganoderma applanatum* (q.v.), but the hymenial surface doesn't bruise as markedly as that of the latter species. Illustrations – Marks *et al.* (1982, p. 88), as *Heterobasidion hemitephrum*; Fuhrer & Robinson (1992, p. 76), as *Fomitopsis hemitephrum*; Mallett & Grgurinovic (1996, fig. 19), as *Fomitopsis hemitephra*; May *et al.* (2003, plate 43).

Fomitopsis lilacinogilva (Berk.) T.E. Wright & J.R. Deschamps – Its lilac colouration distinguishes this fungus from all other polypores found on logs anmd stumps in Tasmania. Illustrations – Macdonald & Westerman (1979, p. 115), as *Trametes lilacino-gilva*; McCann (2003, p. 78).

Ganoderma applanatum (Pers.) Pat. – One of the best-known polypores worldwide, the 'Artist's Conk' is a large brown, bracket-forming fungus noted for its white hymenial surface that readily bruises brown when marked. Illustrations – Macdonald & Westerman (1979, p. 109); Shepherd & Totterdell (1988, p. 135); Fuhrer & Robinson (1992, p. 77); Young (2000, plate 15); McCann (2003, p. 75); Robinson (2003, p. 47).

Gloeoporus taxicola (Pers.:Fr.) Gilb. & Ryvarden – A soft, resupinate polypore with the hymenial surface made up of purple-vinaceous folds and reticulations, the growing edge much paler. Found on the undersides of wet, dead logs. Illustration – Fuhrer & Robinson (1992, pp. 72–3), as *Merulius ravenelii*.

Grifola colensoi (Berk.) G. Cunn. – The compound fruit body, up to 40 cm diameter, is made up of numerous, large overlapping lobes up to 15 cm long radiating outwards from a common attachment. The abhymenial surface is brown to blackish, whereas the hymenial surface is cream to buff at first, becoming darker with age. Illustration – Shepherd & Totterdell (1988, p. 136), as *G.* aff. *frondosa*. Many or all Tasmanian records of *G. frondosa* are probably misidentifications of *G. colensoi*.

Junghuhnia rhinocephala (Berk.) Ryvarden – The coffee, bay, chestnut, or rusty colours of this small shelf-like or sheet-forming polypore, and especially its distinctive, pleasant, sweet odour, persisting long after drying, make this species recognisable in the field. Microscopically, the abundant crystal-coated 'metuloids' aid in identification. Illustrations – Berkeley (1859, plate 182, fig. 8), as *Polyporus rhinocephalus*; Hood (1992, fig. 70), as *Trichaptum rhinocephalum*.

Mycoacia subceracea (Wakef.) G. Cunn. – Forming golden yellow patches on the undersides of fallen branches or small logs, this resupinate fungus has its spore-bearing basidia located on small spines. Illustrations – Fuhrer (2001, p. 109); McCann (2003, p. 72).

Neolentiporus maculatissimus (Lloyd) Rajchenb. – A species that forms medium-sized brackets on the sides of trees and logs, the pores of the hymenial surface often exceeding 1 mm diameter, with the brownish abhymenial surface varying from almost smooth in youth to markedly scaly. Illustrations – Fuhrer (2001, p. 121); May *et al.* (2003, plate 48).

Podoscypha petalodes (Berk.) Pat. – Forming orangy brown, leathery rosettes usually near the base of trees, this fungus has concentric bands on its abhymenial surface and a smooth hymenial surface. Illustrations – Fuhrer (2001, p. 133); May *et al.* (2003, plate 59); McCann (2003, p. 83).

Polyporus melanopus (Sw.:Fr.) Fr. – A tough, leathery polypore on wood with a dark brown stipe, white hymenial surface and a smooth, off-white, brown or dark blood-red pileus. Illustrations – Hood (1992, fig. 91); McCann (2003, p. 81), as *Polyporus* sp.

Postia caesia (Schrad.:Fr.) P. Karst. – This is a species complex, the species of which have small, sausage-shaped spores. All forms, whether soft and spongy, or firm and thin, are sessile on wood and turn greenish blue when bruised. Australian and New Zealand forms described under *Polyporus setiger* Cooke belong to this complex. Its appropriate generic position as a *Postia, Tyromyces* or an *Oligoporus* is yet to be determined. Illustrations – Hood (1992, fig. 81), as *Tyromyces setiger*; Courtecuisse & Duhem (1995, fig. 100), as *Oligoporus caesius*; Hood (2003, fig. 83), as *Tyromyces setiger*.

Postia dissecta (Lév.) Rajchenb. – A thin polypore with individual fruit bodies rarely exceeding 3 cm diameter, forming tiered shelves often at the end of cut logs. Pileus brownish, often with concentric bands, the hymenial surface white. Illustration – Hood (1992, fig. 93), as *Polyporus exiguus*.

Postia pelliculosa (Berk.) Rajchenb. – A spongy polypore with a brown, hairy abhymenial surface and a white or pinkish hymenial surface. It also occurs with a black, hairy abhymenial surface and a yellow hymenial surface. Illustrations – Marks *et al.* (1982, p. 87), as *Tyromyces pelliculosus*; Hood (1992, fig. 82); McCann (2003, p. 79).

Pycnoporus coccineus (Fr.) Bondartsev & Singer – A polypore that forms conspicuous orange-red brackets or shelves on dead wood. Illustrations – Macdonald & Westerman (1979, p. 113), as *P. cinnabarinus*; Bougher & Syme

(1998, pp. 330–1); Fuhrer (2001, p. 127); May *et al.* (2003, plate 50); Robinson (2003, p. 53); McCann (2003, p. 78).

Ryvardenia campyla (Berk.) Rajchenb. – A variable polypore species that often forms a rosette of overlapping tongue-shaped lobes. Its colour may be white, as in the type specimen, or range through various shades of brown and black, and the surface may vary from smooth to rugose. Illustrations – Cunningham (1965, fig. 15), as *Grifola campyla*; Marks *et al.* (1982, p. 88), as *Grifola campyla*; McCann (2003, p. 76).

Ryvardenia cretacea (Lloyd) Rajchenb. – A very large bracket on standing and fallen trees in wet forests, the abhymenial surface is variably coloured, being greyish, off-white or pale brown with a white hymenial surface. Although firm with a chalky texture in youth, the fungus becomes waterlogged in age and falls to the ground as an insect-riddled mass after one or two seasons. Illustrations – Marks *et al.* (1982, p. 86), as *Piptoporus cretaceus*; Fuhrer (2001, p. 120).

Trametes hirsuta (Wulfen:Fr.) Lloyd – A polypore with a grey, off-white or pallid brown, hairy abhymenial surface and a white hymenial surface. Illustration – Fuhrer (2001, p. 128).

Trametes versicolor (L.:Fr.) Lloyd – One of the best-known polypores worldwide, the thin, many-zoned abhymenial surface can have a myriad of colours. Illustrations – Macdonald & Westerman (1979, p. 107); Hood (1992, figs. 110–1); Bougher & Syme (1998, pp. 340–1); Fuhrer (2001, p. 129); McCann (2003, p. 78).

Tyromyces merulinus (Berk.) G. Cunn. – This is an orange-red, usually resupinate polypore, but is also found with some shelf-like growth. Illustrations – Fuhrer & Robinson (1992, p. 78); Hood (1992, fig. 78).

[Russulales]

Clavicorona piperata (Kauffman) Leathers & A.H. Sm. – This whitish, pale pink, pale fawn or pale grey species with a peppery taste is separable from other white-spored coral fungi by its habit on decaying wood and its unique branching pattern, each tier or whorl producing up to six branches, giving it a candelabra-like appearance. It is believed (see Bougher & Syme 1998) that the similar-appearing *Clavicorona pyxidata* (Pers. : Fr.) Doty may not occur in Australia and that Australian records of that species may be misidentifications of the present species. Another species reputed to occur in Australia is *Clavicorona colensoi* (Berk.) Corner, differing in its fainter or delayed peppery taste and its finer stems and branches. Some records of this species may just be small representatives of *C. piperata*. Illustrations – Macdonald & Westerman (1979, p. 99), as *C. pyxidata*; Shepherd & Totterdell (1988, p. 126), as *C. pyxidata*; Fuhrer & Robinson (1992, p. 64), as *C.* aff. *piperata*, but which may be *C. colensoi*; Bougher & Syme (1998, pp. 314–5); Fuhrer (2001, p. 86); McCann (2003, p. 85, lower left and lower right, the latter possibly *C. colensoi*); Robinson (2003, p. 37).

Mucronella pendula (Massee) R.H. Petersen – Found on surfaces of cut logs or on their sheltered undersides, these small, white, stalactite-like oddities may form small, pendulous colonies. Illustrations – Grgurinovic & Mallett (1996, fig. 47); Shepherd & Totterdell (1988, p. 129), as *Myxomycidium pendulum*; Fuhrer (2001, p. 90); May *et al.* (2003, plate 20); McCann (2003, p. 72).

Stereum hirsutum (Willd.:Fr.) Pers. – A very variable shelf-like 'thelephore' with yellow, orange and brownish colours. The abhymenial surface is densely covered with soft hairs. Illustrations –Shepherd & Totterdell (1988, p. 133), as *S. complicatum*; Hood (1992, fig. 39); Mallett & Grgurinovic (1996, fig. 20); Bougher & Syme (1998, pp. 338–9); Fuhrer (2001, p. 135); McCann (2003, p. 83); Robinson (2003, p. 45).

Stereum illudens Berk. – The purple-vinaceous shades of the hymenial surface contrast with the brown zones of the abhymenial surface. Illustrations – Macdonald & Westerman (1979, p. 121), as *Xylobolus illudens*; Fuhrer & Robinson (1992, p. 74–5); Fuhrer (2001, p. 136); May *et al.* (2003, plate 58); McCann (2003, p. 84).

Stereum ostrea (Blume & Nees:Fr.) Fr. – Generally larger and thinner than *S. hirsutum*, which this species resembles due to its yellow-orange colours, the hairs on the upper surface are finer and less dense. Illustrations – Macdonald & Westerman (1979, p. 119); Fuhrer & Robinson (1992, p. 72); Hood (1992, plate 3), as *S. fasciatum*; Hood (2003, fig. 62); May *et al.* (2003, plate 57); McCann (2003, p. 84).

Stereum rugosum Pers. – The grey lower surface helps distinguish this species from *S. illudens* in the field. Unlike European representatives of the species, Tasmanian specimens do not exude a red latex when injured. Illustrations – Fuhrer (2001, pp. 131 and 137); McCann (2003, p. 84).

[Thelephorales]

Phellodon niger (Fr.:Fr.) P. Karst. – Growing close to the soil amongst litter, this blackish, leathery fungus has concentric bands on its abhymenial surface, and a tendency for pilei and stipes to fuse together, often resulting in distorted fruiting bodies. The basidia are located on small spines on the hymenial surface. Illustrations – Shepherd & Totterdell (1988, p. 131); Fuhrer (2001, p. 110); Robinson (2003, p. 41), as *Phellodon* aff. *niger*.

[Tremellales]

Exidia glandulosa (Bull.:Fr.) Fr. – This black, blackish brown or grey-brown, gelatinous or rubbery jelly fungus covers rotting logs and, unlike the related genus *Tremella*, often has a roughened spore-bearing surface. Illustration – McCann (2003, p. 91).

Pseudohydnum gelatinosum (Scop.:Fr.) P. Karst. – A mycological oddity, this species is a 'jelly fungus' with a spore-bearing surface composed of translucent spines. Illustrations – Macdonald & Westerman (1979, p. 143); Fuhrer & Robinson (1992, p. 80); Hood (1992, fig. 22); Fuhrer (2001, p. 142); Young (2000, plate 24), as *Tremellodon gelatinosum*; McCann (2003, p. 91).

Tremella fimbriata Pers.:Fr. – A brown jelly fungus with lobes that are either flattened or inflated. The spore-bearing surface is smooth, not roughened as in *Exidia glandulosa* (q.v.). Illustrations – Arora (1986, plate 173), as *T. foliacea*; McCann (2003, p. 92), as *T. frondosa*.

Tremella fuciformis Berk. – Common on fallen logs in wet forests, the whitish colour of this convoluted jelly fungus differentiates it from other species of the genus. Illustrations – Shepherd & Totterdell (1988,

p. 143); Fuhrer & Robinson (1992, p. 80); Fuhrer (2001, p. 141); May *et al.* (2003, plate 60); McCann (2003, p. 92).

Tremella mesenterica Retz.:Fr. – Similar to *T. fuciformis* (q.v.) in its brain-like, convoluted form, but differs in its yellow to orange colours and its preference for drier environments. Illustrations – Shepherd & Totterdell (1988, p. 143); Grgurinovic & Mallett (1996, fig. 19); Fuhrer (2001, pp. 138 and 141); May *et al.* (2003, plate 62); McCann (2003, p. 92); Robinson (2003, p. 57).

APPENDIX 2
Additions and corrections to records of gilled Basidiomycota in Ratkowsky & Gates (2002)

[Agaricales]

Cheimonophyllum candidissimum (Berk. & M.A. Curtis) Singer – The small, fan-shaped, fruit bodies are white, soft-fleshed, and occur on rotting wood. Illustration – McCann (2003, p. 42).

Dermocybe canaria E. Horak – A medium to large fungus, yellow in all its parts, that turns brown with age. Illustration – McCann (2003, p. 20).

Macrolepiota clelandii Grgur. – This species was listed in Ratkowsky & Gates (2002) as *M. konradii* (Huijsman ex P.D. Orton) M.M. Moser. However, Vellinga (2003) showed that the name *M. konradii*, as well as the names *M. gracilenta* (Krombh.) Wasser, *M. procera* (Scop. : Fr.) Singer, and *M. mastoidea* (Fr. : Fr.) Singer, refer to European species and have been misapplied by Australian authors to what is really a single, native species, *M. clelandii*. Illustrations – see the list in Ratkowsky & Gates (2002).

Mycena albidofusca Grgur. – This is a small species with a brown pileus and a blister-like or whitish central disc and translucent-striate margin. Illustrations – Grgurinovic (2003, plate 14); McCann (2003, p. 53).

Mycena carmeliana Grgur. – A brown species with orange hues, recognised by its sulcate margin, bleach odour, and orange basal disc. Illustration – Grgurinovic (2003, plate 28).

Mycena mulawaestris Grgur. – A medium-sized species with a dark brown, glutinous pileus. Illustration – Grgurinovic (2003, plate 21).

Mycena nargan Grgur. – A medium to large, conical, dark-brown species, distinguishable by small, white particles that cover the pileus in youth. Illustration – Grgurinovic (2003, plate 23).

Mycena vinacea Grgur. – This species was listed in Ratkowsky & Gates (2002) as *Mycena pura* (Pers.:Fr.) P. Kumm. According to Grgurinovic (2003), all Australian records purporting to be *M. pura* are either *M. vinacea* Cleland or another related species, *M. nullawarrensis* Grgur., with the latter not yet known outside Victoria. Tasmanian material fits the description of *M. vinacea*, and, to the two illustrations cited in Ratkowsky & Gates (2002) as *M. pura*, one can add Grgurinovic (2003, plate 3), McCann (2003, p. 54), and Robinson (2003, p. 25, as *M. pura*).

Pholiota aurivella (Batsch.:Fr.) P. Kumm. – Characterised by a lemon-yellow or golden-brown, thickly glutinous pileus in which dark brown or tawny brown scales are immersed in the gluten layer.

[Russulales]

Lactarius stenophyllus Berk. – Pileus centrally depressed, with lemon-coloured shades and concentric zones that may fade in age or which are sometimes indistinct, lamellae adnate to subdecurrent, close to crowded, yellow with pale peach or apricot hues. Stipe stout, white or tinted pale peach or pale apricot. Latex white, with a bitter aftertaste. Illustration – Berkeley (1859, plate 181, fig. 8).

Lentinellus hepatotrichus (Berk.) D.A. Reid – This species, in common with the other species of the genus, is characterised by conspicuously serrate or eroded lamellar margins and amyloid, verrucose spores. The sessile, dark brown pileus is generally densely hairy, with tufts of shaggy hairs covering most of the upper surface. Spores small, 3–5 x 3–4 µm. A member of the *L. ursinus* (Fr. : Fr.) Kühner complex and separated from *L. pulvinulus* (q.v.) mainly by its smaller spores. Illustration – Fuhrer & Robinson (1992, p. 47), as *Lentinellus* sp.

Lentinellus omphalodes (Fr.) P. Karst. – This is the only one of the Tasmanian species of the genus with a well-developed stipe, which may be central or eccentric. We have recently learned (R.H. Petersen, pers. comm., 7 January 2004) that this species should now be called *L. micheneri* (Berk. & M.A. Curtis) Pegler.

Lentinellus pulvinulus (Berk.) Pegler – The sessile, light brown to buff pileus is pubescent near the attachment but tends to be glabrous near the margin. Spores 5–7 x 4–6 µm. Believed to be closely related to *L. flabelliformis* (Bolton : Fr.) Ito. Separated from *L. hepatotrichus* (q.v.) mainly by its larger spores.

DISTRIBUTION OF THE WESTERN PARAGALAXIAS (*PARAGALAXIAS JULIANUS*) (PISCES: GALAXIIDAE) ON THE WESTERN CENTRAL PLATEAU, TASMANIA

by Mark Nelson

(with one text-figure and one appendix)

NELSON, M., 2004 (29:x): Distribution of the Western paragalaxias (*Paragalaxias julianus*) (Pisces: Galaxiidae) on the Western Central Plateau, Tasmania. *Papers and Proceedings of the Royal Society of Tasmania* 138: 61–65. ISSN 0080–4703. Inland Fisheries Service. PO Box 288, Moonah, Tasmania 7009, Australia.

The known distribution of the rare Tasmanian endemic fish species Western paragalaxias (*Paragalaxias julianus* McDowell & Fulton, 1978) is extended from 17 to 63 sites restricted to the Tasmanian Central Plateau in a region known as the Western Lakes in the World Heritage Area. The species was found in catchments, some lakes where it had not previously been recorded and from a wider range of habitat types than previously described.

Key Words: *Paragalaxias julianus*, Western Lakes, fish surveys, electrofishing.

INTRODUCTION

The Western Paragalaxias, *Paragalaxias julianus* McDowall & Fulton, 1978, is the largest of four endemic Tasmanian *Paragalaxias* species, the others being *P. eleotroides* McDowall & Fulton, 1978, *P. dissimilis* (Regan, 1906) and *P. mesotes* McDowall & Fulton, 1978. It may reach 100 mm in length (Fulton 1990) and varies in colour from dark brown to black on the back and sides with irregular patches on the sides. Background colour is yellowish-olive with a belly of silvery-olive (McDowall 1996). A comprehensive description is given by McDowall (1996, 1998).

Paragalaxias julianus is restricted to the Western Lakes region of the Central Plateau and is known from a number of lakes in the upper Little Pine and Ouse rivers catchments and from waters in an area known as the "Nineteen Lagoons". *P. eleotroides* and *P. dissimilis* are found in the Great Lakes and *P. mesotes* occurs in Arthurs and Woods lakes.

The origins of these species are uncertain. Fulton (1988) suggests all four species evolved in the Great Lakes area, but the genus predates the glacial periods because of its degree of dissimilarity to any of the other galaxiids. McDowall (1998) proposes that *P. julianus* occupied its present range only since the last glacial retreat, 15,000–25,000 years ago. McDowall (1998) further proposes the possibility that a species of *Paragalaxias,* not dissimilar to *P. julianus,* was widespread in central Tasmania and dispersed through the area following the last glacial retreat. Speciation would have occurred in the interim.

P. julianus is listed as rare under the *Tasmanian Threatened Species Protection Act 1995* because of its limited distribution, relatively small number of possibly fragmented localities, and the potential risk of decline due to introduced species and changes in habitat quality.

The Western Lakes Fishery Management Plan (Inland Fisheries Service 2002) indicated a need for surveys to clarify the species' distribution and conservation status. This paper reports on such surveys in the James River system, Ouse and Little Pine rivers and the "Nineteen Lagoons" region.

METHODS

Sites in the Western Lakes region of the Central Plateau were accessed by walking, limiting sampling capability.

Fish sampling was conducted using portable, battery-powered (24V, 7Ah) backpack electrofisher units (Smith-Root Model 12-B). Due to the low water conductivity in this region (Mean = 32.7 µS/cm, SD = 14.6) high power outputs were required. At each site sampling was conducted over a 10–15 minute period (electrofisher 'on' time when electrical current was passed through the water). Sites were sampled once only. Physical parameters recorded at each site were water temperature and electrical conductivity (WTW Model LF330), percent substrate type (Bedrock, Boulder >256 mm; Cobble 64–256 mm; Pebble 16–64 mm; Gravel 4–16 mm; Sand 1–4 mm; Silt/Clay <1 mm) and sampling period. Species identity and fork length were recorded for each fish collected.

Ninety-two sites were sampled in a five-week period. Site selection was based on information from prior surveys indicating known locations and expected distribution of *P. julianus.* Catchments where previous surveys failed to locate the species were also targeted (e.g., James R, lower Little Pine R systems).

RESULTS

Fish Species

Sites sampled and fish species recorded are detailed in appendix 1. Forty-six sites (50%) sampled contained *P. julianus* (appendix 1, fig. 1). A further 17 locations are known from the literature (Fulton 1988, Sloane & French 1991, Hydro Tasmania unpubl. data). Four fish species were recorded: the introduced brown trout (*Salmo trutta* Linnaeus, 1758), the climbing and spotted galaxias (*Galaxias brevipinnis* Günther, 1866 and *Galaxias truttaceus* Valenciennes, 1846 and the Western paragalaxias (*P. julianus*). The three native species were frequently recorded in the same water bodies (43.5% of sites) while *P. julianus* was occasionally found with only *G. brevipinnis* (21.7% of sites) and infrequently with only *G. truttaceus* (6.5% of sites). *P. julianus* was also recorded as the only fish species at a number of sites (28.3% of sites).

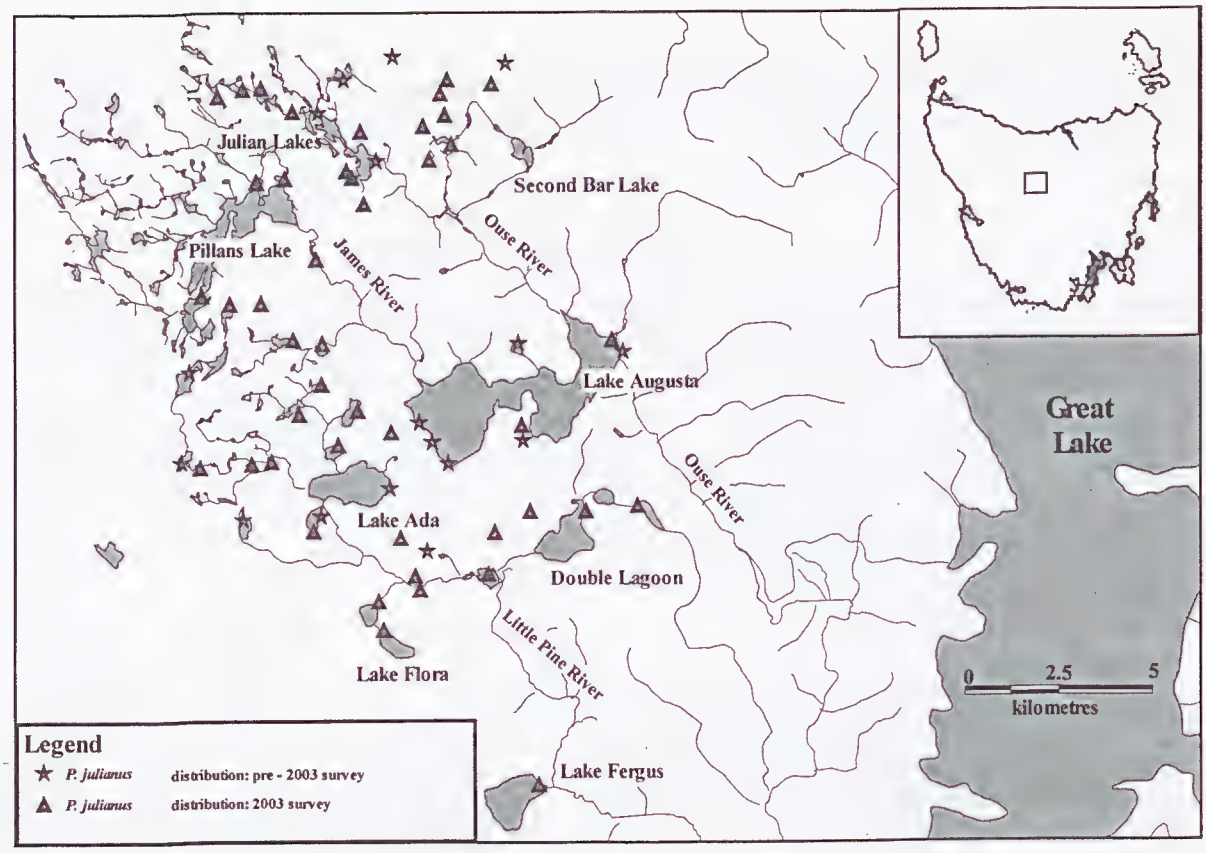

FIG. 1 — Collection sites in the Western Lakes for Paragalaxias julianus.

A total of 562 individuals of *P. julianus* were collected, ranging from 16 to 91 mm (mean=52.6 ± 14 SD) in length.

Habitat

Most water bodies contained shorelines of rock that graded into a uniform silt/sand bottom. *P. julianus* were most commonly found among uniform boulder (>256 mm diameter, 80% of sites) or cobble (64–256 mm diameter, 11% of sites) substrates, and frequently in a mix of both but with boulder dominant (74% of mixed substrate sites with boulder dominant). Of the remainder, two sites were individual boulders in a sand and silt substrate, one site a pebble (16–24 mm diameter) substrate and one site a silt substrate. Occasionally individuals were located in small piles of cobbles surrounded by silt substrate. Some individuals were located hiding under individual rocks of cobble or boulder size.

Field observations indicated that *P. julianus* preferred uniform cobble substrate in mixed habitat.

Distribution

The known distribution of *P. julianus* has now been significantly expanded. New areas include the James River system and Pillans Lake, and the middle and lower reaches of the Little Pine River as far down as Lake Fergus. The species range also includes the upper Lake Ada catchment incorporating Sandy and Tin Hut lakes, and the unnamed river system draining into the northwest corner of Julian Lakes, as well as the Stumps and Wadleys lakes system which is a sub-catchment of the James River system above Lake Augusta. All sites where the species occurred are above 1000 m elevation (appendix 1). The range area (extent of occurrence) is approximately 200 km^2.

The species was not located in one of the two northwest Julian Lakes catchments that drain into the main Julian Lake (fig. 1), nor were any specimens found in any of the lakes draining into Pillans Lake, although in many drainages no barriers to upstream movement were apparent.

DISCUSSION

Paragalaxias julianus is widespread within a restricted area delimited by the upper catchments of the Ouse and Little Pine rivers. Prior surveys indicated the species was common within a more limited range which included lakes in the Little Pine-Christys Creek system, between Lake Baillie and Lunka Lake, the Ouse River system above Lake Augusta, as well as the Carter Lakes and Lake Dudley (Sloane & French 1991). Clearly, the known distribution has not expanded beyond the expected range; rather, the species is widespread within this range. Sloane & French (1991) considered the species to be locally quite common and findings from the present study support this. *P. julianus* was frequently found in numbers exceeding those of the other galaxias species. However, at several sites only one or two specimens were located after intensive sampling, indicating that the current recorded distribution pattern is also partly a reflection of sampling effort. Due to the rapid survey technique used, small populations may have been missed during sampling. There is, therefore, the

potential for *P. julianus* to be present in some areas where it was not found during these surveys.

Although the surveys focused on lakes and relatively few riverine environments, *P. julianus* was not found in running water habitats. Several specimens were located in river lagoons and marginal river environments suggesting that it has a strong preference for standing water. It is possible that individuals were being forced into less favourable habitats by the dry conditions during the study period.

The absence of this species in catchments flowing into Pillans Lake indicates that the species may have moved up through the system to this current limit. Since data indicate a preference for lentic environments, dispersal upstream through riverine channels would be limited and slow. Fulton (1988) suggested the possibility that the species moved across catchments from the Ouse River system to the Little Pine River system in the area of Lake Augusta. This seems a likely scenario as the Little Pine River system was independent of the Great Lake system before construction of hydro-electric infrastructure and flows into the middle Derwent River, and the species has now been located in all adjacent catchments across the top of its known range.

It is unlikely that the species exists outside its known range which encompasses all the catchments in the upper Ouse and Little Pine rivers. The presence of trout also may have restricted distribution and abundance within this range but no pre-trout data are available. Trout predation or competition may reduce habitat availability by restricting the species to shallow backwaters and edgewaters and deterring them from moving into and spawning in or adjacent to open water (P. Davies pers. comm.). A common observation during this survey was for adult native fish to be seen swimming freely in open waters away from protective habitat in what were assumed to be trout-free waters. In contrast, where trout were known to be present, adult native fish were only collected from rocky substrates and were rarely visible.

Trout were not recorded in many lakes sampled but the backpack electrofishing technique used is not efficient for sampling trout in shallow lake margins. A fright effect can occur in open water through the fish sensing the electric field before stunning can occur, and through fish seeing operators before they come into capture range. Some trout-free lakes containing *P. julianus* may occur, but this is as yet unconfirmed.

In this study *P. julianus* were most abundant in uniform boulder or cobble substrates and frequently in a mix of both. Whilst McDowall & Fulton (1978) describe the species as being found beneath rocks on lake beds particularly where rocks are lying spaced apart on a gravelly substrate, they considered it less common among piles of rocks.

Much of the basic biology of *P. julianus* remains unknown. The species spends its entire life-cycle in freshwater, spawning in spring with eggs laid in masses on the sheltered, inland-facing side of rocks in shallow water, and the larvae are pelagic (P. Davies, pers. comm.). Information required for management to conserve the species includes life history; habitat requirements for spawning and all life stages; impacts of trout; and impacts of water management for hydro-electricity. A better understanding of trout-free areas would also assist in the future management of the species. It is unclear if the species distribution is stable, declining or expanding; future monitoring programs are necessary to determine this.

ACKNOWLEDGEMENTS

This work was funded through the World Heritage Area Fauna Program, Nature Conservation Branch, Department of Primary Industries Water and Environment, and conducted with in-kind support from the Inland Fisheries Service. Michael Driessen organised WHA funding. Michael Schottmeier, Brett Mawbey and Keith Breheny provided field support. Mick Howland of Hydro Tasmania provided some distribution data. Peter Davies of Freshwater Systems provided some unpublished information. Thanks also to Andrew Taylor for assistance with the mapping graphics and Jean Jackson, Stuart Chilcott and Adam Uytendaal for reviewing the manuscript.

REFERENCES

FULTON, W., 1988: The freshwater fish fauna of Tasmania's Western Central Plateau. *Inland Fisheries Commission Occasional Report* 88-02. 23 pp.

FULTON, W., 1990: *Tasmanian Freshwater Fishes.* University of Tasmania Hobart. Fauna of Tasmania Handbook No. 7. 80 pp.

INLAND FISHERIES SERVICE, 2002: *Western Lakes Fisheries Management Plan.* 40 pp.

MCDOWALL, R.M., (ed.) 1996: *Freshwater Fishes of South-Eastern Australia.* Reed Books, Sydney. 247 pp.

MCDOWALL, R.M., 1998: Phylogenetic relationships and ecomorphological divergence in sympatric and allopatric species of *Paragalaxias* (Teleostei: Galaxiidae) in high elevation Tasmanian lakes. *Environmental Biology of Fishes* 53: 235–257.

MCDOWALL, R.M. & FULTON, W., 1978: A further new species of *Paragalaxias* Scott from Tasmania with a revised key to the species. *Australian Journal of Marine and Freshwater Research* 29: 659–665.

SLOANE, R.D. & FRENCH, G.C., 1991: Trout Fishery Management Plan, Western Lakes – Central Plateau: Tasmanian World Heritage Area. Unpublished report to Department of Parks, Wildlife and Heritage.

(accepted 2 August 2004)

APPENDIX 1
Fish species caught during the survey for *Paragalaxias julianus*

#	Site	Date (2003)	Easting AGD 66	Northing AGD 66	Altitude m a.s.l.	*Paragalaxias julianus*	*Galaxias brevipinnis*	*Galaxias truttaceus*	*Salmo trutta*
1	Carters Lake	3 Feb	461300	5365300	1150	*	*	*	
2	Emma Tarns	4 Feb	457614	5361922	1145		*		
3	Emma Tarns	4 Feb	457535	5361880	1145	*	*		
4	Hood Lagoon	4 Feb	457991	5360717	1148	*			
5	unnamed lagoon	4 Feb	458135	5360294	1161	*			
6	Little Pine River	4 Feb	458356	5360339	1161				*
7	Little Pine River	4 Feb	458832	5360523	1142				*
8	Lake Kay	4 Feb	460261	5360783	1145	*			
9	Lake Agnes	4 Feb	459022	5361294	1152				
10	Rocky Lagoon	5 Feb	458306	5363301	1158				
11	unnamed lake	5 Feb	452392	5362957	1166				
12	Ada Lagoon	5 Feb	454869	5362085	1159	*	*	*	*
13	Double Lagoon	5 Feb	463269	5362690	1161	*	*		
14	unnamed lagoon	5 Feb	464224	5365033	1157				
15	Lake Augusta	5 Feb	463972	5367717	1151				*
16	Thomsons Rvt	5 Feb	464083	5367894	1156	*	*		*
17	Thomsons Rvt lagoon	5 Feb	464520	5368229	1164		*		*
18	Little Pine River	6 Feb	462195	5354325	1041				*
19	Lake Fergus	6 Feb	461803	5354378	1047	*	*		
20	Bull Lagoons	6 Feb	460089	5355964	1156		*	*	
21	unnamed lake	7 Feb	455092	5372137	1170		*	*	
22	unnamed lake	7 Feb	456417	5372025	1217	*	*	*	
23	unnamed lagoon	11 Feb	458904	5370060	1224				
24	Pillans Lake	11 Feb	453135	5372675	1203	*	*	*	
25	Pillans Lake	11 Feb	453119	5372698	1203	*	*	*	*
26	Pillans Lake	12 Feb	451437	5369239	1201	*	*	*	
27	Hunters Lake	12 Feb	451813	5368460	1218			*	
28	unnamed lake	12 Feb	452298	5368986	1220	*	*	*	
29	Wadleys Lake	12 Feb	453261	5369002	1190	*	*	*	*
30	unnamed lake	13 Feb	451286	5371762	1212		*		
31	unnamed lake	13 Feb	450585	5371708	1216		*	*	
32	unnamed lake	13 Feb	449350	5371899	1228		*		
33	unnamed lake	13 Feb	449748	5371044	1245		*	*	
34	unnamed lake	13 Feb	450361	5371160	1228		*	*	
35	unnamed lake	13 Feb	451091	5371084	1236		*	*	
36	unnamed lake	14 Feb	452328	5373188	1216		*	*	*
37	unnamed lake	14 Feb	456056	5372823	1214	*	*		*
38	Lake Botsford	17 Feb	459104	5363402	1161				*
39	Ouse River	17 Feb	465395	5364999	1134		*		*
40	Little Blue Lagoon	18 Feb	457253	5365090	1158	*	*	*	
41	Sandy Lake	18 Feb	455631	5364702	1168	*			
42	unnamed lake	18 Feb	454431	5365638	1171	*	*	*	*
43	unnamed lake	18 Feb	453162	5365032	1179		*	*	
44	unnamed lake	18 Feb	453345	5365946	1180		*		
45	unnamed lake	18 Feb	455120	5366554	1181	*	*	*	*
46	James River	20 Feb	457892	5366857	1171		*	*	*
47	James River	20 Feb	455692	5369606	1177		*	*	*
48	James River lagoon	20 Feb	454953	5370333	1189	*			*
49	Lake Howe	20 Feb	453814	5370062	1223		*		
50	unnamed lake	20 Feb	454246	5367901	1199	*		*	
51	Stumps Lake	20 Feb	455141	5367788	1162	*	*	*	*
52	Lake Flora	21 Feb	457020	5359068	1145	*	*	*	
53	O'Dells Lake	21 Feb	456865	5359942	1145	*	*	*	
54	First Lagoon	23 Feb	464863	5362849	1155	*			
55	Ouse River	24 Feb	459503	5371432	1226				*
56	Second Bar Lake	24 Feb	461536	5373133	1230				*
57	unnamed lagoon	24 Feb	460342	5372210	1221		*		*

APPENDIX 1, cont.

#	Site	Date (2003)	Easting AGD 66	Northing AGD 66	Altitude m a.s.l.	*Paragalaxias julianus*	*Galaxias brevipinnis*	*Galaxias truttaceus*	*Salmo trutta*
58	unnamed lake	24 Feb	455889	5373037	1218	*	*	*	*
59	unnamed lake	24 Feb	456316	5374227	1224	*	*	*	
60	Lake Ila	25 Feb	458420	5373364	1221	*	*		*
61	Thomsons Lake	25 Feb	459111	5373839	1228	*			
62	Grubb Lake	25 Feb	460364	5375655	1225	*	*		
63	First Bar Lake	25 Feb	458980	5375776	1220	*			*
64	unnamed lake	25 Feb	458763	5375361	1216	*			*
65	unnamed lake	25 Feb	458906	5374716	1216	*			
66	unnamed river	25 Feb	458233	5374383	1217	*	*		*
67	unnamed lake	26 Feb	454231	5374820	1224	*			
68	unnamed lake	26 Feb	454158	5375521	1226		*		
69	unnamed lake	26 Feb	453264	5375530	1227	*	*	*	*
70	unnamed lake	26 Feb	452707	5375490	1230	*	*	*	
71	unnamed lake	26 Feb	451933	5375277	1227	*	*	*	
72	unnamed lake	26 Feb	451050	5376096	1245			*	
73	unnamed lake	26 Feb	451333	5376432	1243		*		
74	unnamed lake	26 Feb	453781	5375816	1242		*	*	
75	Pillans Lake	27 Feb	453993	5372796	1204	*	*		
76	unnamed lake	27 Feb	454158	5373070	1207		*	*	
77	unnamed lake	27 Feb	453778	5373621	1216		*		*
78	Tin Hut Lake	4 Mar	456232	5365752	1172	*		*	
79	East Rocky lagoon	4 Mar	460454	5362051	1152	*			
80	Lake Chipman	4 Mar	461553	5362690	1147	*	*	*	*
81	Little Pine Lagoon	5 Mar	465895	5348953	1020		*	*	*
82	unnamed lake	11 Mar	451618	5372864	1218		*	*	
83	unnamed lake	12 Mar	450103	5374919	1255		*	*	
84	Lake Gwendy	12 Mar	449664	5374783	1255		*	*	
85	Lake Lexie	12 Mar	448829	5374816	1264		*	*	
86	Pencil Pine Tarn	12 Mar	448447	5374083	1256		*		
87	unnamed lake	12 Mar	448921	5373395	1256		*	*	
88	unnamed lake	14 Mar	451727	5363709	1178		*	*	
89	unnamed lake	14 Mar	451384	5364019	1193	*	*		*
90	Terry Tarn	14 Mar	450656	5363586	1196		*	*	*
91	unnamed lake	14 Mar	452970	5364122	1170	*		*	*
92	unnamed lake	14 Mar	453580	5364195	1169	*			*

* indicates presence of species.
Sampling effort – 15 min. electrofisher 'on' time per site.

RECONNAISSANCE LIMNOLOGY OF TASMANIA VIII. TASMANIAN COASTAL LAGOONS – EPICENTRES OF ENDEMISM IN THE AUSTRALIAN AQUATIC MICROBIOTA

by R. G. J. Walsh, R. J. Shiel and P. A. Tyler

(with two text-figures, one plate and seven tables)

WALSH, R. G. J., SHIEL, R. J. & TYLER, P. A., 2004 (29:x): Reconnaissance limnology of Tasmania VIII. Tasmanian coastal lagoons – epicentres of endemism in the Australian aquatic microbiota. *Papers and Proceedings of the Royal Society of Tasmania* 138: 67–76. ISSN 0080–4703. Lower Basin Laboratory, Murray-Darling Freshwater Research Centre, PO Box 3428 Mildura, Victoria 3502, Australia (RGJW); School of Earth and Environmental Sciences, University of Adelaide, South Australia 5005, Australia (RJS); School of Ecology and Environment, Deakin University, PO Box 423, Warrnambool, Victoria 3280, Australia. ptyler@deakin.edu.au (PAT*) * Author for correspondence.

Two clusters of coastal lagoons, one near Strahan on Tasmania's west coast, the other near St Helens on the north-east coast, are the prime known epicentres of novelty and endemism in the Australian freshwater algal flora. The algae inhabiting these acid, dystrophic lagoons have a very limited distribution. Other dystrophic lagoons may have one or two, but not all, of this suite of endemics. The Strahan dune lakes, especially Lake Garcia, also have the greatest microfaunal diversity yet recorded from any Tasmanian waterbody, including several endemic species. The St Helens sites are less rich in species of microfauna, perhaps because of climatic differences or perhaps because of less intensive sampling there, but they, too, contain endemic taxa. The lagoons in both areas lie outside the formal protection of national parks, but present land management does provide a measure of protection.

Key Words: coastal lagoons, dystrophic waters, algae, microfauna, endemism.

INTRODUCTION

Australian coastal lagoons, principally some in Tasmania, have been recognised as the strongholds of novel and uniquely Australian freshwater algae (Tyler 1992, 1996a). The results of a broad survey of Tasmanian coastal lagoons were presented earlier (Bowling *et al.* 1993, Walsh *et al.* 1995). With more taxonomic studies (Croome *et al.* 1998) and recent field work in north-east Tasmania, and on islands of Bass Strait (Rolfe *et al.* 1999, Tyler 1996b, Walsh 1995; Walsh *et al.* 2001), it can now be said that the presently known epicentres of endemicity and novelty in the freshwater algal flora are clusters of lagoons near Strahan, western Tasmania, and at Stieglitz, near St Helens, north-eastern Tasmania. These same lagoons also contain endemic taxa of microfauna. Some, but not all, of the suite of endemics found in these two sets of lagoons occur in other lagoons dotted along the Tasmanian coastline, on islands in Bass Strait and on islands off the Queensland coast (Croome & Tyler 1985, 1988, Croome *et al.* 1998, Ling *et al.* 1989, Tyler 1996a,b). Some physicochemical and limnological properties of some of the natural lagoons have been investigated by a number of authors and their unique or restricted algal flora and their microfauna have been reviewed (Bowling *et al.* 1993, Koste & Shiel 1986, 1987, Shiel *et al.* 1989, Tyler 1996a, b, Walsh *et al.* 2001). This paper presents further detail on key lagoons on Tasmania's west coast, near Strahan, with two nearby, man-made lakes included for comparison, and at Stieglitz in the north-east of Tasmania.

METHODS

Geomorphological analyses of the lagoons were based on aerial photographs, topographical maps, ground photographs and field investigations. Sampling and analyses for chemical parameters were by the methods of Bowling *et al.* (1993). Plankton and littoral microfaunal samples were collected, and *in situ* measurements made, at three to five month intervals, between August 1991 and November 1994, from nine lagoons and two man-made lakes on Tasmania's west coast (fig. 1). The sampling effort for this period is indicated in Walsh (1996). Plankton and littoral microfauna also were collected from the west coast dune lakes during seven surveys for Tasmanian microfauna in the period 1984–97; methods and sampling effort for these surveys were consistent throughout, and are given in Koste & Shiel (1986, 1987) and Shiel *et al.* (1989). The lagoons at Stieglitz were visited only occasionally, most intensively in February 1999. Microscopical observations were made in Strahan and St Helens and recorded by videomicroscopy. Collections are held by the authors. For deposition of type material refer to the taxonomic papers cited herein.

RESULTS

Site Descriptions

Table 1 gives brief details of the lagoons and reservoirs on the west coast included in this study. Those from St Helens are briefly described in the text. Photographs have been published previously of Lake Garcia, Lake Bantic and Hibb's Lagoon (Bowling *et al.* 1993, Croome & Tyler 1988a) and of the three Stieglitz lagoons (Tyler 1996b). Preliminary data on some of the lagoons included here are given by Bowling *et al.* (1993) and Tyler (1996b). Parting Creek Dam, at Zeehan, and Lake Cumberland (pl. 1) are artificial reservoirs, each created, in the late 19th Century, simply by building a dam across a valley. The catchments of both are clothed in native western Tasmanian vegetation and water quality is essentially that of natural lagoons.

The natural lagoons of the west coast included in this study lie in sand dunes behind Ocean Beach, near Strahan (fig. 1), where there is a complex, vegetated, but eroding,

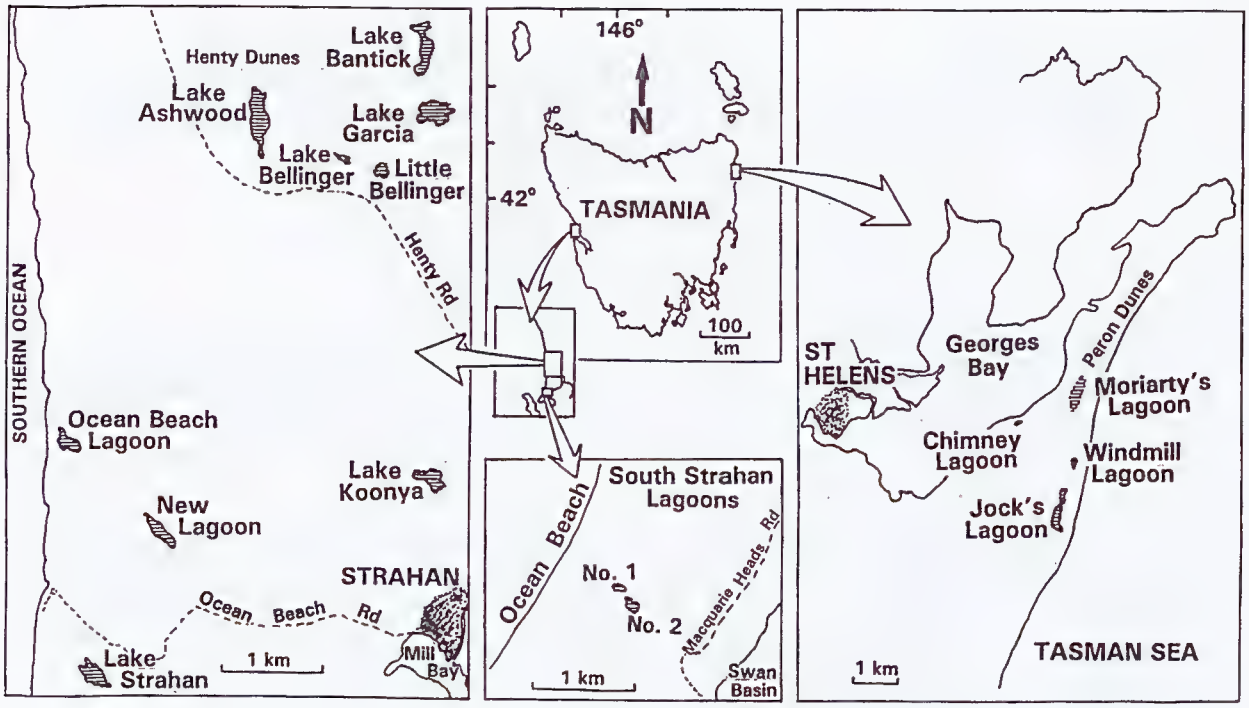

FIG. 1— Map showing location of lagoons studied. The two reservoirs, Parting Creek Dam and Lake Cumberland (not shown), are accessed from Zeehan, 46 km north of Strahan.

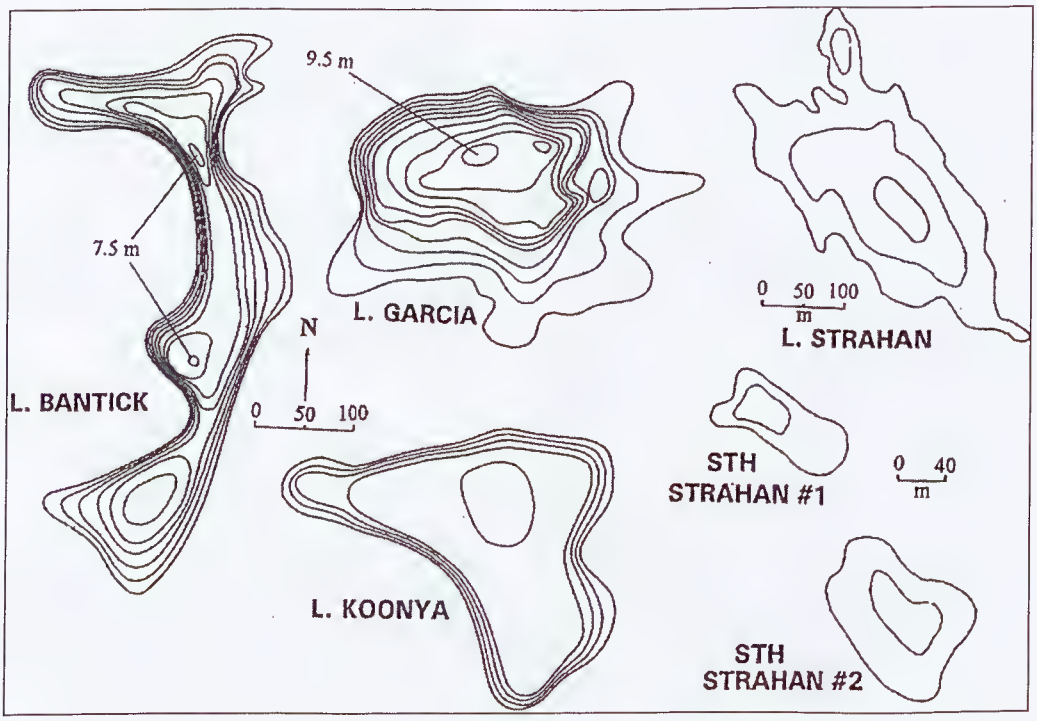

FIG. 2 — Bathymetric maps of selected coastal lagoons near Strahan. Contours are at 1 m intervals.

PLATE 1
Lake Cumberland, a reservoir created late in the nineteenth century.

system of parabolic dunes of Pleistocene origin, extending up to 7 km inland. The source of sand for these dunes is believed to be siliceous, glacial and glaciofluvially derived sediments from the granitic lower gorge of the Little Henty and Henty Rivers (Banks *et al.* 1977). A number of Holocene, unvegetated, active and transgressive dunes occur immediately behind the beach, advancing inland at the rate of 17 m per year.

The source of sand for these dunes is the present Ocean Beach and blow-outs of the older Pleistocene dunes. Dunes just north of Strahan rise to 90 m; vegetated dunes further inland reach a maximum of 147 m (Banks *et al.* 1977). There is a distinct contrast in the degree of soil development between unvegetated dunes and those, fully vegetated, inland. The progressive development, and increase in soil depth, with increasing distance inland, suggests a progressive increase in the age of dunes and this implies a source of sand different from the Henty River source of today. The age of dune building for Ocean Beach is thought to be similar to that in north-east Tasmania (Bowden 1978, 1983), King and Flinders Islands (Jennings 1959, 1961, Kershaw & Sutherland 1972) and Bruny Island (Banks *et al.* 1977, Walsh *et al.* 1995). The area in which the west coast dunes lie experiences the strong winds of the Roaring Forties. The average annual rainfall is 1500 mm, with an average of 240 rainy days per year.

Australian coastal lagoons have been classified by Timms (1982, 1992). The lagoons in the Strahan area are principally perched lakes (Timms' type i), lying on soils or organic mats developed within longitudinal or parabolic dunes. Hibbs Lagoon (Bowling *et al.* 1993, fig. 9) and Lake Koonya do not fit into Timms' classification. Their origins are indicated by Bowling *et al.* (1993).

The Stieglitz lagoons are located on a narrow peninsula, 10 km long, forming the southern shore of Georges Bay (fig. 1). The backbone of the peninsula is an outcrop of Devonian granite. Long shore drift has built up an extensive beach, with a single foredune, along much of this peninsula. Between the foredune and the granite lie a number of freshwater lagoons and wetlands. In their geomorphology they are similar to those of Bruny Island (Walsh *et al.*1995). Photographs and preliminary data for these lagoons are given by Tyler (1996b).

Moriarty's Lagoon (fig. 1) is a shallow depression at the northern end of the granitic ridge, lying between it and the dunes to the north. In essence it is a swamp, heavily vegetated with *Baumea, Juncus* and other aquatic plants. It appears to be a combination of Timms' types ii and iv. In summer it dries up over most of its area.

Windmill Lagoon is located immediately behind the foredune, between it and the granite ridge. It is 4.5 m deep adjacent to the dune and has much of its area as open water. In addition there are stands of emergent *Triglochin* and *Eleocharis* in shallower areas. It is a Timms' type iv lagoon.

Jocks Lagoon is similar in geomorphology to Windmill Lagoon but may have also some features of Timms' type ii. It is shallow (z_{max}. ca. 2.0 m), astatic and vegetated over most of its area.

Morphometry and Physicochemical Attributes

Available morphometric data are given in table 1. Bathymetric maps for some lagoons are shown in figure 2. Lake Strahan, South Strahan Lagoons and New Lagoon are astatic; the latter three may dry up in some years. Of the natural lagoons, only Hibbs Lagoon, Lake Mallana and Lake Koonya have inflow and outflow creeks. The morphological data show that the only natural lagoons likely to display seasonal stratification are Lake Garcia, Lake Bantic, Lake Mallana, Lake Koonya and Hibbs Lagoon.

Lake Garcia (z_{max} 9.5 m) is known to stratify (Bowling *et al.* 1993, fig. 10), with diminution in oxygen concentrations accompanying the thermocline. Additional measurements (unpublished) suggest that it stratifies in September and

TABLE 1
Morphometry and brief description of coastal lagoons and reservoirs in the Strahan district, western Tasmania.

Site	Zmax m	Surface area (ha)	Description	Lake Type*
Lake Garcia	9.5		Holocene parabolic/longitudinal dune on siliceous sands.	Perched lagoon type i
Lake Bantic	7.5		Holocene parabolic/longitudinal dune on siliceous sands.	Perched lagoon type i
Lake Strahan	2.5	003.00	Holocene parabolic/longitudinal dune on siliceous sands.	Perched lagoon type i
New Lagoon	< 1.0	001.00	Holocene parabolic/longitudinal dune on siliceous sands.	Perched lagoon type i
South Strahan No. 1	1.5	002.00	Holocene parabolic/longitudinal dune on siliceous sands.	Perched lagoon type i
South Strahan No. 2	1.5	001.00	Holocene parabolic/longitudinal dune on siliceous sands.	Perched lagoon type i
Lake Mallana	4.5	001.00	Tertiary sediments and Holocene siliceous dunes.	Dune contact type iv
Lake Koonya	4.5	002.00	Tertiary sediments and Holocene siliceous dunes.	Slope change
Hibbs Lagoon	8.0		River valley and siliceous sands	Natural impoundment
Lake Cumberland	4.0		Reservoir	Reservoir
Parting Creek Dam	5.5		Reservoir	Reservoir

* Lake type designated after Timms (1982).

turns over in May, giving approximately nine months of stratification. Despite this long period the lowest hypolimnetic oxygen concentration observed was about 5% of saturation value.

At the time of year when nearby lakes, such as Lake Garcia, are stratified, Lake Bantic may or may not be so (Bowling *et al.* 1993). The relatively long fetch of Lake Bantic (Bowling *et al.* 1993, figs 6, 7) may prevent long lasting stratification in the windy climate of Tasmania's west coast. The thermal profile of Lake Mallana was not measured during this study, but it is known to stratify (Bowling *et al.* 1993). The suspected incipient meromixis of Hibbs Lagoon (Bowling *et al.* 1993) was confirmed by this study. Though only 4.0 m deep, Lake Koonya was thermally stratified on the one occasion examined. Another shallow lake in the vicinity, Little Bellinger, has also been observed to stratify (Bowling *et al.* 1993). Of the lagoons in the north-east, even the deepest, Windmill, is unlikely to stratify. Moriarty's Swamp is dry over much of its area in summer. Small pools of water remain in the lowest-lying parts of the swamp.

Some physical and chemical conditions of the lagoons and reservoirs studied are given in table 2. The full, electronic database "STRAHLITZ" is available from the authors. The lagoons are all of moderate salinity (mostly < 500 $\mu S\ cm^{-1}$). Ternary diagrams of major ions (not presented) confirm earlier data (Bowling *et al.* 1993) that ionic proportions are close to those of seawater.

The coastal lagoons and reservoirs of the west coast are, with the exception of Lake Bantic (see below), typically dystrophic. With g_{440} values ranging from 3.0 to 59.1, they rank as moderately to highly dystrophic on a Tasmania-wide scale (Bowling *et al.* 1986). This is the expected condition of "dim red window" (Tyler 1992) waters of western Tasmania. Euphotic depths determined quantaspectrometrically during this study ranged from 0.8–2.3 m. Quantaspectroradiometric scans of Lake Strahan and others of comparable dystrophy reveal rapid attenuation of wavelengths less than about 500 nm. At a depth of 0.5 m in such lakes wavelengths <500-550 nm are totally quenched (Bowling *et al.* 1986). As expected of dystrophic waters, pH values are low (pH 3.5–4.5).

An unexplained curiosity is that Lake Bantic, only 1 km from Lake Garcia (fig. 1), and surrounded by the same vegetation, is considerably less dystrophic than that lake and all neighbouring lagoons of this cluster. The reasons for this are not known but a pedological explanation is suspected. In keeping with the less dystrophic conditions the pH of Lake Bantic (pH 4.8–5.8) is a little higher than that of neighbouring dystrophic lagoons. Further data on the west coast lagoons are given by Walsh (1996).

Available physicochemical data for the north-east lagoons are given in table 2. Salinity values are higher that those of most west coast lagoons, especially for Moriarty's Swamp. Their pH values are also a little higher but their g_{440} values are comparable. Ionic proportions are close to those of seawater.

Biological features

Many of the natural west coast lagoons have emergent stands of aquatic macrophytes, either as fringing zones or patches in the shallows. Common species are *Eleocharis sphacelata* R. Br., *Triglochin procera* R. Br., *Restio tetraphyllus* Labill., *Baumea* sp. and *Chorisandra* sp. *Sphagnum* spp. also occur around some lagoons and *Chara* sp. covers the floor of the optically deep Lake Bantic.

The microinvertebrates found in west coast lagoons are listed in table 3. Typically, the planktonic microcrustacean community is monospecific, with the calanoid copepod *Calamoecia tasmanica tasmanica* (Smith) the usual dominant species. It is highly characteristic of dystrophic coastal lagoons throughout Tasmania (Walsh & Tyler 1998). The exceptions to this are Lake Bantic, where the cladoceran *Ceriodaphnia planifrons* Smith occurred as subdominant, Parting Creek Dam, where the cladoceran *Bosmina meridionalis* Sars was subdominant, Lake Cumberland where *B. meridionalis* was the only planktonic crustacean and Lake Mallana where the cladoceran *Daphnia* sp. occurred on one occasion only.

Chydorid cladocerans (1–4 spp.) occurred in the littoral zone of most lagoons, usually species of *Alona, Alonella, Camptocercus, Chydorus, Graptoleberis* or *Rak.* The genera

TABLE 2
Summary of some physicochemical conditions* of some lagoons and reservoirs on Tasmania's coast

Lagoon	pH	K_{25}, S cm^{-1}	g440 m^{-1}	Z_{eu} m
L. Garcia	4.3-5.6	70-146	3.2-10.4	2.1-2.3
L. Bantic	4.8-5.9	68-138	0-0.9	7.7-11.2
L. Ashwood	4.6-5.2	127-152	4.9-11.1	
L. Koonya	3.7-4.2	107-122	27.9-31.8	1.2
L. Strahan	4.2-5.1	169-362	6.9-50.5	0.8-0.9
L. Mallana	3.5-4.2	113-167	15.1-27.5	1.1
South Strahan Lagoons 1&2	3.5-4.0	245-411	25.2-59.1	
New L.	3.7-4.5	176-212	29.5-37.7	
Ocean Beach L.	4.6-4.7	550-569	13.9-14.3	
L. Cumberland	4.2-4.7	48-73	3.0-11.0	
Hibbs L.	6.1-6.8	133-160	4.4-10.8	1.9
Parting Creek Dam	4.1-5.9	55-84	5.7-16.1	1.7
Jocks Lagoon	4.6-4-9	350-361	22.0	
Windmill Lagoon	5.9-6.2	450-516	5.3	
Moriarty Swamp	6.1-6-9	733-815	16.1	

* Data from the present study and from Bowling *et al.* 1993.

Ilyocryptus and *Scapholeberis* occurred amongst emergent macrophytes and *Pseudomoina lemnae* (King) was common in the astatic South Strahan Lagoons. A suite of cyclopoid copepods also occurred in the littoral of most lagoons, viz. species of *Eu-, Macro-, Meso-, Micro-, Para-, Thermo-* or *Tropocyclops*, with an occasional record of primarily epibenthic or epiphytic canthocamptid harpacticoids, e.g., *Canthocamptus* sp. Ostracods were notably sparse, although the presence of occasional individuals of, e.g., *Limnocythere* in the littoral zone of some dune lakes indicates that some species may be present seasonally.

Preliminary studies of the rotifer fauna of the west coast lagoons showed them to be "unexpectedly rich in species" (Koste *et al.* 1988 p. 128) including many new records for Tasmania and two species new to science. On any visit, between 10 and 35 rotifer species were recorded in the zooplankton of any particular lagoon; rotifers were commonly the numerically dominant zooplankters, with the most common taxa being various species in the genera *Conochilus, Keratella, Lecane, Polyarthra, Synchaeta* and *Trichocerca.* Notably, on any given sampling day, each lagoon had a dominant taxon different from those of neighbouring lagoons. For example, in Lake Garcia dominant rotifers were *Keratella cochlearis* (Gosse) and *Conochilus dossuarius* (Hudson) while in Lake Ashwood, on the same day, dominants were *Keratella javana* Hauer and *Conochilus hippocrepis* (Schrank). Because of the vegetated nature of the sampling sites in each lagoon, rotifer assemblages invariably were a mixture of true plankters and littoral taxa. The lagoons also contain some species of rotifers endemic to Tasmania (table 6).

Also notable in collections from the west coast lagoons was a diverse array of testate Rhizopoda, a group poorly reported from Tasmania. Genera noted in the Strahan lagoons include *Arcella, Centropyxis, Corythion, Cucurbitella, Difflugia, Euglypha, Hyalosphaenia, Lesquereusia* and *Trinema.* Testate rhizopods have long been thought to be cosmopolitan, like the ciliated Protozoa (Finlay 1998, Finlay *et al.* 1996, 1999). However, there is recent and increasing evidence that there is regionalism, if not endemism, in the Rhizopoda (Meisterfeld & Tan 1998). The status of the poorly known Tasmanian testate amoebae remains to be investigated. A new species of the ciliated Protozoa (Ciliophora), *Lembadion curvatum* Esteban, Finley, Olma & Tyler, 2000, was discovered recently in Lake Bantic (Esteban *et al.* 2000).

The considerable attention to date paid to the cluster of dystrophic lagoons on Tasmania's west coast has stemmed largely from the number of endemic or novel algae that live there. Tyler (1996a) recognises frail endemics with specific habitat preferences, met by the west coast lagoons and a few other places, and robust endemics that are more widely distributed and which tolerate a wider range of water conditions. A number of coastal lagoons dotted around the Tasmanian coast contain one or more frail endemics. The lagoons near Strahan, either collectively or singly, contain the full suite of frail endemic species described to date (table 5). Floristic and taxonomic studies are incomplete. Other new species are likely from these lagoons and certainly there are known species of chrysophytes and desmids not yet recorded from Australia but known to occur near Strahan and Stieglitz. A distinctive form of the desmid *Pleurotaenium tridentulum* Wolle G.S. West, with torsion of the corpus (Ling & Tyler 2000), is known only from five lagoons: at Strahan (Lakes Garcia and Ashwood), Stieglitz (Jocks and Windmill Lagoon) and Millers Lagoon in southwest Tasmania.

The three lagoons near St Helens on Tasmania's north-east coast, have not been studied in detail, but their value as sites of diversity and endemism is proven (tables 6–7). The microcrustacean fauna (table 4) has been studied only briefly, but all three lagoons have as the dominant calanoid *Calamoecia tasmanica tasmanica* (Smith), a species which is highly characteristic of dystrophic lagoons (Walsh & Tyler 1998). In keeping with the shallow, vegetated nature of the Stieglitz lagoons, the cladoceran assemblage is that of shallow waters, *viz.* the daphnids *Ceriodaphnia* and *Simocephalus* and a suite of chydorids from the genera *Alona, Alonella,*

TABLE 3
Microinvertebrates and small macroinvertebrates from eight localities near Strahan on four dates

Faunal group	No. taxa	No. genera	Genera/taxa
Rhizopoda	23	11	*Arcella, Centropyxis, Corythion, Cucurbitella, Difflugia, Euglypha, Hyalosphaenia, Lesquereusia, Pontigulasia Trinema, Zivkovicia*
Rotifera	108	40	Bdelloidea indet., *Rotaria, Anuraeopsis, Ascomorpha, Brachionus, Cephalodella, Collotheca, Colurella, Conochilus Dicranophorus, Dipleuchlanis, Euchlanis, Filinia, Gastropus Hexarthra, Keratella, Lecane, Lepadella, Lindia, Microcodon, Monommata, Notommata, Ploesoma, Polyarthra, Pompholyx, Proales, Proalides, Proalinopsis, Resticula, Scaridium, Squatinella, Synchaeta, Testudinella, Trichocerca, Trichotria, Tripleuchlanis*
Cladocera	16	12	*Alona, Alonella, Camptocercus, Ceriodaphnia, Chydorus. Dunhevedia, Graptoleberis, Macrothrix, Pleuroxus, Rak, Scapholeberis, Simocephalus*
Copepoda	8	7	*Calamoecia, Canthocamptus, Eucyclops, Macrocyclops, Mesocyclops, Paracyclops, Tropocyclops*
Ostracoda	4	3	*Newnhamia,* indet. genus/genera
Macroinverte-brates	10	10	Turbellaria: cf. *Mesostoma*; Oligochaeta: Naididae; Insecta: Collembola, Diptera: Chironomidae, Coleoptera: Dytiscidae, Hemiptera: Notonectidae, Odonata: Zygoptera, Trichoptera; Amphipoda; Acari Hydrachnidae/Oribatidae

TABLE 4
Microinvertebrates and small macroinvertebrates from four waterbodies at Stieglitz on four dates

Faunal group	No. taxa	No. genera	Genera/taxa
Rhizopoda	16	8	*Arcella, Centropyxis, Cucurbitella, Difflugia, Euglypha, Lesquereusia, Netzelia, Pontigulasia*
Rotifera	64	29	*Bdelloidea indet., Ascomorpha, Brachionus, Cephalodella, Colurella, Conochilus, Dicranophorus, Euchlanis, Filinia, Gastropus, Hexarthra, Keratella, Lecane, Lepadella, Macrochaetus, Monommata, Mytilina, Notommata, Pompholyx, Ploesoma, Proales, Proalides, Resticula, Scaridium, Synchaeta, Testudinella, Trichocerca, Trichotria, Tripleuchlanis*
Cladocera	16	12	*Alona, Alonella, Camptocercus, Ceriodaphnia, Chydorus, Dunhevedia, Graptoleberis, Macrothrix, Pleuroxus, Rak, Scapholeberis, Simocephalus*
Copepoda	9	9	*Boeckella, Calamoecia, Gladioferens, Eucyclops, Macrocyclops, Mesocyclops, Paracyclops, Canthocamptus, Mesochra*
Ostracoda	7	at least 4	*Cypretta, Limnocythere, Newnhamia,* indet. genus/genera
Macroinverte-brates	2	2	Acari Hydrachnidae/Oribatidae

Camptocercus, Chydorus, Graptoleberis and *Pleuroxus.* The Rotifera were comparably diverse, with most genera and many species, some of them Tasmanian endemic species (table 6), shared with the Strahan dune lakes. Of the three Stieglitz lagoons sampled, the greatest microfaunal diversity occurred in Jock's Lagoon (32 taxa).

As a group, the Stieglitz lagoons contain all the endemic algae found in the west coast lagoons (table 5). Floristic studies are incomplete but, as with the west coast lagoons, they are known to contain protistans not yet recorded for Australia and also probable new species. Windmill Lagoon and Moriarty's Swamp, in particular, are especially rich and diverse in desmids, chrysophytes and dinophytes. The Stieglitz lagoons also contain some Tasmanian endemics among the rotifers (table 7) and a chydorid crustacean, *Alona rusticoides* Smirnov & Timms, endemic to Tasmania (Smirnov & Timms 1983). As with the west coast lagoons, those near Stieglitz are likely to harbour other species new to Tasmania, or new to science. They have been sampled at one time of year only, in summer, and on few occasions. Moriarty's Swamp, in particular, changes considerably with season, being inundated with water in winter but drying, or nearly so, in summer. Proper attention to seasonality would be highly likely to reveal more than this limited study has done.

DISCUSSION

Among the cluster of coastal lagoons near Strahan are some that are too shallow to stratify. Others, with depths in excess of about 4.0 m, especially if sheltered from the prevailing

westerly winds, do stratify. This is probably aided by the strong thermal gradients that develop in dystrophic lakes (Jones & Arvola 1984, Bowling & Salonen 1990). As an example, Lake Garcia stratifies early in the season and stratification persists until late, giving a stratified period of 8–9 months. This is comparable to that for highly dystrophic and sheltered Lake Chisholm in northern Tasmania forests (Bowling & Tyler 1988). In contrast, the limited numbers of measurements of clear-water Lake Bantic suggest a much shorter period. Rather surprisingly, while hypolimnetic oxygen concentrations do progressively decline in Lake Garcia, anoxia never occurs, despite the long period of stratification. Of the lagoons near St Helens, Moriarty's Swamp and Jocks Lagoon are too shallow to stratify and the limited data available suggest that the deeper Windmill Lagoon does not stratify either.

The physicochemical hallmark of the lagoons and reservoirs studied is low pH, dystrophy, moderate salinity and seawater ionic proportions. This is usual for almost all surface waters of western Tasmania (Tyler 1992) and some coastal lagoons elsewhere. These conditions favour chromophytic phytoflagellates as dominants of the phytoplankton (Croome & Tyler 1987b) and the majority of the endemic algae are of this type (tables 5, 7). The waters of the lagoons are strictly of the "dim red window" type (Bowling *et al.* 1986, Tyler 1992). Though the limited number of samples does not permit analysis of variability of physicochemical features, nothing in this study changes the earlier view (Bowling *et al.* 1993) that though there may be considerable variability it will not be sufficient to change the general limnological characters i.e., the lagoons will always be dystrophic and acid. This is probably significant for the maintenance of the characteristic populations of phytoflagellates and other organisms.

The west coast lagoons have a rich diversity of algae and rotifers, despite the view of Timms (1986) that rotifers are rare or absent from acidic dune lakes. A brief biogeography of Tasmania's Rotifera, given by Shiel *et al.* (1989), noted that the highest diversity and endemism was found to the west of the island, particularly around the Strahan dune lakes area. Lake Garcia, for example, remains the site of the highest rotifer species richness from a single collection in Tasmania (35 rotifer species). The endemic rotifers of the Strahan and Stieglitz lagoons are listed in table 6. In addition the west coast lagoons are the only known Australian sites for *Euchlanis triquetra* Ehrenberg and *Testudinella ahlstromi* Hauer. Eleven of Tasmania's 13 endemic rotifer species were previously thought to occur only in western dystrophic waters (Shiel *et al.* 1989). However, two of them have since been reported in acidic coastal or dune lakes elsewhere – *Testudinella tasmaniensis* Koste & Shiel from SW Western Australia (Storey *et al.* 1993), and *Lecane eylesi* Russell (=*L. tasmaniensis* Shiel & Koste) from the Chatham Islands (Russell 1953) and the west coast of the South Island of New Zealand (Shiel & Green 1996). It is possible that more of the western Tasmanian endemics may be more widely distributed but, on present evidence, the western Tasmania rotifer species assemblage contains the highest proportion of indigenous taxa in any Australasian region.

In contrast to the richness of the rotifer communities of the dune lagoons, species diversity of microcrustacea is low. During this study only one species of calanoid copepod was present, though, previously (Walsh unpublished), *Calamoecia australis* (Searle) was recorded from Lake Garcia and *Gladioferens spinosus* Henry from Hibbs Lagoon. Cladoceran diversity also tended to be low and the Harpacticoida and Ostracoda were represented by only one or two species. This is in contrast to the lagoons on the east and far north-east coasts of Tasmania (Walsh 1996), where there are typically 3–7 spp. present. This is attributed to differences in basin morphometry, complexity and cover of the aquatic macrophyte commmunity.

Considerable interest in the west coast lagoons centres on their harbouring endemic algae. The combination of low salinity, seawater ionic order, low pH and dystrophy appears to favour a small suite of species that are not found outside this sort of habitat. A further restriction is that the epicentre of this endemicity appears to be the coastal lagoons, not the remote montane lakes with apparently suitable water chemistry. These endemics have been called frail endemics, in contrast to those that apparently have more catholic tolerances and wider distributions (Tyler 1996a). While the lagoons near Strahan, and those near Stieglitz, are clearly the two strongholds, one or more species may occur in other dystrophic lagoons, dotted around Tasmania (Bowling *et al.* 1993, Tyler 1996a, Walsh *et al.* 1995), on the islands of Bass Strait (Walsh *et al.* 2001) and on islands off the Queensland coast (Croome *et al.* 1998). It is anticipated that frail endemic algae will only be found elsewhere outside Tasmania in waterbodies of this physicochemical nature, moreover only in complying waterbodies that also lie in native catchments or are surrounded by a buffer zone of such vegetation (cf. Walsh *et al.* 2001).

The occurrence of *Prorocentrum foveolata* Croome & Tyler together with *P. playfairi* Croome & Tyler in Moriarty Swamp is notable. *P. playfairi* is widely but sparsely distributed in Tasmania (Croome & Tyler 1987a). It is found in dystrophic lagoons of low to moderate salinity with the exception of Bruny Island (Walsh *et al.* 1995), where salinities are higher. *P. foveolata*, on the other hand, has its stronghold on the mainland of Australia, with salinities considerably higher than the typical *P. playfairi* habitats, and only a toehold in northeastern Tasmania (Tyler 1996b). The two species are known to coexist only in Moriarty's Swamp and in Reedy Lagoon on Flinders Island, Bass Strait (Walsh *et al.* 2001).

The presence of endemic algae, crustaceans and rotifers in these two groups of lagoons posed the question of what other protistan groups may also have endemic species there. In particular we wondered about the Ciliophora. It is widely believed that the ciliates are universally distributed (Finlay 1998, Finlay *et al.* 1996) but, we argued, that is an opinion based almost entirely on Northern Hemisphere experience. Surely, in the epicentres of Australian protistan novelty and endemism, we had the best chances of detecting endemism among the ciliates. A study carried out on mainland Australia, however, found that of 85 ciliate species in Tower Hill lakes, Victoria, all were previously known (Esteban *et al.* 2000, Finlay *et al.* 1999). Samples from the three St Helens lagoons and from Lake Bantic and Lake Garcia were examined. Only one new species, *Lembadion curvatum*, was found, in Lake Bantic (Esteban *et al.* 1999). However, the examinations were brief and cursory. The two clusters of lagoons in Tasmania are clearly prime sites in the debate about microbial biogeography and more detailed examination of their ciliate fauna is warranted.

Hibbs Lagoon was included in this study because of the interest of incipient meromixis rather than because of endemic algae. The two reservoirs were included because they demonstrate that frail endemics can colonise new waterbodies if water quality conditions are met (table 2). Because these two nineteenth century reservoirs were each

TABLE 5
Occurrence of novel or endemic protists, referred to by the code given in Table 7, in freshwater coastal lagoons and reservoirs of Tasmania.

Lagoon	Protist						
Lake Garcia	Du	Pp		Pt	Ss	Tt	Tv
Lake Bantic	Du	Pp	Lc	Pt	Ss	Tt	
Lake Ashwood				Pt		Tt	
Lake Koonya						Tt	
Lake Strahan	Du	Pp		Pt	Ss	Tt	Tv
Lake Mallana	Du	Pp		Pt		Tt	
Ocean Beach Lagoon						Tt	
Lake Cumberland	Du					Tt	
Parting Creek Dam	Du			Pt	Ss	Tt	Tv
Jocks Lagoon		Pp		Pt	Ss	Tt	
Windmill Lagoon	Du	Pp			Ss	Tt	
Moriarty Swamp	Du	Pp	Pf		Ss		

TABLE 6
Distribution of some microfauna, endemic to Australia, found in lagoons near Strahan and near St Helens (Stieglitz)

Species	Lagoon	Other localities
Lecane sp. nov. (R)	Jocks	
Notommata tyleri Koste, Shiel & Tan (R)	Garcia	Tasmania (central plateau)
Testudinella tasmaniensis Koste & Shiel (R)	Ashwood, Ocean Beach, Windmill.	Dune lake, SW-Western Australia.
Testudinella unicornuta Koste & Shiel (R)	Garcia, Strahan, Ashwood, Jocks.	western Tasmania
Trichotria buchneri Koste, Shiel & Tan (R)	Garcia, Ashwood, Ocean Beach.	western Tasmania
Alona rusticoides Smirnov & Timms (C)	Jocks, Windmill	Tasmania

R=Rotifera, C=Cladocera

TABLE 7
Endemic or novel freshwater protist (algae unless otherwise indicated) found in one or more of the coastal lagoons or reservoirs on Tasmania's coast

Species	Code	Reference	**Comments, Distribution**
Prorocentrum playfairi	Pp	Croome & Tyler 1987a	Tasmania and Bass Strait islands
Prorocentrum foveolata	Pf	Croome & Tyler 1987a	Mainland Australia, toehold in Tasmania
Thecadiniopsis tasmanica	Tt	Croome *et al.* 1987	Tasmania and Bass Strait islands
Dinobryon unguentariforme	Du	Croome *et al.* 1988	Tasmania, Queensland islands
Tessellaria volvocina	Tv	Tyler *et al.* 1989	Widespread in Australia
Pleurotaenium tridentalum forma	Pt	Ling & Tyler 2000	Widespread in Tasmanian coastal lagoons
Staurastrum sp.	Ss	Undescribed. See King & Tyler 1981, fig. 6b	Widespread in Tasmanian coastal lagoons
Lembadion curvatum Ciliophora	Lc	Esteban *et al.* 2000	Only Lake Bantic

formed by damming a valley in the wilderness, conditions in the new waterbodies, once natural processes of decay of flooded vegetation had run their course, would be much as in a natural lake surrounded by native vegetation. Tyler (1996a) and Walsh *et al.* (2001) claim that this native water quality, or at least lack of arable or pastoral agriculture nearby, is the key criterion for survival of a population of frail endemics.

The lagoons near Strahan lie in Crown land but outside national parks. The cluster centred on Lake Garcia and the South Strahan Lagoons (fig. 1) lies in land under the management of Forestry Tasmania. Much of the land in the vicinity of the lagoons is used for coniferous plantations. Forestry Tasmania has been acquainted with the floristic values of lakes under their aegis. They have responded by declaring a 50 m buffer zone around all mapped lagoons and entering on Management Decision Classification maps additional Special Management Zones, where water quality must not be compromised by harvesting operations. Smaller ponds and rush grown pools will be considered also under the Forest Practices Code of Tasmania (Forestry Commission Tasmania 1994, R. A. Hamilton pers. comm.). Hibbs Lagoon lies outside the south-western World Heritage Area (Tyler 1992) but in the South West Conservation Zone. Lake Strahan, Lake Koonya and New Lagoon are managed by the Tasmanian Parks and Wildlife Service. This authority was made aware of the value of lagoons >10 years ago and is said (N. Ricketts pers. comm. 1998) to be pursuing protection measures; none is yet in place. The lagoons near Stieglitz lie on Crown land gazetted as a State Recreation Reserve. This affords some protection but, as in the vicinity of Strahan, there is community concern about the loss of recreational amenity if the lands are gazetted as a higher order of reserve.

This paper concludes a series concerned with a limnological reconnaissance of Tasmanian coastal lagoons. The island State boasts, in its remote, montane wilderness, a lakeland of unsurpassed beauty, diversity and limnological interest. Some of its attributes, especially the more glamorous, have been chronicled elsewhere (e.g., Tyler 1974, 1986, 1992, 1993, Tyler & Wickham 1988, Tyler & Vyverman 1995, Vyverman *et al.* 1995, Hodgson *et al.* 1997). This series has concentrated more on the aquatic biota of small, lowland lakes and coastal lagoons, places that are frequently passed by in favour of more attractive highland lakes, and frequently looked upon as places to be drained or filled in. But it is these rush-grown lagoons that are the epicentres of endemism and novelty in the microflora and microfauna. Proof of this endemism has been sought (Tyler 1992). It rests on the fact that frail endemics have been found in so few other places in Australia, despite widespread sampling (e.g., Croome & Tyler 1985, 1988b, Ling & Tyler 2000). Nonetheless, it is not possible to sample every lagoon in the continent and the occurrence of endemics in Queensland, and on stepping stones in Bass Strait (Rolfe *et al.*, Walsh *et al.* 2001) indicates that a search elsewhere in Australia, in lagoons with appropriate water quality and with native vegetation surrounding them, could be fruitful. Areas that spring readily to mind are near Lismore, New South Wales, where Playfair (1915) recorded endemic algae, and in the south west of Western Australia, where Segers & Shiel (2003) recorded endemic rotifers and Frey (1991) documented a suite of endemic chydorid cladocerans. It would be gratifying if novelty and uniqueness among the Australian aquatic microbiota were not largely a Tasmanian monopoly.

ACKNOWLEDGEMENTS

This study was financed by the Plomley Foundation, the National Estate Grants Programme (Project 9111), the University of Tasmania and Deakin University. We thank the National Parks and Wildlife officers in Strahan and the Landcare Group in St Helens for advice and assistance. The CSIRO Science Endowment Fund provided a dissecting microscope used for part of the microfauna survey. Dorothy Berner, Temple University, Philadelphia, is thanked for identifying the Lake Garcia/Lake Bantik *Ceriodaphnia*. We thank Carol Williams and Todd Dudley, both of St Helens, for valuable advice and liaison.

BIBLIOGRAPHY

BANKS, M.R., COLHOUN, E.A. & CHICK, N.K., 1977: A reconnaissance of the geomorphology of central western Tasmania. *In* Banks, M. R. & Kirkpatrick, J. B. (Eds): *Landscape & Man: The interactions between Man and environment in Western Tasmania.* Royal Society of Tasmania, Hobart: 29–54.

BOWDEN, A.R., 1978: Geomorphic perspective on shallow ground water potential, coastal north-eastern Tasmania. *Australian Water Resources Council, Technical Paper* 36.

BOWDEN, A.R., 1983: Relict terrestrial dunes: Legacies of former climate in coastal north-east Tasmania. *Zeitschrift für Geomorphologie* N.F. 45: 153–174.

BOWLING, L.C. & SALONEN, K., 1990: Heat uptake and resistance to mixing in small humic lakes and of forests in Southern Finland. *Australian Journal of Marine and Freshwater Research* 41: 747–755.

BOWLING, L.C. & TYLER, P.A., 1988: Lake Chisholm, a polyhumic forest lake in Tasmania. *Hydrobiologia* 161: 55–67.

BOWLING, L.C., STEANE, M.S. & TYLER, P.A., 1986: The spectral distribution and attenuation of underwater irradiance in Tasmanian inland waters. *Freshwater Biology* **16**: 313–335.

BOWLING, L.C., BANKS, M.R., CROOME, R.L. & TYLER, P.A., 1993: Reconnaissance Limnology of Tasmania II. Limnological features of Tasmanian freshwater coastal lagoons. *Archiv für Hydrobiologie* 126: 385–403.

CROOME, R.L. & TYLER, P.A., 1985: Distribution of silica-scaled Chrysophyceae (Paraphysomonadaceae and Mallomonadaceae) in Australian inland waters. *Australian Journal of Marine and Freshwater Research* 36: 839–853.

CROOME, R.L. & TYLER, P.A., 1987a: *Prorocentrum playfairi* and *Prorocentrum foveolata*, two new dinoflagellates from Australian freshwaters. *British Phycological Journal* 22: 67–75.

CROOME, R.L. & TYLER, P.A., 1987b: Phytoflagellates and their ecology in Tasmanian polyhumic lakes. *Hydrobiololgia* 161: 245–253.

CROOME, R.L., HALLEGRAEFF, G.M. & TYLER, P.A., 1987: *Thecadiniopsis tasmanica* gen. et sp. nov. (Dinophyta : Thecadiniaceae), a new peridinioid dinoflagellate from Tasmanian freshwaters. *British Phycological Journal* 22: 325–333.

CROOME, R.L., LING, H.U. & TYLER, P.A., 1988a: *Dinobryon unguentariforme* (Chrysophyceae), an unusual new species from Australia. *British Phycological Journal* 23: 129–133.

CROOME, R.L. & TYLER, P.A., 1988b: Further observations of silica-scaled Chrysophyceae (Paraphysomonadaceae and Mallomonadaceae) from Australian freshwaters. *Nova Hedwigia* 46: 481–489.

CROOME, R.L., KRISTIANSEN, J. & TYLER, P.A., 1998: A description of *Mallomonas marsupialis* (Synurophyceae) a new species from Australia with comments on the endemicity

of Australian freshwater algae. *Nordic Journal of Botany* 18: 633–639

ESTEBAN, G.F., FINLAY, B.J., OLMO, J.L. & TYLER, P. A., 2000: Ciliated protozoa from a volcanic crater lake in Victoria, Australia. *Journal of Natural History* 34: 159–189.

FINLAY, B.J., 1998: The global diversity of protozoa and other small species. *International Journal of Parasitology* 28: 29–48.

FINLAY, B.J., ESTEBAN, G.F. & FENCHEL, T., 1996: Global diversity and body size. *Nature* 383: 132–133.

FINLAY, B.J., ESTEBAN, G.F., OLMO, J.L. & TYLER, P.A., 1999: Global distribution of free-living microbial species. *Ecography* 22: 138–144.

FREY, D.G., 1991: The species of *Pleuroxus* and of three related genera (Cladocera, Chydoridae) in southern Australia and New Zealand. *Records of the Australian Museum* 43: 291–372.

HODGSON, D.A., TYLER P.A. & VYVERMAN, W., 1996: The palaeolimnology of Lake Fidler, a meromictic lake in south west Tasmania and the significance of recent human impact. *Journal of Paleolimnology* 18: 313–333.

JENNINGS, J.N., 1959: The coastal geomorphology of King Island, Bass Strait, in relation to changes in relative level of land and sea. *Records of the Queen Victoria Museum, Launceston* 11: 1–39

JENNINGS, J.N. 1961: Sea level changes in King Island, Bass Strait. *Zeitschrift für Geomorphologie, Supplement* 3: 80–84.

JONES, R.I. & ARVOLA, L., 1984: Light penetration and some related characteristics in small forest lakes in Southern Finland. *Internationale Vereinigung für Theoretische und Angewandte Limnologie, Verhandlungen* 22: 811–816.

KERSHAW, R.C. & SUTHERLAND, F.L., 1972: Quaternary geomorphology of Flinders Island. *Records of the Queen Victoria Museum, Launceston* 43: 1–28.

KING, R.D. & TYLER, P.A., 1981: Limnology of Perched Lake, south-west Tasmania. *Australian Journal of Marine and Freshwater Research* 32: 501–515.

KOSTE, W. & SHIEL, R.J. 1986: New Rotifera (Aschelminthes) from Tasmania. *Transactions of the Royal Society of South Australia* 111: 93–109.

KOSTE, W. & SHIEL, R.J., 1987: Tasmanian Rotifera: Affinities with the Australian fauna. *Hydrobiologia* 147: 31–443.

KOSTE, W., SHIEL, R.J. & TAN, L.W., 1988: New rotifers (Rotifera) from Tasmania. *Transactions of the Royal Society of South Australia* 112: 119–131.

LING, H.U., CROOME, R.L. & TYLER, P.A., 1989: Freshwater dinoflagellates of Tasmania, a taxonomic and ecological survey. *British Phycological Journal* 24: 111–129.

LING, H.U. & TYLER, P.A., 2000: Australian freshwater algae (exclusive of diatoms). *Bibliotheca Phycologia* 105: 1–643, 159 pl. J. Cramer, Berlin and Stuttgart.

MEISTERFELD, R. & TAN, L.W., 1998: First records of testate amoebae (Protozoa: Rhizopoda) from Mount Buffalo National Park, Victoria: preliminary notes. *The Victorian Naturalist* 115: 231–238.

PLAYFAIR, G.I., 1915: Freshwater algae of the Lismore District, with an appendix on the algal fungi and schizomycetes. *Proceedings of the Linnean Society of New South Wales* 40: 310–62.

ROLFE, S.F., KEW, P.L. & TYLER, P.A., 2001: Reconnaissance limnology of Tasmania.VI. Physicochemical features of coastal lagoons of the Bass Strait islands. *Archiv für Hydrobiologie* 150: 693–704.

RUSSELL, C.R. 1953: Some Rotatoria of the Chatham Islands. *Records of the Canterbury Museum* 6: 237–244.

SEGERS, H. & SHIEL, R.J., 2003: Microfaunal diversity in a biodiversity hotspot: new rotifers from south-western Australia. *Zoological Studies* 42: 516-521.

SHIEL, R.J. & GREEN, J.D., 1996: Rotifera recorded from New Zealand, 1859-1995, with comments on zoogeography. *New Zealand Journal of Zoology* 23: 193–209

SHIEL, R.J., KOSTE, W. & TAN, L.W., 1989: Tasmania revisited; rotifer communities and habitat heterogeneity. *Hydrobiologia* 186/187: 239–245.

SMIRNOV, N.N. & TIMMS, B.V., 1983: A revision of the Australian Cladocera (Crustacea). *Records of the Australian Museum, Supplement* 1: 1–132.

STOREY, A.W., HALSE, S.A. & SHIEL, R.J., 1993: The aquatic invertebrate fauna of the Two Peoples Bay area, south-western Australia. *Journal of the Royal Society of Western Australia* 76: 25–32.

TIMMS, B.V., 1982: Coastal dune waterbodies of north eastern New South Wales. *Australian Journal of Marine and Freshwater Research* 33: 203–222.

TIMMS, B.V., 1986: The coastal dune lakes of Eastern Australia. *In* De Deckker, P. & Williams, W. D. (Eds): *Limnology in Australia.* CSIRO, Melbourne & W. Junk, Dordrecht: 421–432.

TIMMS, B.V., 1992: *Lake Geomorphology.* Gleneagles Publishing, Adelaide.

TYLER, P. A., 1974: Limnological studies. *In* Williams, W.D. (Ed.): Biogeography and Ecology in Tasmania. *Monographia Biologicae* 25: 29–61. W. Junk, The Hague.

TYLER, P.A., 1986: Anthropological limnology in the Land of Moinee. *In* De Deckker, P. & Williams, W. D. (Eds): *Limnology in Australia.* CSIRO, Melbourne & W. Junk, Dordrecht: 532–537.

TYLER, P.A., 1992: A Lakeland from the Dreamtime: The Second Founder's Lecture. *British Phycological Journal* 27: 353–368.

TYLER, P.A., 1996a: Endemism in freshwater algae. In Kristiansen, J. (Ed.) Biogeography of Freshwater Algae. *Developments in Hydrobiology* 118 (*Hydrobiologia* 336): 127–135.

TYLER, P.A., 1996b: The significance of north-east Tasmania for the biogeography of endemic Australian freshwater algae. *Records of the Queen Victoria Museum, Launceston* 103: 133–135.

TYLER, P.A. & WICKHAM, R.P., 1988: Yan Yean revisited - a bicentennial window on Australian freshwater phycology. *British Phycological Journal* 23: 105–114.

TYLER, P.A. & VYVERMAN, W.G., 1995: The microbial market place - trade-offs at the chemocline of meromictic lakes. *Progress In Phycological Research* 11: 325–370.

TYLER, P.A., PIPES, L., CROOME, R.L. & LEEDALE, G.F., 1989: *Tessellaria volvocina* (Chrysophyta) rediscovered. *British Phycological Journal* 24: 329–337.

TYLER, P.A., SHERWOOD, J.E., MAGILTON, C.J. & HODGSON, D.A., 1996: Limnological and geomorphological considerations underlying Pedder 2000 - the campaign to restore Lake Pedder. *Archiv für Hydrobiologie* 136: 343 –361.

VYVERMAN, W., VYVERMAN, R., HODGSON, D. & TYLER, P.A., 1995: Diatoms from Tasmanian mountain lakes: a reference data set (TASDIAT) for environmental reconstruction and a systematic and autecological study. *Bibliotheca Diatomologica* 33: 1–193, 42 pl.

WALSH, R.G.J., 1996: Limnology of Tasmanian freshwater coastal dune lakes with particular reference to the microcrustacea. Unpubl. PhD thesis, University of Tasmania, Hobart.

WALSH, R.G.J., VYVERMAN, W.G. & TYLER, P.A., 1995: Reconnaissance limnology of Tasmania III. Coastal lagoons of Bruny Island. *Archiv für Hydrobiologie* 136: 247–260.

WALSH, R.G.J. & TYLER, P.A., 1998: Reconnaissance limnology of Tasmania IV. The distribution and ecological preferences of Tasmanian species of freshwater calanoid copepods (Crustacea: Centropagidae). *Archiv für Hydrobiologie* 141: 403–420.

WALSH, R.G.J., SHIEL, R.J. & TYLER, P.A., 2001: Reconnaissance limnology of Tasmania VII. Coastal lagoons of Bass Strait islands, with reference to endemic microflora and microfauna. *Archiv für Hydrobiologie* 152: 489–510.

(accepted 2 August 2004)

MR GORDON HALE, 1921–2004 HONORARY LIFE MEMBER, ROYAL SOCIETY OF TASMANIA: OBITUARY

by M. R. Banks

(with one plate)

BANKS, M. R., 2004 (29:x): Mr Gordon Hale 1921–2004, Honorary Life Member, Royal Society of Tasmania: Obituary. *Papers and Proceedings of the Royal Society of Tasmania* 138: 77. ISSN 0080–4703. School of Earth Sciences, University of Tasmania. Private Bag 79, Hobart Tasmania 7001, Australia.

Mr Gordon Hale

Gordon Hale was born in Hobart on 19 June 1921 and died in Hobart on 18 August 2004. During his lifetime he knew severe hardship but gave much to the Tasmanian community through his profession as engineering geologist, through active membership in professional societies, including the Royal Society of Tasmania, and in war veterans' bodies. He was widely known in Tasmania and beyond, and widely respected.

He completed his secondary education at Hobart High School in 1939, and attained, early in 1940, the rank of Sergeant in the Citizen Military Forces, with which he had served since 1937. A month after transferring to the A.I.F. in December 1941 he was sent to Singapore where he fought in the Battle for Singapore as a member of the 2/29th Battalion until the surrender in February 1942. As a prisoner of war, he was part of a wood-cutting gang but found time to further his education by taking courses in the P.O.W. camp and was subsequently awarded a scholarship based on these studies. Gordon was discharged from the Army in December 1945.

Early in 1946 he commenced studies in Engineering at the University of Tasmania under the Commonwealth Reconstruction and Training Scheme. In 1947 he transferred to Science and, under the influence of the late Professor S. W. Carey, developed a lifelong interest in geology. He graduated in Geology at the end of 1951 with first class honours for a research project based on field mapping and studies of clay deposits in the Dover area. This project was the basis of his first two papers, published in the *Papers and Proceedings of the Royal Society of Tasmania* in 1953.

For several months early in 1952 he worked as Demonstrator in Geology at the University of Tasmania. Then, in April, he joined the staff of the Tasmanian Museum and Art Gallery as the first Curator of Geology at that institution. In that capacity he planned and supervised design and construction of exhibits for the Geology Gallery. He was also Honorary Part-time Lecturer in Geology at the University, teaching mineralogy and geological mapping, subjects he made interesting.

Several years later the Hydro Electric Commission moved to appoint their first engineering geologist. Gordon applied and was successful, commencing work with the Commission in March 1956. He subsequently became Geologist-in-Charge and then Chief Geologist. He retired from that position in 1982 and since then has devoted his time to, *inter alia*, hobbies such as fishing, gardening, wood carving and golf.

Gordon Hale was elected Honorary Treasurer of the Royal Society of Tasmania in 1953 and occupied that position for 24 years, seeing the Society through some lean years in the 1960s, and was a member of the Standing Committee for five years. He was elected Junior Vice-President for 1977 and, in the custom usual at that time, became Senior Vice-President in 1978. The Society conferred Honorary Life Membership on him in 1979. Between 1953 and 1970 he had eight papers published by the Society on a variety of Tasmanian geological topics. He also published material in the *Journal of the Geological Society of Australia*, and in engineering journals.

The Royal Society of Tasmania was not Gordon's only interest. He contributed in an executive capacity to the Geological Society of Australia, particularly to the Tasmania Division, and to several veterans' organisations. However, the Royal Society of Tasmania gained greatly from Gordon Hale's services and we salute and thank him for it.

(accepted 4 October 2004)

ROYAL SOCIETY OF TASMANIA PAPERS AND PROCEEDINGS
GUIDE TO AUTHORS

The Royal Society of Tasmania, which was founded in 1843, is the oldest scientific society in Australia and New Zealand and the third oldest Royal Society in the Commonwealth. Since 1849, it has published annual volumes of refereed scholarly papers about Tasmania in the *Papers and Proceedings of the Royal Society of Tasmania* and, from time to time, monographs and special, generally thematic, issues of the journal. Its subscribers include learned societies, research institutions and universities all over the world.

Scope

Papers and Proceedings of the Royal Society of Tasmania publishes research that focuses on Tasmania or is particularly relevant to Tasmanians. Although the subject matter is usually within the natural sciences or history, papers in the arts, social sciences or other disciplines are encouraged. Papers should embody the results of a significant piece of original work or offer an original synthesis or review.

Papers may be submitted by members of the Society or by non-members. Submission implies that the contents are original and have not been published previously in any form, and that no similar manuscript will be submitted elsewhere.

Copyright

Verbatim quotations of text must be acknowledged and the source given (with the relevant page number/s). Authors must specifically acknowledge the source of illustrations that have been previously published elsewhere and are not their property, and must obtain permission for publication of text or illustrations covered by copyright. Permission to use material previously published by the Royal Society of Tasmania can be obtained upon application to the Council.

Address for Submissions

Honorary Editor, The Royal Society of Tasmania, GPO Box 1166, Hobart, Tas 7001, Australia.
Please include your email address and the name of the person the editor can contact with editorial queries, proofs etc. Also note whether electronic versions of the text of the paper (preferably in *Word*) and of the figures (in *PICT, TIF, JPG* or *EPS*) are available.

Refereeing Policy

The Council of the Society will take into consideration the advice of at least two reviewers before deciding for or against accepting the paper for publication. That decision will be final. If the paper is not accepted, one copy will be retained by the Society, the others returned to the author. Once accepted, papers and their copyright belong to the Society. However, an author may copy his or her paper for distribution as a reprint, and reproduction of synopses in abstracting journals is authorised.

Style

Referees are not expected to correct grammatical or spelling mistakes; papers should be well written, with the minimum of jargon. Remember that many of the readers of this journal are not specialists in your field; do not exclude them.

The Editor reserves the right to adjust the text for clarity, conformity to style, and publication standards. In general, the editor follows the conventions in the current edition of the *Style Manual for Authors, Editors and Printers* published by the Australian Government Publishing Service, and the spelling in the *Macquarie Dictionary*.

Text format

- use 11 or 12 point serif type
- print double-spaced (*not* one-and-a-half spaced)
- do not justify (i.e., use ragged right)
- number all pages consecutively, including references, figure legends, appendices
- number every fifth line (automatic in *Word*) to assist reviewers
- send three copies of the paper (including good copies of the illustrations)
- note whether electronic versions of the text (*Word*) and figures (*PICT, TIF, JPG* or *EPS*) are available
- supply key words (2–10) for the use in abstracting journals
- include an abstract of no more than 200 words

Citation format:

- published material e.g., Brown (1983), Brown & Green (1985), Brown *et al.* (1987), Brown *et al.* (in press), (Brown 1983)
- note any information supplied personally to the author(s) e.g., (T.O. White pers. comm.); do not include in the list of references; obtain permission from the informant (preferably in writing) to quote him or her
- include the relevant page number of a lengthy cited work e.g., (1983, p. 110)
- do not refer to papers 'in preparation' without an explanatory note to the editor

References format:

The reference list should conform to the format used in recent volumes of the journal, with the exception of two minor changes:

- journal titles to be given in full (not abbreviated)
- book titles to be in upper and lower case, italicised (not all-capitals)

Tables and Illustrations:

- number consecutively in the order of the first reference to them in the text

Tables:
The preferred dimensions for tables are either (a) 65 lines or less in depth, each line of no more than 130 characters and spaces in length, or (b) 42 lines or less in depth, each line of no more than 190 characters and spaces. These dimensions include the title, explanatory material and column headings. Tables:

- should be 'stand-alone', with sufficient information for the table to be understood without reference to the text
- explain symbols and abbreviations (e.g., n.d. = no data) in the title
- should have the fewest possible lines; do not use the grid 'default' in *Word*

Illustrations (figures and plates):
The maximum dimensions for illustrations, when printed, are 250 by 167 mm, including captions. Wherever possible, illustrations will be fitted into a single column (width 80 mm). Illustrations:

- preferably in black and white; colour illustrations may be used but authors will be expected to bear the extra cost of printing.
- supply captions for all illustrations.
- use keys within the artwork to explain symbols used in the illustrations.
- add bar scales or objects of known or stated dimensions to show the scale of illustrations wherever appropriate.
- write the author's name and the figure or plate number in soft pencil on the back of each illustration.
- lines, letters and symbols must be of a size and weight to stand the likely reduction to the printed size without breaking up, becoming too faint, filling in or becoming too small for ready legibility; the smallest letter or number, after reduction, should be not less than 2 mm high and, on the axes of graphs, 2.5 or 3 mm high.
- electronic figures should be made available in PICT, TIF, JPG or EPS formats.
- DO NOT supply figures and/or plates in a Word document. If electronic files are not available, please supply high-quality hard copy.

Appendices
Material presented as Appendices (labelled A, B, C, etc.) are accepted at the editor's discretion, but may be printed in a smaller type than the body of the paper.

Conventions
The Botanical, Zoological and Stratigraphic Codes of Nomenclature should be fully observed.
Use of SI units of measurement is strongly preferred where consistent with the means of measurement.

Costs
To keep publication costs down, texts should be concise, and tables and illustration should be used sparingly, both for economy and for maximum effect in the published form. Grants from author's institutions or elsewhere to support publication should be secured if possible. Authors are responsible for the costs of changes, other than minor corrections, to proofs. Page charges will normally be levied on the eleventh and each subsequent page of a paper as printed. The author will be charged the cost of printing colour illustrations.

Museum Victoria
71417

PAPERS AND PROCEEDINGS OF THE ROYAL SOCIETY OF TASMANIA
VOLUME 138

Contents

page

HARLOW, L. D., WATKINS, W. B. & KOUTOULIS, A. — An ultrastructural and functional assessment of nasal cilia and spermatozoa in an infertile human male and healthy controls 1

EVERARD, J. L., SUTHERLAND, F. L. & ZWINGMANN, H. — A Cretaceous phonolite dyke from the Tomahawk River, northeast Tasmania 11

MORRIS, D. I. — *Laxmannia morrisii* Keighery (Anthericaceae) a synonym of *L. squarrosa* Lindl., not a native of Tasmania 35

KIRKPATRICK, J. B., LEAMAN, T., PENNINGTON, A. & POLLARD, T. — Characteristics and dynamics of the sand dune vegetation at North Bay, Tasmania 37

LEESON, K. E. & KIRKPATRICK, J. B. — Vegetation patterns associated with a large rock plate in the Meehan Range, Tasmania 47

GATES, G. M. & RATKOWSKY, D. A. — A preliminary census of the macrofungi of Mt Wellington, Tasmania – the non-gilled Basidiomycota 53

NELSON, M. — Distribution of the Western paragalaxias (*Paragalaxias julianus*) (Pisces: Galaxiidae) on the Western Central Plateau, Tasmania 61

WALSH, R. G. J., SHIEL, R. J. & TYLER, P. A. — Reconnaissance limnology of Tasmania VIII. Tasmanian coastal lagoons – epicentres of endemism in the Australian aquatic microbiota 67

BANKS, M. R. — Mr Gordon Hale 1921–2004, Honorary Life Member, Royal Society of Tasmania: Obituary 77

Instructions to Authors 79